LOW-LYING q^3 BARYONS AND GROUND STATE PENTAQUARKS IN SU(3) FLAVOR SYMMETRY

Kai   Xu

A Thesis Submitted in Partial Fulfillment of the Requirements for the

Degree of Doctor of Philosophy in Physics

Suranaree University of Technology

Academic Year 2018

แบริออนที่พลังงานต่ำและควาร์กห้าตัวที่สถานะพื้นภายใต้สมมาตร

SU (3) FLAVOR SYMMETRY

นายไข่ ฉู

วิทยานิพนธ์นี้เป็นส่วนหนึ่งของการศึกษาตามหลักสูตรปริญญาวิทยาศาสตรดุษฎีบัณฑิต

สาขาวิชาฟิสิกส์

มหาวิทยาลัยเทคโนโลยีสุรนารี

ปีการศึกษา 2561

LOW-LYING q³ BARYONS AND GROUND STATA

# PENTAQUARKS IN SU(3) FLAVOR SYMMETRY

Suranaree University of Technology has approved this thesis submitted in partial fulfillment of the requirements for the Degree of Doctor of Philosophy.

Thesis Examining Committee

_____
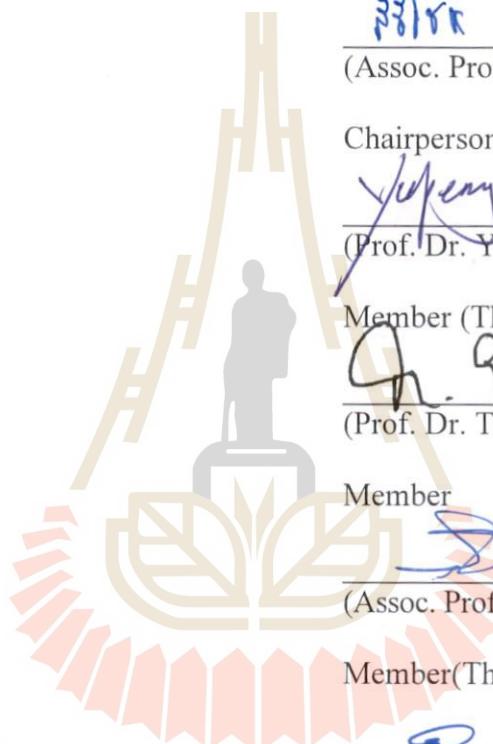
(Assoc. Prof. Dr. Sirichok Jungthawan)

Chairperson

_____
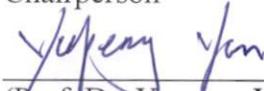
(Prof. Dr. Yupeng Yan)

Member (Thesis Advisor)

_____
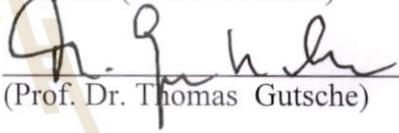
(Prof. Dr. Thomas Gutsche)

Member

_____

(Assoc. Prof. Dr. Sorakrai Srisuphaphon)

Member(Thesis Co-Advisor)

_____

(Asst. Prof. Dr. Ayut Limphirat)

Member

_____

(Asst. Prof. Dr. Khanchai Khosonthongkee)

Member

_____   _____

(Assoc. Prof. Flt. Lt. Dr. Kontorn Chamniprasart) (Assoc. Prof. Dr. Worawat Meevasana)

Vice Rector for Academic Affairs   Dean of Institute of Science

and Internationalization

ไข่ ฉู : แบริออนที่พลังงานต่ำและควาร์กห้าตัวที่สถานะพื้นภายใต้สมมาตร SU(3) FLAVOR SYMMETRY (LOW-LYING q^3 BARYONS AND GROUND STATE PENTAQUARKS IN SU(3) FLAVOR SYMMETRY) อาจารย์ที่ปรึกษา : ศาสตราจารย์ ดร.ยูเป็ง แยน , 89 หน้า

การศึกษาสเปกตรัมมวลของอนุภาคแบริออนมีมานานกว่าทศวรรษแล้วแต่ทว่าผลลัพธ์เชิง ทฤษฎีนั้นยังคงไม่สอดคล้องกับข้อมูลจากการทดลองดังเช่นผลการทำนายเชิงทฤษฎีโดยใช้ แบริออนที่มีควาร์กสามตัวนั้น ไม่เพียงแต่สถานะกระตุ้นที่พลังงานสูงแม้แต่การทำนายมวลของ สถานะกระตุ้นที่พลังงานต่ำอย่างมวลของอนุภาคสั่นพ้องโรเปอร์ N(1440) มีความผิดพลาดเช่นกัน โดยพบว่ามวลของ N(1440) มีขนาดใหญ่กว่า N(1520) และ N(1535)

งานวิจัยนี้มุ่งศึกษามวลของอนุภาคแบริออนโดยใช้แบบจำลองควาร์ก โดยที่อนุภาค แบริออนมีควาร์กสามตัวและห้าตัวเป็นองค์ประกอบและยึดเหนี่ยวกันภายใต้พลังงานศักย์ คอร์เนล อีกทั้งยังศึกษาอนุภาคสั่นพ้องโรเปอร์ N(1440) สถานะกระตุ้นคลื่นพี N(1535) และ แบริออนที่มีสามควาร์กในพลังงานต่ำชั้นอื่น ๆ ซึ่งจากการวิจัยพบว่า N(1685) อาจเป็นสถานะที่ ประกอบด้วยควาร์กห้าตัวที่เบาที่สุดโดยไม่มีควาร์กชนิดเอสเป็นองค์ประกอบ นอกจากนี้ยังศึกษา สถานะควาร์กห้าตัวที่สถานะพื้นโดยมีควาร์กหนักแฝงอยู่ซึ่งอยู่ในรูป $q^3Q\bar{Q}$ (q=u, d, s ใน สมมาตรเฟลเวอร์ SU(3) และ Q=c, b) อีกด้วย

สาขาวิชาฟิสิกส์	ลายมือชื่อนักศึกษา_____
ปีการศึกษา 2561	ลายมือชื่ออาจารย์ที่ปรึกษา_____

KAI XU : LOW-LYING q^3 BARYONS AND GROUND STATE
PENTAQUARKS IN SU(3) FLAVOR SYMMETRY. THESIS ADVISOR :
PROF. YUPENG YAN, Ph.D. 89 PP.

GROUP THEORY/BARYON SPECTRUM/CONSTITUENT QUARK
MODEL/PENTAQUARK/MODEL PARAMETERS

Baryon mass spectrum has been studied over decades, but theoretical results are still largely inconsistent with experimental data. No need to mention the higher excited states, even the low-lying resonances, for example, theoretical works in the three-quark picture always predict a larger mass for the Roper resonance $N(1440)$ than for $N(1520)$ and $N(1535)$.

In our work baryon mass spectra are evaluated in the constituent quark model with Cornell potential, assuming that baryons consist of the q^3 as well as $q^4\bar{q}$ pentaquark component. The roper resonance N(1440) and the P-wave excitation state N(1535) and other low-lying q^3 baryons are interpreted. N(1685) could be the lowest non-strange pentaquark state. The ground pentaquark states of hidden heavy $q^3 Q\bar{Q}$ (q = u,d,s quark in SU(3) flavor symmetry; Q = c, b quark) system are also studied.

School of Physics   Student's Signature _Kai Xu_

Academic Year 2018   Advisor's Signature _Yupeng Yan_

ACKNOWLEDGEMENTS

I would like to express my gratitude to the many people for their encouragement, assistance, and support which enabled me to complete my PhD studies.

My deepest gratitude goes first and foremost to my thesis advisor Prof. Dr. Yupeng Yan and co-advisor Asst. Dr. Sorakrai Srisuphaphon and Prof. Dr. Thomas Gutsche for their constant support, patient guidance, consideration, and assistance throughout the study. Without their help, this work would not be possible. And also great thanks go to Prof. Dr. Thomas Gutsche for his tutoring and help before and after I stay in Tuebingen University, I really learned a lot in that year. I would like to thank Dr. Ayut Limphirat and Dr. Khanchai Khosonthongkee for every help and suggestion they give on my living and work.

I would like to thank for the support of SUT-PhD/13/2554 Scholarship of Suranaree University of Technology, Center of excellence in High Energy Physics and Astrophysic (COE) and also Higher Education Research Promotion and National Research University Project of Thailand, Office of the Higher Education Commission. Many thanks are also for our theoretical physics group in Suranaree University of Technology and the teachers and members in the group for valuable lessons, discussions and suggestions.

Last but not least, I would like to extent my immense gratitude to my mother for her continuous love, understanding, encouragement and support throughout the progress and for motivating me to complete my study.

Kai Xu

CONTENTS

CONTENTS (Continued)

LIST OF TABLES

LIST OF TABLES (Continued)

LIST OF TABLES (Continued)

LIST OF FIGURES

CHAPTER I

INTRODUCTION

In recent decades, hadron physicists have expended great effort hunting for evidence of the multiquark states. Since the arguable state of $\Theta^+(1540)$ was proposed as the first observed pentaquark, tremendous progress on experimental and theoretical explorations of the multiquark states has been achieved. Disregarding the large number of XYZ tetraquark candidates, in recent years the LHCb Collaboration has reported and confirmed the observation of three narrow pentaquark-like states: $P_c(4312)^+$, $P_c(4440)^+$, and $P_c(4457)^+$. All three pentaquark-like states may have the quark content of $uudc\bar{c}$ (Aaij et al., 2015; Aaij et al., 2019), but their internal structures as well as quantum numbers are still unclear.

Probably the most successful and complete description of hadron structure is provided by the constituent quark model which was proposed by Murray Gell-Mann and George Zweig in 1964 (Gell-Mann, 1964). Within this framework quarks were introduced as algebraic entities acting as elementary and fundamental constituents of matter. Since quarks are confined they do not appear as free asymptotic particles but only as constituents of the color singlet hadrons. Hence, there is only a qualitative understanding about the nature and dynamical origin of the constituent quarks which occur as quasiparticles, believed to be current quarks surrounded by a cloud of virtual quarks and gluons by which effective quark masses are put into these current quarks. These dressed current quarks of different flavor correspond to different constituent quarks effectively in the low energy system, as well for heavy quarks like c and b quark in heavy quark system.

Baryons and baryon resonances have been studied for decades, but theoretical results are still largely inconsistent with experimental data. The study of baryon excitation states is the main way to reveal the baryon mass spectrum in which the levels are labelled as: $N_{J^P}(mass)$, but even the lowest-mass nucleon resonance, the Roper resonance $N_{1/2^+}(1440)$ has been problematic. In the constituent quark model of the three-quark picture with one-gluon-exchange (Capstick and Isgur, 1986), for example, the Roper $N_{1/2^+}(1440)$ should have a mass 80 MeV above the first $J = 1/2$ negative-parity state $N_{1/2^-}(1535)$ mass, but not almost 100 MeV below it as the level ordering shown in Figure 1.1.

From 1960s, the final breakthrough of the quark model was provided by direct evidence for quarks in deep inelastic scattering experiments at SLAC in 1968 (Bloom et al., 1969). Despite the success of the quark model, detailed observables related to spectrum, production and decay properties of observed hadrons still pose major challenges to the theoretical understanding. A very good review paper, "Baryon Spectroscopy" (Klempt and Richard, 2010) not only introduces the newly discovered baryon and heavy baryon, but also explains the
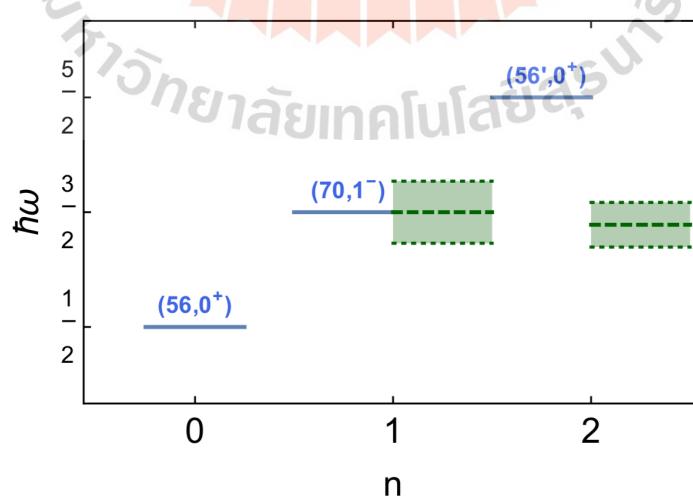
Figure 1.1 The level ordering produced in the constituent quark model.

experiments and relevant models.

The baryons are experimentally well established and studied in different production processes where the most important ones are introduced in the following:

a. Pion- (Kaon-) nucleon elastic and charge exchange scattering: The baryon spectroscopy was firstly defined from $\pi^{\pm}N$ elastic scattering, large numbers of baryon resonances are reported with ratings from one-star to four-stars, practically only the four-star resonances are confirmed. The total and differential cross section for several different center of mass energies are studied in different accelerators, beams and detectors. The s, t, u-channel exchange in these pion-nucleon scattering are counted theoretically for different particles. The kaon nucleon elastic scattering which can produce hyperon spectrum is also studied in the same way. Figure 1.2 courtesy of the COMPAS group, IHEP, Protvino, Russia (Tanabashi et al., 2018) is an example. In this for example, the total cross section for $\pi^{-}p$ scattering exhibits three distinctive peaks at the $\Delta_{3/2^+}(1232)$, at 1.5 GeV, and at 1.7 GeV; a fourth enhancement at 1.9 GeV is faint, a further peak at 2.2 GeV leads into the continuum.

b. Inelastic pion and kaon nucleon scattering and other reactions: inelastic scattering is a similar scattering process as elastic scattering just with the kinetic energy of an incident particle not conserved, so the incident particle will take certain values of momentum within a range above the threshold. N(1535) is produced in the process of η scattering and N(1520) is weakly coupled to the ηN channel but are also from $N\eta$ production which is a S-D wave interference with the dominant N(1535) contribution (Arndt et al., 2005). Decay widths and branching ratios are also largely studied in these reactions.

c. Photoproduction: Since quite some missing resonances decoupled

from the pion nucleon elastic scattering escape detection because of their low helicity amplitudes, photoproduction brought us a new method of studying baryon spectrum. The missing ones may show up in photoproduction of multi-particle final states. And the cross sections for photoinduced reactions shows the structures of some baryon resonances. Photoproduction of pseudoscalar mesons include pions, η, $\eta^{'}$ and kaons; Photoproduction of multi-mesonic final states include vector mesons, like ρ, ω, ϕ. And these couplings to the nucleon can be described by the generalized parton distributions (GPDs) (Collins et al., 1997). γN production give us an access to the transverse and longitudinal helicity amplitudes of more
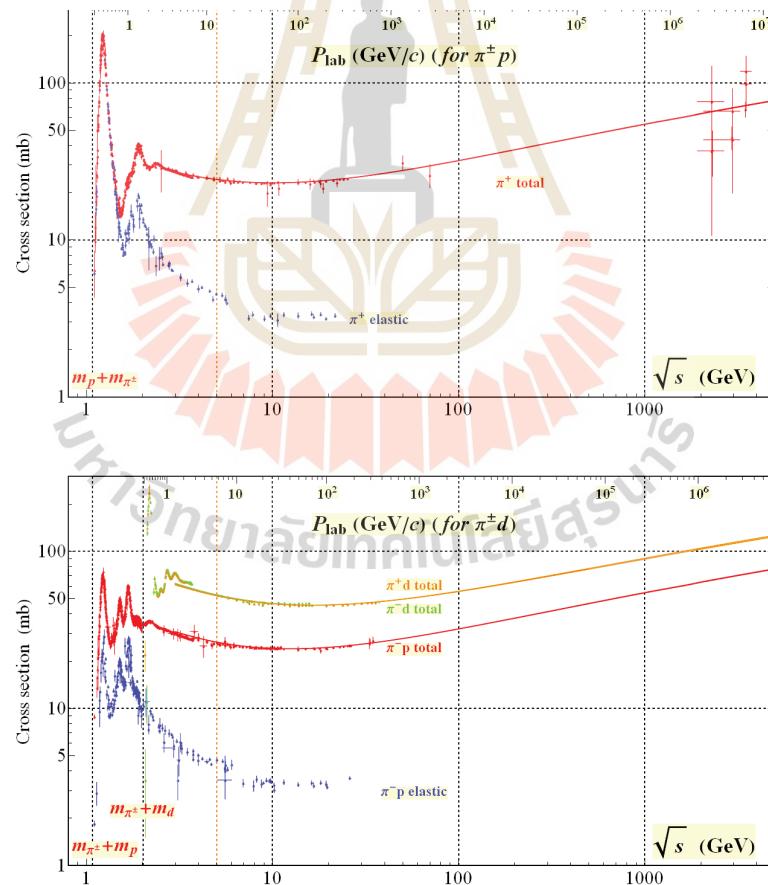
Figure 1.2 The total and elastic cross sections for $\pi^{\pm}$ scattering off protons.

resonances, roper for example, and photoproduction of η, $\eta^{'}$ mesons also show us the helicity amplitude of more resonances like N(1535) and N(1520).

d. Partial-wave analyses: Partial-wave analyse is a very important tool for determining masses, widths, and quantum numbers from the data of other methods, the helicity amplitudes it provided are indispensable complements for the complete information of the nucleon resonance. Most partial-wave analyses are performed at a few places only like SAID group (Arndt et al., 2008), MAID (Drechsel et al., 2007), EBAC (Juliá-Díaz et al., 2008), the Giessen model (Feuster and Mosel, 1999; Shyam et al., 2010) and the Bonn-Gatchina model (Anisovich et al., 2005).

By applying the above approaches, more baryon resonances have been discovered and confirmed and the internal structures of some resonance states have been revealed by the properties like Breit-Wigner amplitudes, transitions amplitudes, and form factors. In general, the theoretical models are also supposed to explain the experimental phenomena and data observed in the above production processes.

In this work, we propose to study the baryon spectrum, assuming that baryons consist of the q^3 component as well as the $q^4\overline{q}$ pentaquark component. The research takes an advantage from the fact that we are one of few research groups in the world, that is able to systematically construct the wave function of multi quark system. Permutation groups are applied to analyze the symmetries of different multi-quark system including baryon, meson, tetraquark and pentaquark, all possible quark configurations of the color, flavor, spin and spatial degrees of freedom are worked out in the language of permutation groups, and the corresponding wave functions are constructed systematically in the form of Yamanouchi basis. The spatial wave functions of various symmetries are derived

in the harmonic-oscillator interaction.

The existence of multiquark components in hadrons has been raised recently in quark models. For instance, the role of 5-quark components has been explored in the pion and electromagnetic decays and transition form factors of the $N_{1/2^+}(1440)$ resonance (Juliá-Díaz and Riska, 2006). It is also revealed, in our previous work on the annihilation reactions $\bar{p}p \to \phi X$ and also a number of works of others, that the proton may possess a considerable $q^4\bar{q}$ component. This thesis shows that the ordering problem of the Roper $N(1440)$, $N(1520)$ and $N(1535)$ may be solved by introducing the $q^4\bar{q}$ contribution.

a. Roper resonance

The Roper resonance $N(1440)1/2^+$ is a four-star resonance with pole mass ≈ 1.37 GeV and width ≈ 0.18 GeV (Burkert and Roberts, 2019). From the experimental results of Figure 1.3, the transverse helicity amplitudes of the transition $\gamma^*N \to P_{11}(1440)$ are calculated within the light-front relativistic quark model assuming that the $P_{11}(1440)$ is the first radial excitation of the q^3 ground state (Aznauryan, 2007). From the clear evidence in front, nowadays it's widely judged that the Roper is mainly the first radial excitation of the nucleon.

The experimental data on $A_{1/2}$ are taken from: circles [blue] -analysis of single-pion final states (Aznauryan et al., 2009); triangles [green] -analysis of $ep \to e'\pi^+\pi^-p'$ (Mokeev et al., 2008; Mokeev et al., 2016); square [black] -CLAS Collaboration result at the photoproduction point (Aznauryan et al., 2009); and triangle [black] -global average of this value (Tanabashi et al., 2018).

b. $N(1535)$ and $N(1520)$

A similar study of helicity amplitudes $A_{1/2}^P$ and $S_{1/2}^P$ for the electromagnetic transition $\gamma^*N \to N^*(1535)$ (Jido et al., 2008; An and Zou, 2009) showed $q^4\bar{q}$ component is more compact than q^3 component. The first one clearly shows
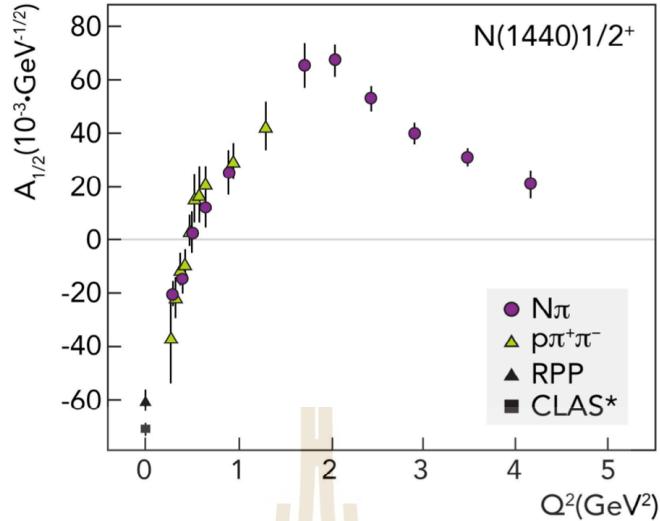
Figure 1.3 Experimental date of the transverse helicity amplitudes for Roper-resonance electroproduction $\gamma^* p \to N(1440)$

that the $A^p_{1/2}$ amplitude as a q^3 state is smaller than the experimental results, while An and Zou bring us a much better description of the empirical results by introducing $25\% \sim 65\%$ $q^4\bar{q}$ component. The decay width of $N(1535) \to N\eta$, $\Gamma_{N(1535) \to N\eta} \equiv (65 \pm 25\text{MeV})$ (Tanabashi et al., 2018) is as large as the decay width of $N(1535) \to N\pi$, $\Gamma_{N(1535) \to N\pi} \equiv (67.5 \pm 19\text{MeV})$ (Tanabashi et al., 2018), N(1535) must couple to the η meson much more strongly than predicted by flavor symmetry concluded from (Olbrich et al., 2018). Further more, only flavor symmetry can't describe the decays $N(1535) \to N\eta$ and $\Lambda(1670) \to \Lambda\eta$ in corresponding baryon octet $N(1535), \Lambda(1670), \Sigma(1620)$, while $N(1650) \to N\eta$ and $\Lambda(1800) \to \Lambda\eta$ in $N(1650), \Lambda(1800), \Sigma(1750)$ decays are in agreement with flavor symmetry. Like the study (Parganlija et al., 2013) about the pseudoscalar mixing angle of η and η', η is mixed by two pure pseudoscalar isosinglet states, $\eta_N \equiv (\bar{u}u + \bar{d}d)/\sqrt{2}$, $\eta_s \equiv \bar{s}s$ and $\theta_P \simeq -44.6°$, we believe that N(1535) could contain quite some amount of $uuds\bar{s}$ pentaquark component.

On the contrary to $N_{1/2^-}(1535)$, the S-D wave interference state

$N_{3/2^-}(1520)$ branching ratio of $\Gamma_{\eta N}/\Gamma_{tot}$ is less than 1% almost zero. While the study of $N_{3/2^-}(1520)$ which was reported in 2014 by the CBELSA/TAPS Collaboration (Hartmann et al., 2014) still did not draw the final conclusion, however (Ramalho and Pena, 2017) states that $\gamma N \to N(1520)$ form factors are dominated by the meson cloud contributions which means N(1520) may not be pure q^3 state as well. So we believe that N(1520) could couple to non strange pentaquark state.

This thesis is organized as follows. The construction of wave function of multi quark system are in Chapter II and the details are presented in Appendix B. All possible quark configurations of the color, flavor, spin and spatial degrees of freedom are worked out in the language of permutation groups, and the corresponding wave functions are constructed systematically in the form of Yamanouchi basis. We estimation of the mass of low-lying q^3 states, low-lying light $q^4\bar{q}$ and hidden heavy pentaquark states in Chapter III. The ordering problem of the Roper, N(1535)and N(1520) are also discussed in this section. Chapter IV discussed the possibility that N(1685) could be the lowest pentaquark state. Finally, the conclusions are given in Chapter V.

CHAPTER II

CONSTRUCTION OF WAVE FUNCTION OF

MULTI QUARK SYSTEM

2.1 q^3, q^2Q Baryon Wave Functions

Permutation groups are applied to analyze the symmetries of baryon and pentaquark states. All possible quark configurations of the color, flavor, spin and spatial degrees of freedom are worked out in the language of permutation groups, and the corresponding wave functions are constructed systematically in the form of Yamanouchi basis. Here we present the ground q^3 baryon states for example, the total wave function consists of the color, spatial, spin and flavor parts.

$$
\begin{aligned}
\Psi^{(q^3)}_{Octet} &= \frac{1}{\sqrt{2}}\psi^c_{[111]}\psi^o_{[3]}(\phi_{[21]_\lambda}\chi_{[21]_\lambda} + \phi_{[21]_\rho}\chi_{[21]_\rho}), \\
\Psi^{(q^3)}_{Decuplet} &= \psi^c_{[111]}\psi^o_{[3]}\phi_{[3]sym}\chi_{[3]sym}
\end{aligned}
\tag{2.1}
$$

Where ψ^c, ψ^o, ϕ and χ are respectively the color, spatial, flavor and spin parts of the q^3 cluster, same notation for pentaquark as well, and the specific wave function in form of Yamanouchi basis as,

$$
\begin{aligned}
\phi_{[21]_\lambda} &= \frac{1}{\sqrt{6}}(2uud - duu - udu), \quad \phi_{[21]_\rho} = \frac{1}{\sqrt{2}}(udu - duu), \\
\chi_{[21]_\lambda} &= \frac{1}{\sqrt{6}}(2\uparrow\uparrow\downarrow - \downarrow\uparrow\uparrow - \uparrow\downarrow\uparrow), \quad \chi_{[21]_\rho} = \frac{1}{\sqrt{2}}(\uparrow\downarrow\uparrow - \downarrow\uparrow\uparrow),
\end{aligned}
\tag{2.2}
$$

$$
\phi_{[3]sym} = \frac{1}{\sqrt{3}}(uud + duu + udu), \quad \chi_{[3]sym} = \uparrow\uparrow\uparrow,
\tag{2.3}
$$

$$\Psi^c_{[111]} = \frac{1}{\sqrt{6}} \left[(RG - GR)B + (GB - BG)R + (BR - RB)G \right] \quad (2.4)$$

The spatial wave functions of various symmetries, which are derived in the harmonic-oscillator interaction are described in are applied as complete bases to evaluate the low-lying baryon resonances. The detailed are shown in Section 2.3.

The heavy baryon which includes two light quarks and one single charm quark or bottom quark q^2Q has the same color wave function as the low-lying baryons. Requiring the q^2 in the heavy baryon to be antisymmetric, the general wave functions are,

$$\Psi^{(q^2)}_{[2]_A} = \Psi^c_{[11]} \Psi^{sf}_{[x]_s},$$
$$\Psi^{sf}_{[x]_s} = \sum_{i,j=S,A} a_{ij} \Psi^s_{[X]_i} \Psi^f_{[Y]_j} \quad (2.5)$$

The possible $\Psi^{(q^2)}_{sf}$ wave function are,

$$\Psi^{sf}_{[x]_s} = \Psi^s_{[2]_S} \Psi^f_{[2]_S}, \ \Psi^s_{[11]_A} \Psi^f_{[11]_A} \quad (2.6)$$

So the total q^2Q wave function is the coupling of $\Psi^{sf}_{[x]_s}$ with the single heavy quark, which is,

$$\Psi(q^2Q) = \Psi^c_{[111]} \Psi^o_{[3]} \ \left(\Psi(q^2)^{sf}_{[x]_s} \ \otimes \ \Psi(Q)^{sf} \right) \quad (2.7)$$

2.2 $q^4\bar{q}$, $q^3Q\bar{Q}$ Pentaquark Wave Functions

The Young tabloid construction of the $q^4\bar{q}$ configuration is shown as,

The total wave function of the q^4 configuration may be written in the general form,

$$\Psi_{total} \quad = \quad \sum_{i,j=\rho,\lambda,\eta} a_{ij} \; \psi^c_{[211]_i} \psi^{osf}_{[31]_j}, \tag{2.8}$$

with

$$\psi^{osf}_{[31]_{\rho,\lambda,\eta}} \quad = \quad \sum_{i,j=S,A,\rho,\lambda,\eta} b_{ij} \psi^o_{[X]_i} \psi^{sf}_{[Y]_j},$$
$$\psi^{sf}_{[Y]} \quad = \quad \sum_{i,j=S,A,\rho,\lambda,\eta} c_{ij} \psi^s_{[x]_i} \psi^f_{[y]_j}, \tag{2.9}$$

where ψ^c, ψ^{osf}, ψ^{sf}, ψ^s, and ψ^f are respectively the color, spatial-spin-flavor, spin-flavor, spin, and flavor parts of the q^4 cluster. S, A, ρ, λ, and η stand for fully symmetric, fully antisymmetric, ρ-type, λ-type, and η-type functions. The coefficients in Eqs. (2.8) and (2.9) can be determined by enacting the permutations (12), (23) and (34) of the S_4 group on both sides of the general wave functions. The fully antisymmetric wave function for the q^4 configuration is worked out as

$$\psi = \frac{1}{\sqrt{3}} \left(\psi^c_{[211]_\lambda} \psi^{osf}_{[31]_\rho} - \psi^c_{[211]_\rho} \psi^{osf}_{[31]_\lambda} + \psi^c_{[211]_\eta} \psi^{osf}_{[31]_\eta} \right) \tag{2.10}$$

After solving the general equations, the coefficients of all general wave functions can be decided. The detailed configurations of the spatial-spin-flavor as well as spin-flavor wave functions are worked out in the form of a Yamanouchi basis, as shown in Appendix A.

All possible spatial-spin-flavor configurations in the form of Yamanouchi basis are showed in Table 2.1 and q^4 configuration all possible spin-flavor configurations in Table 2.2:

Table 2.1 All possible spatial spin flavor configurations q^4 in permutation symmetry.

$[31]_{OSF}$	
$[4]_O$	$[31]_{SF}$
$[1111]_O$	$[211]_{SF}$
$[22]_O$	$[31]_{SF}, [211]_{SF}$
$[211]_O$	$[31]_{SF}, [211]_{SF}, [22]_{SF}, [1111]_{SF}$
$[31]_O$	$[4]_{SF}, [31]_{SF}, [211]_{SF}, [22]_{SF}$

Table 2.2 All possible spin-flavor configurations of q^4 in permutation symmetry.

$[4]_{FS}$			
$[4]_{FS}[22]_F[22]_S$	$[4]_{FS}[31]_F[31]_S$	$[4]_{FS}[4]_F[4]_S$	
$[31]_{FS}$			
$[31]_{FS}[31]_F[22]_S$	$[31]_{FS}[31]_F[31]_S$	$[31]_{FS}[31]_F[4]_S$	$[31]_{FS}[211]_F[22]_S$
$[31]_{FS}[211]_F[31]_S$	$[31]_{FS}[22]_F[31]_S$	$[31]_{FS}[4]_F[31]_S$	
$[22]_{FS}$			
$[22]_{FS}[22]_F[22]_S$	$[22]_{FS}[22]_F[4]_S$	$[22]_{FS}[4]_F[22]_S$	$[22]_{FS}[211]_F[31]_S$
$[22]_{FS}[31]_F[31]_S$			
$[211]_{FS}$			
$[211]_{FS}[211]_F[22]_S$	$[211]_{FS}[211]_F[31]_S$	$[211]_{FS}[211]_F[4]_S$	$[211]_{FS}[22]_F[31]_S$
$[211]_{FS}[31]_F[22]_S$	$[211]_{FS}[31]_F[31]_S$		
$[1111]_{FS}$			
$[1111]_{FS}[211]_F[31]_S$	$[1111]_{FS}[22]_F[22]_S$		

2.3 Spatial Wave Function

Here we introduce jacobi coordinates, a complete basis of certain symmetry may be constructed with q^3 systems in the harmonic oscillator interaction.

$$H = \frac{p_\lambda^2}{2m} + \frac{p_\rho^2}{2m} + \frac{1}{2}C\left(\lambda^2 + \rho^2\right) \tag{2.11}$$

where

$$\vec{\rho} = \frac{1}{\sqrt{2}}(\vec{r_1} - \vec{r_2}) \quad \vec{\lambda} = \frac{1}{\sqrt{6}}(\vec{r_1} + \vec{r_2} - 2\vec{r_3}) \tag{2.12}$$

In the center of mass system, with $\vec{R} = 1/\sqrt{3}(\vec{r_1} + \vec{r_2} + \vec{r_3})$, we have:

$$\vec{r_{12}} = \sqrt{2}\vec{\rho} \quad \vec{r_{13}} = \frac{1}{\sqrt{2}}(\vec{\rho} + \sqrt{3}\vec{\lambda}) \quad \vec{r_{23}} = \frac{1}{\sqrt{2}}(-\vec{\rho} + \sqrt{3}\vec{\lambda}) \tag{2.13}$$

The spatial wave functions of the q^3 as well as the subsystem of $q^3 Q\bar{Q}$ pentaquarks with the permutation symmetries $[3]_S$ are listed in Table C.1 from Appendix C up to $N' = 22$, where l_ρ, l_λ, and are L' are limited to 0, 1 and 2 only. Note that we have set $M' = 0$ and used the abbreviation,

$$\sum_{\{n_i, l_i, m_i\}} C_{n_\rho, l_\rho, m_\rho, n_\lambda, l_\lambda, m_\lambda} \psi_{n_\rho l_\rho m_\rho}(\vec{\rho}) \psi_{n_\lambda l_\lambda m_\lambda}(\vec{\lambda})$$

$$\equiv \sum_{\{n_i, l_i\}} C_{n_\rho, l_\rho, n_\lambda, l_\lambda} \psi(n_\rho, l_\rho, n_\lambda, l_\lambda)$$

$$\equiv \sum_{\{n_i, l_i\}} C_{n_\rho, l_\rho, n_\lambda, l_\lambda} (n_\rho, l_\rho, n_\lambda, l_\lambda) \tag{2.14}$$

with $N = 2(n_\lambda + n_\rho) + l_\lambda + l_\rho$ and $\Psi_{n_r l_r m_r}(r) = R_{n_r l_r}(r) Y_{l_r m_r}(\hat{r})$, where the state function reads,

$$R_{nl}(r) = \left[\frac{2\alpha^3 n!}{\Sigma(n + l + 3/2)}\right]^{1/2} (\alpha r)^l e^{-\frac{1}{2}\alpha^2 r^2} L_n^{l+1/2}(\alpha^2 r^2) \tag{2.15}$$

where $L_n^{l+1/2}$ are the associated Laguerre polynomials. The q^3 spatial wave function of different permutation symmetry are specified in Appendix C and all of them correspond to the real harmonic oscillator band.

14

We construct the spatial wave functions of the $q^4\bar{q}$ pentaquark systems in the harmonic oscillator potential for the quark-quark interaction. The relative Jacobi coordinates and the corresponding momenta may be defined respectively as

$$
\begin{aligned}
\vec{x}_i &= \frac{i}{\sqrt{i+i^2}}\left(\frac{\sum_{j=1}^{i} m_j \vec{r}_j}{m_1 + m_2 + ...m_i} - \vec{r}_{i+1}\right), \\
\vec{p}_i &= u_i \frac{d\vec{x}_i}{dt},
\end{aligned}
\tag{2.16}
$$

where u_i are the reduced quark masses defined as

$$
u_i = \frac{(i+1)(\sum_{j=1}^{i} m_j)m_{i+1}}{i \sum_{j=1}^{i+1} m_j}, i = 1, 2, 3, 4
\tag{2.17}
$$

where $\vec{r}_j$ and m_j are the coordinate and mass of the jth quark. We assign x_1, x_2, x_3, and x_4 to be ρ, λ, η, and ξ Jacobi coordinates, respectively.

We start from the q^4 cluster. The q^4 spatial wave function, coupling among the ρ, λ, and η harmonic oscillator wave functions, may take the general form,

$$
\begin{aligned}
\psi_{N'L'M'}^{q^4[X]_y} &= \sum_{\{n_i,l_i\}} A(n_\rho, n_\lambda, n_\eta, l_\rho, l_\lambda, l_\eta) \\
&\quad \times \psi_{n_\rho l_\rho}(\vec{\rho}) \otimes \psi_{n_\lambda l_\lambda}(\vec{\lambda}) \otimes \psi_{n_\eta l_\eta}(\vec{\eta}) \\
&= \sum_{\{n_i,l_i,m_i\}} C_{n_\rho,l_\rho,m_\rho,n_\lambda,l_\lambda,m_\lambda,n_\eta,l_\eta,m_\eta} \\
&\quad \times \psi_{n_\rho l_\rho m_\rho}(\vec{\rho})\psi_{n_\lambda l_\lambda m_\lambda}(\vec{\lambda})\psi_{n_\eta l_\eta m_\eta}(\vec{\eta})
\end{aligned}
\tag{2.18}
$$

where $\psi_{n_i l_i m_i}$ are just harmonic oscillator wave functions and the sum $\{n_i, l_i\}$ is over $n_\rho, n_\lambda, n_\eta, l_\rho, l_\lambda, l_\eta$. N', L', and M' are respectively the total principle quantum number, total angular momentum, and magnetic quantum number of the q^4 cluster. One has $N' = (2n_\rho + l_\rho) + (2n_\lambda + l_\lambda) + (2n_\eta + l_\eta)$ and $\Psi_{n_r l_r m_r}(r) = R_{n_r l_r}(r)Y_{l_r m_r}(\hat{r})$, the definition of the state functions are the same as the ones in 3q states. The $[X]$ and y in the superscript $[X]_y$ represent the irreducible representation $[X]$ and the y-type symmetry of the representation.

The coupling coefficients $A(n_\rho, n_\lambda, n_\eta, l_\rho, l_\lambda, l_\eta)$ as well as $C_{n_\rho, l_\rho, m_\rho, n_\lambda, l_\lambda, m_\lambda, n_\eta, l_\eta, m_\eta}$ shall be determined according to the $[X]_y$, where the representation matrices of the permutations of the S_4 group are applied to both sides of the general form. The explicit forms of the spatial wave functions for the q^4 cluster are presented in Appendix C for the permutation symmetries $\{[4]_S\}$. To save space, the other possible permutation symmetries $\{[31]_{\rho,\lambda,\eta}, [211]_{\rho,\lambda,\eta}$ and $[22]_{\rho,\lambda}\}$ will not be specified here.

The spatial wave function of pentaquark states is simply the product of the q^4 wave function and the harmonic oscillator wave function for the fourth Jacobi coordinate ξ, where the antiquark is assigned the coordinate $\vec{r}_5$. The permutation symmetry of pentaquarks is simply represented by the q^4 cluster since $\psi_{n_\xi, l_\xi}(\vec{\xi})$ is fully symmetric for any permutation between quarks. The total spatial wave function of pentaquarks may take the form,

$$\Psi_{NLM}^{[X]_y} = \psi_{N'L'M'}^{q^4[X]_y} \otimes \psi_{n_\xi, l_\xi}(\vec{\xi}) \tag{2.19}$$

where $\psi_{n_\xi, l_\xi}(\vec{\xi})$ are the harmonic oscillator functions for the Jacobi coordinate ξ and $[X]_y$ stand for all possible permutation symmetries of the q^4 cluster, that is, $[X]_y = \{[4]_S, [31]_{\rho,\lambda,\eta}, [211]_{\rho,\lambda,\eta}, [22]_{\rho,\lambda}\}$. N, L, and M are respectively the total principle quantum number, total angular momentum and magnetic quantum number of the pentaquark, with

$$N = 2n_\rho + l_\rho + 2n_\lambda + l_\lambda + 2n_\eta + l_\eta + 2n_\xi + l_\xi \tag{2.20}$$

In principle, one can construct the spatial wave functions of pentaquarks to any order by applying the representation matrices of the permutations of the S_4 group to the general form in Eq. (2.18). Though we have been dealing with a system where the quark-quark potential is the harmonic oscillator interaction, the spatial wave functions grouped in this work according to the permutation symme-

try can be employed as complete bases to study a system with other interactions.

The spatial wave functions of pentaquarks with the q^4 symmetry $[4]_S$ are shown in Table 2.3, where $\psi^{q^4}_{N'L'M'}$ ($L' = M' = 0$) and $\psi_{n_\xi, l_\xi}(\vec{\xi})$ ($l_\xi = 0$) are the spatial wave functions of the q^4 subsystem and the harmonic oscillator wave function for the $\vec{\xi}$ coordinate, respectively.

Table 2.3 Pentaquark spatial wave functions of symmetric type with principle quantum number, $N \leq 14$.

$\Psi^{q^4\bar{q}}_{000_{[4]_S}}$	$\psi^{q^4}_{000_{[4]_S}}\psi_{0,0}(\vec{\xi})$
$\Psi^{q^4\bar{q}}_{200_{[4]_S}}$	$\psi^{q^4}_{200_{[4]_S}}\psi_{0,0}(\vec{\xi}),\ \psi^{q^4}_{000_{[4]_S}}\psi_{1,0}(\vec{\xi})$
$\Psi^{q^4\bar{q}}_{400_{[4]_S}}$	$\psi^{q^4}_{400_{[4]_S}}\psi_{0,0}(\vec{\xi}),\ \psi^{q^4}_{200_{[4]_S}}\psi_{1,0}(\vec{\xi}),\ \psi^{q^4}_{000_{[4]_S}}\psi_{2,0}(\vec{\xi})$
$\Psi^{q^4\bar{q}}_{600_{[4]_S}}$	$\psi^{q^4}_{600_{[4]_S}}\psi_{0,0}(\vec{\xi}),\ \psi^{q^4}_{400_{[4]_S}}\psi_{1,0}(\vec{\xi}),\ \psi^{q^4}_{200_{[4]_S}}\psi_{2,0}(\vec{\xi}),\ \psi^{q^4}_{000_{[4]_S}}\psi_{3,0}(\vec{\xi})$
$\Psi^{q^4\bar{q}}_{800_{[4]_S}}$	$\psi^{q^4}_{800_{[4]_S}}\psi_{0,0}(\vec{\xi}),\ \psi^{q^4}_{600_{[4]_S}}\psi_{1,0}(\vec{\xi}),\ \psi^{q^4}_{400_{[4]_S}}\psi_{2,0}(\vec{\xi}),\ \psi^{q^4}_{200_{[4]_S}}\psi_{3,0}(\vec{\xi}),$ $\psi^{q^4}_{000_{[4]_S}}\psi_{4,0}(\vec{\xi})$
$\Psi^{q^4\bar{q}}_{1000_{[4]_S}}$	$\psi^{q^4}_{1000_{[4]_S}}\psi_{0,0}(\vec{\xi}),\ \psi^{q^4}_{800_{[4]_S}}\psi_{1,0}(\vec{\xi}),\ \psi^{q^4}_{600_{[4]_S}}\psi_{2,0}(\vec{\xi}),\ \psi^{q^4}_{400_{[4]_S}}\psi_{3,0}(\vec{\xi}),$ $\psi^{q^4}_{200_{[4]_S}}\psi_{4,0}(\vec{\xi}),\ \psi^{q^4}_{000_{[4]_S}}\psi_{5,0}(\vec{\xi})$
$\Psi^{q^4\bar{q}}_{1200_{[4]_S}}$	$\psi^{q^4}_{1200_{[4]_S}}\psi_{0,0}(\vec{\xi}),\ \psi^{q^4}_{1000_{[4]_S}}\psi_{1,0}(\vec{\xi}),\ \psi^{q^4}_{800_{[4]_S}}\psi_{2,0}(\vec{\xi}),\ \psi^{q^4}_{600_{[4]_S}}\psi_{3,0}(\vec{\xi}),$ $\psi^{q^4}_{400_{[4]_S}}\psi_{4,0}(\vec{\xi}),\ \psi^{q^4}_{200_{[4]_S}}\psi_{5,0}(\vec{\xi}),\ \psi^{q^4}_{000_{[4]_S}}\psi_{6,0}(\vec{\xi})$
$\Psi^{q^4\bar{q}}_{1400_{[4]_S}}$	$\psi^{q^4}_{1400_{[4]_S}}\psi_{0,0}(\vec{\xi}),\ \psi^{q^4}_{1200_{[4]_S}}\psi_{1,0}(\vec{\xi}),\ \psi^{q^4}_{1000_{[4]_S}}\psi_{2,0}(\vec{\xi}),\ \psi^{q^4}_{800_{[4]_S}}\psi_{3,0}(\vec{\xi}),$ $\psi^{q^4}_{600_{[4]_S}}\psi_{4,0}(\vec{\xi}),\ \psi^{q^4}_{400_{[4]_S}}\psi_{5,0}(\vec{\xi}),\ \psi^{q^4}_{200_{[4]_S}}\psi_{6,0}(\vec{\xi}),\ \psi^{q^4}_{000_{[4]_S}}\psi_{7,0}(\vec{\xi})$

We construct the spatial wave functions of $q^3Q\bar{Q}$ systems in the harmonic oscillator potential for the quark-quark interaction. A new set of relative Jacobi coordinates was introduced for the $q^3Q\bar{Q}$ system, different from the ones for $q^4\bar{q}$ system, the Hamiltonian for the harmonic oscillator potential is written as

$$H_{q^3Q^2} = \frac{\vec{p_\lambda}^2}{2m} + \frac{\vec{p_\rho}^2}{2m} + \frac{\vec{p_\sigma}^2}{2M} + \frac{\vec{p_\chi}^2}{2u_\chi} + 5C(\vec{\lambda}^2 + \vec{\rho}^2 + \vec{\sigma}^2 + \vec{\chi}^2) \tag{2.21}$$

with u_χ being the reduced quark mass of the fourth Jacobi coordinate, defined as $u_\chi = \frac{5mM}{3m+2M}$, m and M are the mass of light quark and heavy quark respectively. C is the coupling constant, and the relative Jacobi coordinates and the corresponding momenta are defined respectively as

$$\vec{\rho} = \frac{1}{\sqrt{2}}(\vec{r}_1 - \vec{r}_2) \quad \vec{\lambda} = \frac{1}{\sqrt{6}}(\vec{r}_1 + \vec{r}_2 - 2\vec{r}_3)$$

$$\vec{\sigma} = \frac{1}{\sqrt{2}}(\vec{r}_4 - \vec{r}_5) \quad \vec{\chi} = \frac{1}{\sqrt{30}}(2(\vec{r}_1 + \vec{r}_2 + \vec{r}_3) - 3(\vec{r}_4 + \vec{r}_5))$$

$$\vec{p_\rho} = \frac{1}{\sqrt{2}}(\vec{p}_1 - \vec{p}_2) \quad \vec{p_\lambda} = \frac{1}{\sqrt{6}}(\vec{p}_1 + \vec{p}_2 - 2\vec{p}_3) \quad \vec{p_\sigma} = \frac{1}{\sqrt{2}}(\vec{p}_4 - \vec{p}_5)$$

$$\vec{p_\chi} = \frac{\sqrt{5}}{\sqrt{6}}\left(\frac{2M(\vec{p}_1 + \vec{p}_2 + \vec{p}_3) - 3m(\vec{p}_4 + \vec{p}_5)}{3m + 2M}\right)$$

where $\vec{p}_i$ and $\vec{r}_i$ are the momenta and coordinate of ith quark, the antiquark is assigned the coordinate $\vec{r}_5$, the fourth and fifth quark form the third Jacobi coordinate σ and the centers of first three quarks and the last two heavy quarks form the fourth Jacobi coordinate χ. The permutation symmetry of pentaquarks is simply represented by the q^3 cluster since the $\psi_{n_\sigma,l_\sigma}(\vec{\sigma})$ and $\psi_{n_\chi,l_\chi}(\vec{\chi})$ is fully symmetric for any permutation between quarks. The total spatial wave function of pentaquarks may take the form,

$$\Psi_{NLM}^{[X]_y} = \psi_{N'L'M'}^{q^3[X]_y} \otimes \psi_{n_\sigma,l_\sigma}(\vec{\sigma}) \otimes \psi_{n_\chi,l_\chi}(\vec{\chi}) \tag{2.22}$$

which is simply the product of the q^3 spatial wave function shown in Table C.1 and the harmonic oscillator wave functions $\psi_{n_\sigma,l_\sigma}(\vec{\sigma})$ and $\psi_{n_\chi,l_\chi}(\vec{\chi})$ for the Jacobi coordinate σ and χ. $[X]_y$ stands for all possible permutation symmetries of the q^3 cluster, where, $[X]_y = \{[3]_S, [21]_{\rho,\lambda}, [111]_A\}$. N, L, and M are respectively the total principle quantum number, total angular momentum and magnetic quantum

Table 2.4 $q^3Q\bar{Q}$ pentaquark spatial wave functions of symmetric type.

$\Psi_{000_{[5]_S}}^{q^3Q\bar{Q}}$	$\psi_{000_{[3]_S}}^{q^3}\psi_{0,0}(\vec{\sigma})\psi_{0,0}(\vec{\chi})$
$\Psi_{200_{[5]_S}}^{q^3Q\bar{Q}}$	$\psi_{200_{[3]_S}}^{q^3}\psi_{0,0}(\vec{\sigma})\psi_{0,0}(\vec{\chi}),\ \psi_{000_{[3]_S}}^{q^3}\psi_{1,0}(\vec{\sigma})\psi_{0,0}(\vec{\chi}),\ \psi_{000_{[3]_S}}^{q^3}\psi_{0,0}(\vec{\sigma})\psi_{1,0}(\vec{\chi})$
$\Psi_{400_{[5]_S}}^{q^3Q\bar{Q}}$	$\psi_{400_{[3]_S}}^{q^3}\psi_{0,0}(\vec{\sigma})\psi_{0,0}(\vec{\chi}),\ \psi_{200_{[3]_S}}^{q^3}\psi_{1,0}(\vec{\sigma})\psi_{0,0}(\vec{\chi}),\ \psi_{200_{[3]_S}}^{q^3}\psi_{0,0}(\vec{\sigma})\psi_{1,0}(\vec{\chi}),$
	$\psi_{000_{[3]_S}}^{q^3}\psi_{2,0}(\vec{\sigma})\psi_{0,0}(\vec{\chi}),\psi_{000_{[3]_S}}^{q^3}\psi_{1,0}(\vec{\sigma})\psi_{1,0}(\vec{\chi}),\ \psi_{000_{[3]_S}}^{q^3}\psi_{0,0}(\vec{\sigma})\psi_{1,0}(\vec{\chi})$
$\Psi_{600_{[5]_S}}^{q^3Q\bar{Q}}$	$\psi_{600_{[3]_S}}^{q^3}\psi_{0,0}(\vec{\sigma})\psi_{0,0}(\vec{\chi}),\ \psi_{400_{[3]_S}}^{q^3}\psi_{1,0}(\vec{\sigma})\psi_{0,0}(\vec{\chi}),\ \psi_{400_{[3]_S}}^{q^3}\psi_{0,0}(\vec{\sigma})\psi_{1,0}(\vec{\chi}),$
	$\psi_{200_{[3]_S}}^{q^3}\psi_{2,0}(\vec{\sigma})\psi_{0,0}(\vec{\chi}),\ \psi_{200_{[3]_S}}^{q^3}\psi_{1,0}(\vec{\sigma})\psi_{1,0}(\vec{\chi}),\ \psi_{200_{[3]_S}}^{q^3}\psi_{0,0}(\vec{\sigma})\psi_{2,0}(\vec{\chi}),$
	$\psi_{000_{[3]_S}}^{q^3}\psi_{3,0}(\vec{\sigma})\psi_{0,0}(\vec{\chi}),\ \psi_{000_{[3]_S}}^{q^3}\psi_{2,0}(\vec{\sigma})\psi_{1,0}(\vec{\chi}),\ \psi_{000_{[3]_S}}^{q^3}\psi_{1,0}(\vec{\sigma})\psi_{2,0}(\vec{\chi}),$
	$\psi_{000_{[3]_S}}^{q^3}\psi_{0,0}(\vec{\sigma})\psi_{3,0}(\vec{\chi})$
$\Psi_{800_{[5]_S}}^{q^3Q\bar{Q}}$	$\psi_{800_{[3]_S}}^{q^3}\psi_{0,0}(\vec{\sigma})\psi_{0,0}(\vec{\chi}),\ \psi_{600_{[3]_S}}^{q^3}\psi_{1,0}(\vec{\sigma})\psi_{0,0}(\vec{\chi}),\ \psi_{600_{[3]_S}}^{q^3}\psi_{0,0}(\vec{\sigma})\psi_{1,0}(\vec{\chi}),$
	$\psi_{400_{[3]_S}}^{q^3}\psi_{2,0}(\vec{\sigma})\psi_{0,0}(\vec{\chi}),\ \psi_{400_{[3]_S}}^{q^3}\psi_{1,0}(\vec{\sigma})\psi_{1,0}(\vec{\chi}),\ \psi_{400_{[3]_S}}^{q^3}\psi_{0,0}(\vec{\sigma})\psi_{2,0}(\vec{\chi}),$
	$\psi_{200_{[3]_S}}^{q^3}\psi_{3,0}(\vec{\sigma})\psi_{0,0}(\vec{\chi}),\ \psi_{200_{[3]_S}}^{q^3}\psi_{2,0}(\vec{\sigma})\psi_{1,0}(\vec{\chi}),\ \psi_{200_{[3]_S}}^{q^3}\psi_{1,0}(\vec{\sigma})\psi_{2,0}(\vec{\chi}),$
	$\psi_{200_{[3]_S}}^{q^3}\psi_{0,0}(\vec{\sigma})\psi_{3,0}(\vec{\chi}),\ \psi_{000_{[3]_S}}^{q^3}\psi_{4,0}(\vec{\sigma})\psi_{0,0}(\vec{\chi}),\ \psi_{000_{[3]_S}}^{q^3}\psi_{3,0}(\vec{\sigma})\psi_{1,0}(\vec{\chi}),$
	$\psi_{000_{[3]_S}}^{q^3}\psi_{2,0}(\vec{\sigma})\psi_{2,0}(\vec{\chi}),\ \psi_{000_{[3]_S}}^{q^3}\psi_{1,0}(\vec{\sigma})\psi_{3,0}(\vec{\chi}),\ \psi_{000_{[3]_S}}^{q^3}\psi_{0,0}(\vec{\sigma})\psi_{4,0}(\vec{\chi})$

number of the pentaquark ($l_\sigma = 0$, $l_\chi = 0$), with

$$N = 2n_\rho + l_\rho + 2n_\lambda + l_\lambda + 2n_\sigma + l_\sigma + 2n_\chi + l_\chi \qquad (2.23)$$

The spatial wave functions of pentaquarks with the $q^3Q\bar{Q}$ symmetry $[5]_S$ are listed in the Table 2.4 (Up to $N = 14$ energy level is sufficient for the numerical calculations), where $\psi_{N'L'M'}^{q^3}$ ($L' = M' = 0$) and $\psi_{n_\sigma,l_\sigma}(\vec{\sigma})$ ($l_\sigma = 0$), $\psi_{n_\chi,l_\chi}(\vec{\chi})$ ($l_\chi = 0$) are the spatial wave functions of the q^3 subsystem and the harmonic oscillator wave function for the $\vec{\sigma}$ and $\vec{\chi}$ coordinates, respectively. Without any limitation for n_σ and n_χ, all degenerate states of each pentaquark energy level up to $N = 14$ served as a complete basis. $N \leq 8$ states are listed below, the higher ones follow the rule that $N = N_{q^3} + 2(n_\sigma + n_\chi)$.

CHAPTER III

ESTIMATION OF THE MASS OF

LOW-LYING Q^3 STATES AND GROUND

STATE PENTAQUARKS

3.1 Constituent Quark Model and Model Parameters

We apply, as complete bases, the full wave functions of pentaquarks worked out in the previous section to study the pentaquark system described by the Hamiltonian,

$$
\begin{aligned}
H &= H_0 + H_{hyp}^{OGE}, \\
H_0 &= \sum_{k=1}^{N} (m_k + \frac{p_k^2}{2m_k}) + \sum_{i<j}^{N} (-\frac{3}{8}\lambda_i^C \cdot \lambda_j^C)(A_{ij} r_{ij} - \frac{B_{ij}}{r_{ij}}), \\
H_{hyp}^{OGE} &= -C_{OGE} \sum_{i<j} \frac{\lambda_i^C \cdot \lambda_j^C}{m_i m_j} \vec{\sigma}_i \cdot \vec{\sigma}_j,
\end{aligned}
\tag{3.1}
$$

where A_{ij} and B_{ij} are mass dependent coupling parameters, taking the form,

$$
A_{ij} = a\sqrt{\frac{m_{ij}}{m_u}}, \quad B_{ij} = b\sqrt{\frac{m_u}{m_{ij}}}
\tag{3.2}
$$

with m_{ij} being the reduced mass of ith and jth quarks, defined as $m_{ij} = \frac{m_i m_j}{m_i + m_j}$. The hyperfine interaction, H_{hyp}^{OGE} includes only one-gluon exchange contribution, where $C_{OGE} = C_m m_u^2$, with m_u being the constituent u quark mass and C_m a constant. λ_i^C in the above equations are the generators of color SU(3) group. Refer the detailed calculations of hyperfine contributions in different configurations in Appendix A.

The model parameters are determined by fitting the theoretical results to the experimental data of the mass of all the ground state baryons, namely, eight light baryon isospin states, seven charm baryon states, and six bottom baryon states as well as light baryon resonances of energy level $N \leq 2$, including the first radial excitation state $N(1440)$ with mass at 1.5 GeV and a number of orbital excited $l = 1$ and $l = 2$ baryons. All these baryons are believed to be mainly $3q$ states whose masses were taken from Particle Data Group (Tanabashi et al., 2018). The least squares method is applied to minimize the weighted squared distance δ^2,

$$\delta^2 = \sum_{i=1}^{N} \omega_i \frac{(M^{exp} - M^{cal})^2}{M^{exp^2}} \tag{3.3}$$

where ω_i are weights being 1 for all the states except for N(939) and $\Delta(1232)$ which are set to be 100, M^{exp} and M^{cal} are respectively the experimental and theoretical masses. M^{exp} are taken from PDG (Tanabashi et al., 2018). Listed in Tables 3.1, 3.2, 3.3, and 3.4 are the theoretical masses which are calculated in the Hamiltonian in Eq. (3.1) in the q^3 picture and fitted to the experimental data. The last column in Table 3.1 shows the deviation between the experimental and theoretical mean values, $D = 100 \cdot (M^{exp} - M^{cal})/M^{exp}$. Possible assignments of the theoretical results of excited nucleon and Δ resonances below 2.2 GeV to all the known baryon states are presented in Tables 3.2, 3.3, and 3.4 following the $SU(6)_{SF}$ representations. The orbital-spin-flavor wave functions of q^3 baryon states are listed in Appendix B.

The 3 model coupling constants and 4 constituent quark masses are fitted,

$$m_u = m_d = 327 \text{ MeV} , \quad m_s = 498 \text{ MeV} ,$$

$$m_c = 1642 \text{ MeV} , \quad m_b = 4960 \text{ MeV} ,$$

$$C_m = 18.3 \text{ MeV} , \quad a = 49500 \text{ MeV}^2 , \quad b = 0.75$$

Table 3.1 Ground state baryons applied to fit the model parameters.

Baryon	M^{exp}(MeV)	M^{cal}(MeV)	D (%)
N(939)	939	939	0
$\Delta(1232)$	1232	1232	0
$\Lambda(1116)$	1116	1129	-1.16
$\Sigma(1193)$	1193	1163	2.56
$\Sigma^*(1385)$	1385	1372	0.97
$\Xi(1318)$	1318	1329	-0.83
$\Xi^*(1530)$	1533	1510	1.49
$\Omega(1672)$	1672	1662	0.62
$\Lambda_C(2286)$	2286	2272	0.62
$\Sigma_C(2455)$	2454	2428	1.06
$\Sigma_C^*(2520)$	2518	2486	1.26
$\Xi_C(2470)$	2469	2489	-0.82
$\Xi_C^*(2645)$	2646	2633	0.47
$\Omega_C(2695)$	2695.	2751	-2.07
$\Omega_C^*(2770)$	2766	2789	-0.84
$\Lambda_B(5620)$	5620	5599	0.37
$\Sigma_B(5811)$	5811	5781	0.51
$\Sigma_B^*(5832)$	5832	5801	0.54
$\Xi_B(5792)$	5792	5819	-0.47
$\Xi_B^*(5945)$	5950	5953	-0.05
$\Omega_B(6046)$	6046	6097	-0.84

Table 3.2 Nucleon resonances of positive parity applied to fit the model parameters.

$(\Gamma, {}^{2s+1}D, N, L^P)$	Status	J^P	M^{exp}(MeV)	M^{cal}(MeV)
$N(56, {}^28, 0, 0^+)$	****	$\frac{1}{2}^+$	939	939
$N(56, {}^28, 2, 0^+)$	****	$\frac{1}{2}^+$	N(1440)	1499
$N(56, {}^28, 2, 2^+)$	****	$\frac{5}{2}^+$	N(1720)	1655
$N(56, {}^28, 2, 2^+)$	****	$\frac{3}{2}^+$	N(1680)	1655
$N(20, {}^21, 2, 1^+)$	***	$\frac{1}{2}^+$	N(1880)	1749
$N(20, {}^41, 2, 1^+)$	-	$\frac{3}{2}^+$	missing	1749
$N(70, {}^210, 2, 0^+)$	****	$\frac{1}{2}^+$	N(1710)	1631
$N(70, {}^410, 2, 0^+)$	****	$\frac{3}{2}^+$	N(1900)	1924
$N(70, {}^210, 2, 2^+)$	-	$\frac{3}{2}^+$	missing	1702
$N(70, {}^210, 2, 2^+)$	**	$\frac{5}{2}^+$	N(1860)	1702
$N(70, {}^410, 2, 2^+)$	***	$\frac{1}{2}^+$	N(2100)	1994
$N(70, {}^410, 2, 2^+)$	*	$\frac{3}{2}^+$	N(2040)	1994
$N(70, {}^410, 2, 2^+)$	**	$\frac{5}{2}^+$	N(2000)	1994
$N(70, {}^410, 2, 2^+)$	**	$\frac{7}{2}^+$	N(1990)	1994

Table 3.3 Resonances of negative-parity applied to fit the model parameters.

$(\Gamma, {}^{2s+1}D, N, L^P)$	Status	J^P	M^{exp}(MeV)	M^{cal}(MeV)
$N(70, {}^210, 1, 1^-)$	****	$\frac{3}{2}^-$	N(1520)	1380
$N(70, {}^210, 1, 1^-)$	****	$\frac{1}{2}^-$	N(1535)	1380
$N(70, {}^410, 1, 1^-)$	****	$\frac{1}{2}^-$	N(1650)	1672
$N(70, {}^410, 1, 1^-)$	****	$\frac{5}{2}^-$	N(1675)	1672
$N(70, {}^410, 1, 1^-)$	***	$\frac{3}{2}^-$	N(1700)	1672
$\Delta(70, {}^210, 1, 1^-)$	****	$\frac{1}{2}^-$	Δ(1620)	1380
$\Delta(70, {}^210, 1, 1^-)$	****	$\frac{3}{2}^-$	Δ(1700)	1380

Table 3.4 Δ resonance of positive parity applied to fit the model parameters.

$(\Gamma, {}^{2s+1}D, N, L^P)$	Status	J^P	M^{exp}(MeV)	M^{cal}(MeV)
$\Delta(56, {}^48, 0, 0^+)$	****	$\frac{3}{2}^+$	Δ(1232)	1232
$\Delta(56, {}^48, 2, 0^+)$	***	$\frac{3}{2}^+$	Δ(1600)	1791
$\Delta(56, {}^48, 2, 2^+)$	****	$\frac{5}{2}^+$	Δ(1905)	1947
$\Delta(56, {}^48, 2, 2^+)$	****	$\frac{1}{2}^+$	Δ(1910)	1947
$\Delta(56, {}^48, 2, 2^+)$	***	$\frac{3}{2}^+$	Δ(1920)	1947
$\Delta(56, {}^48, 2, 2^+)$	****	$\frac{7}{2}^+$	Δ(1950)	1947
$\Delta(70, {}^210, 2, 0^+)$	*	$\frac{1}{2}^+$	Δ(1750)	1631
$\Delta(70, {}^210, 2, 2^+)$	-	$\frac{3}{2}^+$	$missing$	1702
$\Delta(70, {}^210, 2, 2^+)$	-	$\frac{5}{2}^+$	$missing$	1702

$$\tag{3.4}$$

Similar model parameters were obtained in the previous work (Xu et al., 2019). The parameters fixed in the work are slightly different from the preliminary ones since charm and bottom baryons are included and more accurate method is used for the model fixing. And the u and d constituent quark mass is closer to the quark mass, 330 MeV which was determined by the baryon magnetic moments (Rujula et al., 1975).

In general, all the ground state baryons are well described, with the maximum deviation less than 3%. For excited baryon states, the Roper resonance as the first radial excited state gets a mass around 1.5 GeV which does not agree well with the pole mass on PDG (Tanabashi et al., 2018), but has a 0.56 GeV gap between the ground state nucleon, close to the gap 0.55 GeV between the two lowest-magnitude $J^P = 1/2^+$ poles in Refs. (Segovia et al., 2015; Burkert and Roberts, 2019). The lowest negative-parity nucleon states turn out to be lower than the Roper resonance just as other predictions of the conventional constituent quark models. We assume that the lowest negative-parity baryon resonances may consist of the q^3 component as well as the $q^4\bar{q}$ pentaquark component. The spin-orbit interactions are not included in this work, so the states in the same spatial-spin-flavor configuration as shown in Appendix B have the same mass value. Except for the two missing $\Delta(70, {}^2 10, 2, 2^+)$ states and the two missing nucleon states $N(20, {}^2 1, 2, 1^+)$ and $N(70, {}^2 10, 2, 2^+)$, most positive-parity states are reasonably reproduced.

3.2 Light Pentaquark Spectrum

The mass spectra of the ground state $q^4\bar{q}$ and $q^3 s\bar{s}$ pentaquarks are evaluated in the Hamiltonian in Eq. (3.1), by applying the complete bases of the

pentaquark wave functions derived in our previous work (Xu et al., 2019).

In Table 3.5, $q^4\bar{q}$ ground state pentaquark masses are presented.

Table 3.5 $q^4\bar{q}$ ground state pentaquark masses of numerical calculation results.

$q^4\bar{q}$ configurations	J^P	$M(q^4\bar{q})$ (MeV)
$\Psi^{csf}_{[211]_C[31]_{FS}[4]_F[31]_S}(q^4\bar{q})$	$\frac{1}{2}^-, \frac{3}{2}^-$	2562, 2269
$\Psi^{csf}_{[211]_C[31]_{FS}[31]_F[4]_S}(q^4\bar{q})$	$\frac{3}{2}^-, \frac{5}{2}^-$	2025, 2269
$\Psi^{csf}_{[211]_C[31]_{FS}[31]_F[31]_S}(q^4\bar{q})$	$\frac{1}{2}^-, \frac{3}{2}^-$	2105, 2033
$\Psi^{csf}_{[211]_C[31]_{FS}[31]_F[22]_S}(q^4\bar{q})$	$\frac{1}{2}^-$	2025
$\Psi^{csf}_{[211]_C[31]_{FS}[22]_F[31]_S}(q^4\bar{q})$	$\frac{1}{2}^-, \frac{3}{2}^-$	1683, 2049

In Table 3.6, ground state $q^3 s\bar{s}$ pentaquark masses are showed in $q^4\bar{q}$ configuration.

Table 3.6 $q^3 s\bar{s}$ ground state pentaquark masses of numerical calculation results.

$q^4\bar{q}$ configuration	J^P	$M(q^4\bar{q})$(MeV)
$\Psi^{csf}_{[211]_C[31]_{FS}[4]_F[31]_S}(q^3 s\bar{s})$	$\frac{1}{2}^-, \frac{3}{2}^-$	2762, 2586
$\Psi^{csf}_{[211]_C[31]_{FS}[31]_F[4]_S}(q^3 s\bar{s})$	$\frac{3}{2}^-, \frac{5}{2}^-$	2420, 2546
$\Psi^{csf}_{[211]_C[31]_{FS}[31]_F[31]_S}(q^3 s\bar{s})$	$\frac{1}{2}^-, \frac{3}{2}^-$	2448, 2414
$\Psi^{csf}_{[211]_C[31]_{FS}[31]_F[22]_S}(q^3 s\bar{s})$	$\frac{1}{2}^-$	2393
$\Psi^{csf}_{[211]_C[31]_{FS}[211]_F[31]_S}(q^3 s\bar{s})$	$\frac{1}{2}^-, \frac{3}{2}^-$	2032, 2243
$\Psi^{csf}_{[211]_C[31]_{FS}[211]_F[22]_S}(q^3 s\bar{s})$	$\frac{1}{2}^-$	2165
$\Psi^{csf}_{[211]_C[31]_{FS}[22]_F[31]_S}(q^3 s\bar{s})$	$\frac{1}{2}^-, \frac{3}{2}^-$	2135, 2354

3.3 Possible Mixtures of q^3 and $q^4\bar{q}$ States

Ground state pentaquarks always have a negative parity, thus only $l = 1$ nucleon and Δ orbitally excited states could mix with ground state pentaquarks. Considering the low theoretical masses for the $N(1535)$ and $N(1520)$ resonances in the q^3 picture and their quantum numbers, it is natural to assume that the two baryon resonances may include both the q^3 and $q^4\bar{q}$ pentaquark component contributions. The wave function of these baryon resonances may be expressed as linear combinations of the q^3 state and $q^4\bar{q}$ pentaquark states which have the same quantum numbers as the q^3 state,

$$a_0|q^3\rangle + \sum_\alpha a_\alpha|q^4\bar{q}\rangle^\alpha\,. \tag{3.5}$$

In principle, one can determine the coefficients a_α by solving the coupled equations of all channels including not only the coupling between the q^3 and $q^4\bar{q}$ states and the coupling between the $q^4\bar{q}$ states, but also the contributions of hidden channels such as meson-baryon ones. The mass matrix is usually not Hermitian but complex, thus the bare states and physical states cannot be linked by an unitary transformation. In this work we simplify the problem to the simplest case that the q^3 state mixes with only one $q^4\bar{q}$ pentaquark state which has the lowest mass, eliminating other pentaquark states and meson-baryon channels. As a result, the 2×2 mass matrix will be highly complex, which may be eigendiagonalized by the transformation,

$$
\begin{aligned}
\psi_1 &= \cos\theta|q^3\rangle - \sin\theta|q^4\bar{q}\rangle\,, \\
\psi_2 &= \sin\theta|q^3\rangle + \cos\theta|q^4\bar{q}\rangle.
\end{aligned}
\tag{3.6}
$$

where ψ_1 and ψ_2 are respectively the lower and higher negative-parity physical states, and the mixing angle θ between the q^3 and $q^4\bar{q}$ states is generally complex.

Table 3.7 The mixture of q^3 and $q^4\bar{q}$ components. All four q^3 states take the same mass, 1380 MeV. The chosen pentaquark states and masses are listed as $q^4\bar{q}$ configuration and $q^4\bar{q}$ Mass (in MeV) from Tables 3.5 and 3.6.

ψ_1 State	J^P	θ	ψ_2 State	$q^4\bar{q}$ configuration	$q^4\bar{q}$ Mass
1530	$\frac{1}{2}^-$	$i35.2°$	1882	$q^3s\bar{s}_{[211]_F[31]_S}$	2032
1515	$\frac{3}{2}^-$	$i32.6°$	1899	$q^4\bar{q}_{[31]_F[4]_S}$	2025
		$i31.7°$	1914	$q^4\bar{q}_{[22]_F[31]_S}$	2049
1610	$\frac{1}{2}^-$	$i46.4°$	1893	$q^4\bar{q}_{[31]_F[31]_S}$	2123
1710	$\frac{3}{2}^-$	$i51.5°$	2024	$q^3s\bar{s}_{[22]_F[31]_S}$	2354

The masses of the physical states, M_{ψ_1} and M_{ψ_2} are derived as follows:

$$
\begin{aligned}
M_{\psi_1} &= M_{q^3}\cos^2\theta + M_{q^4\bar{q}}\sin^2\theta - m_\delta\,, \\
M_{\psi_2} &= M_{q^3}\sin^2\theta + M_{q^4\bar{q}}\cos^2\theta + m_\delta\,, \\
m_\delta &= \frac{(M_{q^4\bar{q}} - M_{q^3})}{2}\tan 2\theta\sin 2\theta
\end{aligned}
\tag{3.7}
$$

The mixing angle θ in Eq. (3.7) is determined by adjusting the lower negative-parity states ψ_1 to $N(1535)$, $N(1520)$, $\Delta(1620)$, and $\Delta(1700)$. With both the real and imaginary part of the mixing angle in the domain of $(0, \pi/2)$, the mixing angle and the M_{ψ_2} can be determined without duplication from Eq. (3.7). Thus, one gets four pairs of mixed states as shown in Table 3.7 with all $Re(\theta) = 0$. $N(1520)3/2^-$ and $N(1875)3/2^-$ form a nonstrange pair, and the $N(1535)1/2^-$ and $N(1895)1/2^-$ form a strange pair for the nucleon resonances while the $\Delta(1620)1/2^-$ and $\Delta(1900)1/2^-$ form a nonstrange pair, and the $\Delta(1700)3/2^-$ and $\Delta(1940)3/2^-$ form a strange pair for the Δ resonances. For the pair of N(1520) and N(1875), we have shown in Table 3.7 the results with both the pentaquark states $q^4\bar{q}_{[31]_F[4]_S}$ (2025 MeV) and $q^4\bar{q}_{[22]_F[31]_S}$ (2049 MeV) mixed with the q^3 state.

In the present model one can not rule out either of them.

Table 3.8 Masses of negative-parity resonances after including ground state pentaquark components. The theoretical masses of $N(1535)$, $N(1520)$, $\Delta(1620)$, and $\Delta(1700)$ states take the mean values of their Breit-Wigner mass from (Tanabashi et al., 2018).

Resonance	Status	J^P	M^{exp} (MeV)	M^{cal} (MeV)
$N(1520)$	****	$\frac{3}{2}^-$	1510-1520	1515
$N(1535)$	****	$\frac{1}{2}^-$	1515-1545	1530
$N(1650)$	****	$\frac{1}{2}^-$	1645-1670	1672
$N(1675)$	****	$\frac{5}{2}^-$	1670-1680	1672
$N(1685)$	*	$\frac{1}{2}^-$?	1665-1675	1683
$N(1700)$	***	$\frac{3}{2}^-$	1650-1750	1672
$N(1875)$	***	$\frac{3}{2}^-$	1850-1920	1899/1914
$N(1895)$	****	$\frac{1}{2}^-$	1870-1920	1882
$\Delta(1620)$	****	$\frac{1}{2}^-$	1590-1630	1610
$\Delta(1700)$	****	$\frac{3}{2}^-$	1690-1730	1710
$\Delta(1900)$	***	$\frac{1}{2}^-$	1840-1920	1893
$\Delta(1940)$	**	$\frac{3}{2}^-$	1940-2060	2024

The mass spectrum of the negative-parity nucleon and Δ resonances are listed in Table 3.8 in the q^3 and $q^4\bar{q}$ picture. $N(1650)$, $N(1675)$, and $N(1700)$ are assumed to be mainly pure q^3 states since the q^3 picture reproduces their masses well, as shown in Table 3.3, and hence there is no mixing with pentaquark states. $N(1685)$ could be the lowest pure pentaquark state. The others are q^3 and $q^4\bar{q}$ mixing states taken from Table 3.7.

The mass spectrum of the negative-parity nucleon and Δ resonances are

listed in Table 3.8 in the q^3 and $q^4\bar{q}$ picture. $N(1650)$, $N(1675)$, and $N(1700)$ are assumed to be mainly pure q^3 states since the q^3 picture reproduces their masses well, as shown in Table 3.3, and hence there is no mixing with pentaquark states. $N(1685)$ could be the lowest pure pentaquark state. The others are q^3 and $q^4\bar{q}$ mixing states taken from Table 3.7.

3.4 $q^3Q\bar{Q}$ Pentaquark Spectrum

Motivated by the hidden-charm pentaquark candidates recently found by the LHCb Collaboration (Aaij et al., 2019) we also calculate the mass spectra of hidden heavy pentaquarks of $q^3Q\bar{Q}$ systems. The quark configurations and wave functions of the $q^3Q\bar{Q}$ systems are derived in Appendix B. The spatial wave functions, which are derived in the harmonic oscillator quark-quark interaction and grouped in Appendix C according to the permutation symmetry, are employed as complete bases to study the $q^3Q\bar{Q}$ systems described with the color dependent Hamiltonian in Eq. (3.1). The mass spectra of the hidden charm and hidden bottom pentaquarks of the q^3 color octet configuration are presented in Tables 3.9 and 3.10 separately.

It's noted that the hidden-charm pentaquark mass spectra in this work is slightly higher than the three narrow pentaquarklike states, $P_c(4312)^+$, $P_c(4440)^+$, and $P_c(4457)^+$ measured by LHCb. The predicted values of 4483 and 4495 MeV for the lowest hidden-charm pentaquark in the $[21]_C[21]_{FS}[21]_F[21]_S$ configuration are close to the experimental values of 4440 and 4457 MeV, but still about 100-200 MeV higher than the $P_c(4312)^+$ state. The higher predicted P_c masses may result from the compact spacial configuration in our pentaquark picture. The observed P_c may probably be baryon-meson molecular states or mixtures of compact pentaquark states and molecules. For the hidden-bottom pentaquarks,

Table 3.9 Ground hidden-charm pentaquark $q^3 c\bar{c}$ mass spectrum, where the q^3 and $Q\bar{Q}$ components are in the color octet states.

$q^3 Q\bar{Q}$ configurations	J^P	$S^{c\bar{c}}$	$M(q^3 c\bar{c})$(MeV)
$\Psi^{csf}_{[21]_C[21]_{FS}[21]_F[21]_S}(q^3 c\bar{c})$	$\frac{1}{2}^-$	0	4483
	$\frac{1}{2}^-, \frac{3}{2}^-$	1	4452, 4495
$\Psi^{csf}_{[21]_C[21]_{FS}[3]_F[21]_S}(q^3 c\bar{c})$	$\frac{1}{2}^-$	0	4702
	$\frac{1}{2}^-, \frac{3}{2}^-$	1	4701, 4701
$\Psi^{csf}_{[21]_C[21]_{FS}[21]_F[3]_S}(q^3 c\bar{c})$	$\frac{3}{2}^-$	0	4556
	$\frac{1}{2}^-, \frac{3}{2}^-, \frac{5}{2}^-$	1	4481, 4525, 4598

Table 3.10 Ground hidden-charm pentaquark $q^3 b\bar{b}$ mass spectrum, where the q^3 and $Q\bar{Q}$ components are in the color octet states.

$q^3 Q\bar{Q}$ configurations	J^P	$S^{b\bar{b}}$	$M(q^3 b\bar{b})$(MeV)
$\Psi^{csf}_{[21]_C[21]_{FS}[21]_F[21]_S}(q^3 b\bar{b})$	$\frac{1}{2}^-$	0	10964
	$\frac{1}{2}^-, \frac{3}{2}^-$	1	10954, 10968
$\Psi^{csf}_{[21]_C[21]_{FS}[3]_F[21]_S}(q^3 b\bar{b})$	$\frac{1}{2}^-$	0	11183
	$\frac{1}{2}^-, \frac{3}{2}^-$	1	11183, 11183
$\Psi^{csf}_{[21]_C[21]_{FS}[21]_F[3]_S}(q^3 b\bar{b})$	$\frac{3}{2}^-$	0	11037
	$\frac{1}{2}^-, \frac{3}{2}^-, \frac{5}{2}^-$	1	11012, 11027, 11051

the work predicts the mass of the ground states to be 10.9-11.2 GeV, lying below the threshold of a single bottom baryon and $B(B^*)$ mesons, which is consistent with other work (Gutsche and Lyubovitskij, 2019).

CHAPTER IV

THE LOWEST PENTAQUARK STATE:

N(1685) OR NOT?

In our calculation one non-strange pentaquark with mass 1683 MeV, $1/2^-$ in $\Psi^{sf}_{[31]_{FS}[22]_F[31]_S}(q^4\overline{q})$ configuration was got. Normally, for the resonance mass less than 1.8 GeV, all states are clear in experiment, so where is this state?

Unlike all the other nucleon resonances of low energy the Breit-Wigner (BW) full width is at least 120 MeV, A narrow structure of BW width around 30 MeV was firstly announced in photoproduction of η mesons off the quasi-free neutron by the group (Kuznetsov et al., 2007), the nucleon was observed in the $\gamma d \rightarrow \eta n(p)$ excitation by another two different groups (Jaegle et al., 2011; Akondi et al., 2014). The observations were introduced under the heading of a new one-star isospin $1/2$ nucleon resonance N(1685) since 2012, but was removed from the listings from 2016. From the recent results on N(1685) (Anisovich et al., 2017), a full partial wave analysis without any narrow resonance leads to an excellent description of the data, so it could not be $1/2^+$ positive parity state. During the same period of time group (Kuznetsov et al., 2017) not only observe the narrow resonance $N^+(1685)$ decaying into ηp final state, but also witness another isospin-$1/2$ $N^0(1685)$ resonance decaying into ηn in the $\gamma N \rightarrow \pi \eta N$ reactions. For the $L = 1$ q^3 configuration $70(1, 1^-)$ multiplets with spin $3/2$, $N(1650), N(1700), N(1675)$ which all are well located, we have no possible space to let N(1685) sit in. We may firstly make an assumption that N(1685) could be the lowest ground pentaquark state.

Actually, with very few exceptions, for most combination of quantum numbers experimentally only the lowest lying state is known, while models predict a lot of higher lying states. However, at higher excitation energies not only the ordering but also the match in simple number counting is poor; and above 1.8 GeV the 56 and 70 multiplets have more mixture effect as an old paper (Forsyth and Cutkosky, 1980) mentioned. $[56, 1^-]$ and $[70, 1^-]$ states for $N = 3$ band could be mixed together with great complexity.

The mass spectrum of the negative-parity nucleon and Δ resonances are listed in Table 3.8 in the q^3 and $q^4\bar{q}$ picture. $N(1650)$, $N(1675)$, and $N(1700)$ are assumed to be mainly pure q^3 states since the q^3 picture reproduces their masses well, as shown in Table 3.3, and hence there is no mixing with pentaquark states. $N(1685)$ could be the lowest pure pentaquark state. The others are q^3 and $q^4\bar{q}$ mixing states taken from Table 3.7. Only $N = 1$ oscillator band of Octet states sit wrongly in the nucleon resonance because they couple with other ground state pentaquarks of same quantum numbers, and a better understanding of $N(1440)$, $N(1520)$ and $N(1535)$ may be achieved by studying the helicity amplitude of $N(1440)$, $N(1520)$ and $N(1535)$ with both q^3 and $q^4\bar{q}$ state contributions since there are much more sensitive experimental data available.

While we can't locate $N(1685)$ in the q^3 negative party spectrum. The lowest pentaquark mass we get is 1683 MeV with $J^P = 1/2^-$ right in this region, even though we can't prove that 1683 MeV is just this $N(1685)$ state, to study the property of N(1685) as a non-strange pentaquark state may give us a good understand in experiment at least its low BW width like the charmonium pentaquark $P_c(4450)^+$ (Aaij et al., 2015) with width $39 \pm 5 \pm 19$ MeV.

CHAPTER V

CONCLUSIONS

In the thesis we have worked out all the spatial-spin-flavor as well as spin-flavor configurations of pentaquark systems, and derived explicitly the spatial-spin-flavor as well as spin-flavor wave functions. Spatial wave functions of various permutation symmetries have been constructed for the pentaquark systems where the quark-quark interactions are of the harmonic oscillator type. The constructed spatial wave functions can serve as complete bases for studying systems in other interactions.

The masses of low-lying q^3 states and ground $q^4\bar{q}$ states are evaluated, where all model parameters are predetermined by fitting the theoretical masses to the experimental data for the baryons which are believed to be mainly $3q$ states. In the work we have assumed that the Roper resonance is the first radial excitation state of nucleon.

It is interesting that the theoretical work predicts the pentaquark state with the $[31]_{FS}[22]_F[31]_S$ configuration and the quantum numbers $I(J^P) = \frac{1}{2}(\frac{1}{2}^-)$ has the lowest mass, about 1680 MeV. One may make a bold guess that this $q^4\bar{q}$ pentaquark state could be the isospin-1/2 narrow resonance $N^+(1685)$ which can not be accommodated as a q^3 particle.

The work shows that the ordering problem of the $N(1440)$, $N(1520)$ and $N(1535)$ may be solved by introducing the $q^4\bar{q}$ contribution. The same calculation leads to that the $N(1895)1/2^-$, $N(1875)3/2^-$, $\Delta(1900)1/2^-$, and $\Delta(1940)3/2^-$ resonances may pair respectively with the $N(1535)1/2^-$,

$N(1520)3/2^-$, $\Delta(1620)1/2^-$, and $\Delta(1700)3/2^-$ in the q^3 and $q^4\bar{q}$ interpretation. A better understanding of $N(1440)$, $N(1520)$ and $N(1535)$ may be achieved by studying the helicity amplitude of $N(1440)$, $N(1520)$ and $N(1535)$ with both q^3 and $q^4\,\bar{q}$ state contributions since there are much more sensitive experimental data available.

The mass spectra of ground hidden heavy pentaquark states $q^3Q\bar{Q}$ are accurately evaluated using the same predetermined model parameters. It is found that the hidden charm pentaquark states with the $[21]_C[21]_{FS}[21]_F[21]_S$ configuration have the lowest masses which are slightly larger than the LHCb results. In this communication, however, the work can not draw any conclusion about the nature of P_c states.
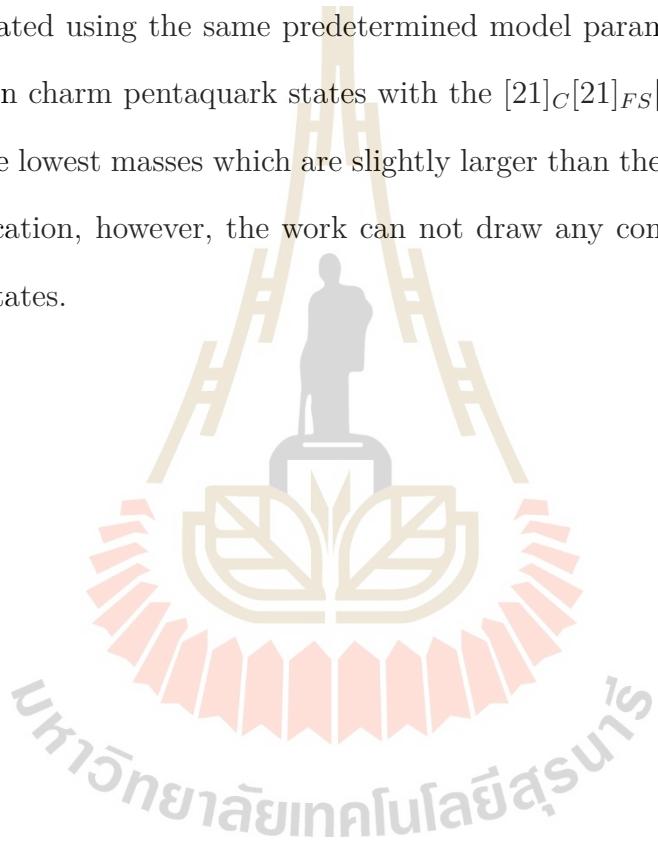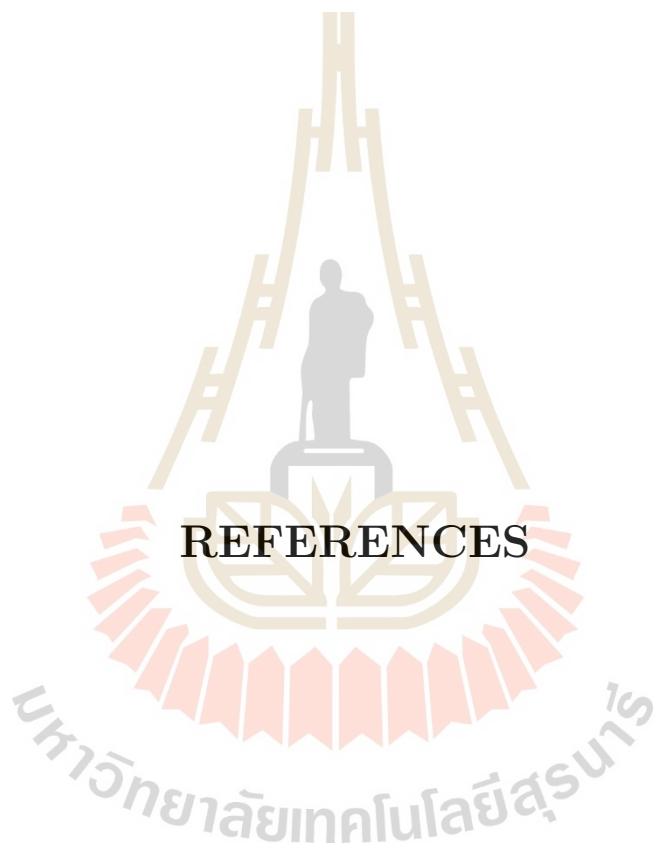
REFERENCES

REFERENCES

Aaij, R., Adeva, B., Adinolfi, M., Affolder, A., Ajaltouni, Z., Akar, S., Albrecht, J., Alessio, F., Alexander, M., Ali, S., Alkhazov, G., Alvarez Cartelle, P., Alves Jr., A. A., Amato, S., Amerio, S., et al. (2015). Observation of $J/\psi p$ Resonances Consistent with Pentaquark States in $\Lambda_b^0 \to J/\psi K^- p$ Decays. **Phys. Rev. Lett.** 115: 072001.

Aaij, R., Beteta, C. A., Adeva, B., Adinolfi, M., Aidala, C. A., Ajaltouni, Z., Akar, S., Albicocco, P., Albrecht, J., Alessio, F., Alexander, M., Alkhazov, G., Alvarez Cartelle, P., Alves Jr., A. A., Amato, S., et al. (2019). Observation of a Narrow Pentaquark State, $P_c(4312)^+$, and of the Two-Peak Structure of the $P_c(4450)^+$. **Phys. Rev. Lett.** 122: 222001.

Akondi, C., Annand, J. R. M., Arends, H. J., Beck, R., Bernstein, A., Borisov, N., Braghieri, A., Briscoe, W. J., Cherepnya, S., Collicott, C., Costanza, S., Downie, E. J., Dieterle, M., Fix, A., Garni, S., et al. (2014). Measurement of the Transverse Target and Beam-Target Asymmetries in η Meson Photoproduction at MAMI. **Phys. Rev. Lett.** 113: 102001.

An, C. S. and Zou, B. S. (2009). The Role of the $qqqq\bar{q}$ components in the electromagnetic transition $\gamma^* N \to N^*(1535)$. **Eur. Phys. J. A** 39: 195–204.

Anisovich, A., Burkert, V., Klempt, E., Nikonov, V. A., Sarantsev, A. V., and Thoma, U. (2017). Scrutinizing the evidence for N(1685). **Phys. Rev. C** 95: 035211.

Anisovich, A. V., Sarantsev, A., Bartholomy, O., Klempt, E., Nikonov, V. A., and Thoma, U. (2005). Photoproduction of baryons decaying into $N\pi$ and $N\eta$. **Eur. Phys. J. A** 25: 427.

Arndt, R. A., Briscoe, W., Strakovsky, I., and Workman, R. (2008). Partial-wave analysis and baryon spectroscopy. **Eur. Phys. J. A** 35: 311.

Arndt, R. A., Briscoe, W. J., Morrison, T. W., Strakovsky, I. I., Workman, R. L., and Gridnev, A. B. (2005). Low-energy ηN interactions: Scattering lengths and resonance parameters. **Phys. Rev. C** 72: 045202.

Aznauryan, I., Burkert, V. D., Biselli, A. S., Egiyan, H., Joo, K., Kim, W., Park, K., Smith, L. C., Ungaro, M., Adhikari, K. P., Anghinolfi, M., Avakian, H., Ball, J., Battaglieri, M., Batourine, V., et al. (2009). Electroexcitation of nucleon resonances from CLAS data on single pion electroproduction. **Phys. Rev. C** 80: 055203.

Aznauryan, I. G. (2007). Electroexcitation of the Roper resonance in relativistic quark models. **Phys. Rev. C** 76: 025212.

Bloom, E. D., Coward, D. H., DeStaebler, H., Drees, J., Miller, G., Mo, L. W., Taylor, R. E., Breidenbach, M., Friedman, J. I., Hartmann, G. C., and Kendall, H. W. (1969). High-Energy Inelastic $e - p$ Scattering at 6° and 10°. **Phys. Rev. Lett.** 23: 930.

Burkert, V. D. and Roberts, C. D. (2019). Roper resonance: Toward a solution to the fifty year puzzle. **Rev. Mod. Phys** 61: 011003.

Capstick, S. and Isgur, N. (1986). Baryons in a relativized quark model with chromodynamics. **Phys. Rev. D** 34: 2809.

Collins, J. C., Frankfurt, L., and Strikman, M. (1997). Factorization for hard exclusive electroproduction of mesons in QCD. **Phys. Rev. D** 56: 2982.

Drechsel, D., Kamalov, S. S., and Tiator, L. (2007). Unitary isobar model – MAID2007. **Eur. Phys. J. A** 34: 69.

Feuster, T. and Mosel, U. (1999). Photon- and meson-induced reactions on the nucleon. **Phys. Rev. C** 59: 460.

Forsyth, C. P. and Cutkosky, R. E. (1980). Masses and Widths of Odd-Parity N and Δ Resonances. **Phys. Rev. Lett.** 46: 576.

Gell-Mann, M. (1964). A Schematic Model of Baryons and Mesons. **Phys. Lett** 8: 214–215.

Gutsche, T. and Lyubovitskij, V. E. (2019). Structure and decays of hidden heavy pentaquarks. **Phys. Rev. D** 100: 094031.

Hartmann, J., Dutz, H., Anisovich, A. V., Bayadilov, D., Beck, R., Becker, M., Beloglazov, Y., Berlin, A., Bichow, M., Brinkmann, K. T., Crede, V., Dieterle, M., Eberhardt, H., Elsner, D., Fornet-Pons, K., et al. (2014). $N(1520)$ $3/2^-$ Helicity Amplitudes from an Energy-Independent Multipole Analysis Based on New Polarization Data on Photoproduction of Neutral Pions. **Phys. Rev. Lett.** 113: 062001.

Jaegle, I., Mertens, T., Fix, A., Huang, F., Nakayama, K., Tiator, L., Anisovich, A. V., Bacelar, J. C. S., Bantes, B., Bartholomy, O., Bayadilov, D., Beck, R., Beloglazov, Y. A., Castelijns, R., Crede, V., et al. (2011). Photoproduction of η'-mesons off the deuteron. **Eur. Phys. J. A** 47: 89.

Jido, D., Doring, M., and Oset, E. (2008). Transition form factors of the $N^*(1535)$ as a dynamically generated resonance. **Phys. Rev. C** 77: 061301.

Juliá-Díaz, B., Lee, T.-S. H., Matsuyama, A., Sato, T., and Smith, L. C. (2008). Dynamical coupled-channels effects on pion photoproduction. **Phys. Rev. C** 77: 045205.

Juliá-Díaz, B. and Riska, D. (2006). The role of $qqqq\bar{q}$ components in the nucleon and the $N(1440)$ resonance. **Nucl. Phys. A** 780: 175–186.

Klempt, E. and Richard, J. M. (2010). Baryon spectroscopy. **Rev. Mod. Phys.** 82: 1095.

Kuznetsov, V., Churikova, S., Gervino, G., Ghio, F., Girolami, B., Ivanov, D., Jang, J., Kim, A., Kim, W., Ni, A., Vorobiev, Y., Yurov, M., and Zabrodin, A. (2007). Evidence for a narrow structure at $W \sim 1.68$ GeV in η photoproduction off the neutron. **Phys. Lett B** 647: 23–29.

Kuznetsov, V., Mammoliti, F., Tortorici, F., Bellini, V., Brio, V., Gridnev, A., Kozlenko, N., Russo, G., Sperduto, M. L., Sumachev, V., and Sutera, C. (2017). Observation of narrow $N^+(1685)$ and $N^0(1685)$ resonance in $\gamma N \to \Pi \eta N$ reactions. **JETP Letters** 106: 693–699.

Mokeev, V. I., Burkert, V. D., Carman, D. S., Elouadrhiri, L., Fedotov, G. V., Golovatch, E. N., Gothe, R. W., Hicks, K., Ishkhanov, B. S., Isupov, E. L., and Skorodumina, I. (2016). New results from the studies of the N(1440)1/2$^+$, N(1520)3/2$^-$, and (1620)1/2$^-$ resonances $ep \to e^{'}\pi^+\pi^-p^{'}$ electroproduction with the CLAS detector in exclusive. **Phys. Rev. C** 93: 025206.

Mokeev, V. I., Burkert, V. D., Elouadrhiri, L., Fedotov, G. V., Golovatch, E. N., Gothe, R. W., Ishkhanov, B. S., Isupov, E. I., Adhikari, K. P., Aghasyan, M., Anghinolf, M., Avakian, H., Bagdasaryan, H., Ball, J., Baltzell,

N. A., et al. (2008). Experimental study of the $P_{11}(1440)$ and $D_{13}(1520)$ resonances from the CLAS data on $ep \to e^{'}\pi^{+}\pi^{-}p^{'}$. **Phys. Rev. C** 86: 035203.

Olbrich, L., Zetenyi, M., Giacosa, F., and Rischke, D. H. (2018). Influence of the axial anomaly on the decay $N(1535) \to N\eta$. **Phys. Rev. D** 97: 014007.

Parganlija, D., Kovacs, P., Wolf, G., Giacosa, F., and Rischke, D. H. (2013). Meson vacuum phenomenology in a three-flavor linear sigma model with (axial-)vector mesons. **Phys. Rev. D** 87: 014011.

Ramalho, G. and Pena, M. (2017). $\gamma^{*}N \to N^{*}(1520)$ form factors in the timelike regime. **Phys. Rev. D** 95: 014003.

Rujula, A. D., Georgi, H., and Glashow, S. L. (1975). Hadron masses in a gauge theory. **Phys. Rev. D** 12: 147.

Segovia, J., El-Bennich, B., Rojas, E., Cloet, I. C., Roberts, C. D., Xu, S. S., and Zong, H. S. (2015). Completing the Picture of the Roper Resonance. **Phys. Rev. Lett.** 115: 171801.

Shyam, R., Scholten, O., and Lenske, H. (2010). Associated photoproduction of K^{+} mesons off protons within a coupled-channels K- matrix approach. **Phys. Rev. C** 81: 015204.

Tanabashi, M., Hagiwara, K., Hikasa, K., Nakamura, K., Sumino, Y., Takahashi, F., Tanaka, J., Agashe, K., Aielli, G., Amsler, C., Antonelli, M., Asner, D. M., Baer, H., Banerjee, S., Barnett, R. M., et al. (2018). Particle Data Group. **Phys. Rev. D** 98: 030001.

Xu, K., Kaewsnod, A., Liu, X. Y., Srisuphaphon, S., Limphirat, A., and Yan, Y.

(2019). Complete basis for pentaquark wave function in group theory approach. **Phys. Rev. C** 100: 065207.

APPENDICES
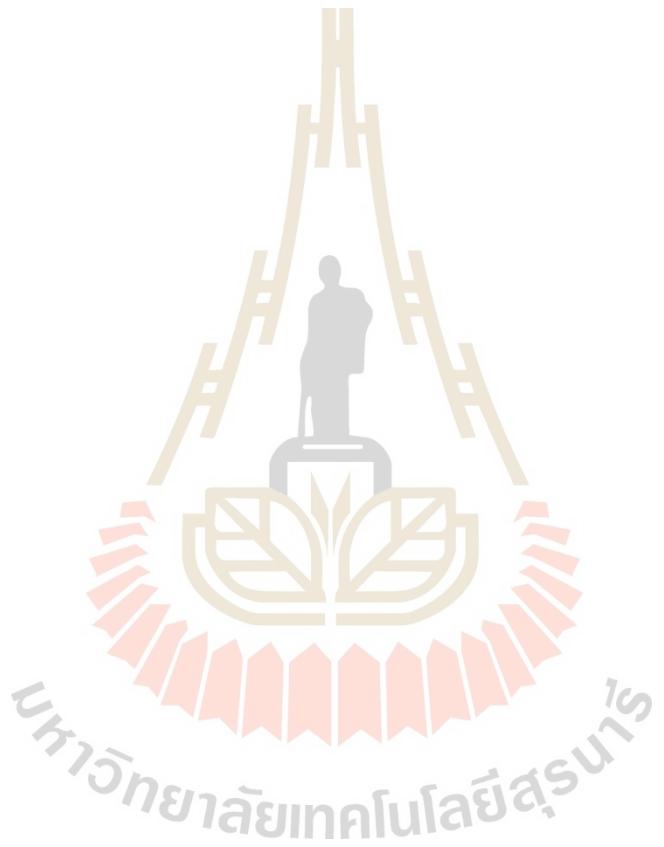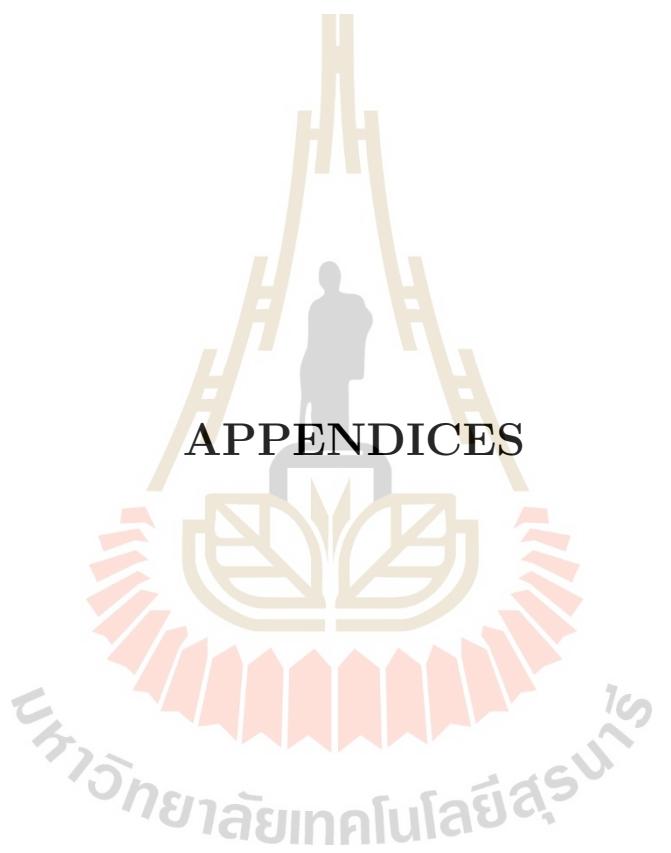
APPENDIX A

GROUP THEORY APPROACH

Pentaquarks are states of four quarks and one antiquark, $q^4\bar{q}$. Pentaquark wave functions contain contributions of the spatial degrees of freedom and the internal degrees of freedom of color, flavor and spin. The internal degrees of freedom are taken to be the three light flavors u, d and s with spin $s = 1/2$ and three possible colors r, g and b.

The quark transforms under the fundamental representation of $SU(n)$, whereas the antiquark transforms under the conjugate representation of $SU(n)$, with $n = 2, 3, 3, 6$ for the spin, flavor, color and spin-flavor degree of freedom, respectively. The algebraic structure of multiquark state consists of the usual spin-flavor and color algebras $SU_{sf}(6) \otimes SU_c(3)$ with $SU_{sf}(6) = SU_f(3) \otimes SU_s(2)$. The n-quark state $|q_1\rangle|q_2\rangle\cdots|q_n\rangle$ forms an m^n dimensional direct product basis of $SU(m)$ ($m = 3$, 3, 3, 2 for the color, spatial, flavor, and spin), which can be decomposed according to the S_4 permutation group.

The construction of $q^4\bar{q}$ states follow the rules that a $q^4\bar{q}$ state must be a color singlet and the $q^4\bar{q}$ wave function should be antisymmetric under any permutation between identical quarks.

In the language of group theory, the permutation symmetry of the four-quark configuration is characterized by the S_4 Young tabloids [4], [31], [22], [211] and [1111].

The total pentaquark wave function should be a color singlet demands that the color part of the pentaquark wave function must be a $[222]_1$ singlet.

Since the color part of the antiquark in pentaquark states is a $[11]_3$ an-

titriplet

$$\psi_{[11]}^c(\bar{q}) = \boxed{\begin{array}{c} \\ \\ \end{array}} \tag{A.1}$$

the color wave function of the four-quark configuration must be a $[211]_3$ triplet

$$\psi_{[211]}^c(q^4) = \tag{A.2}$$

The total states of q^4 is antisymmetric implies that the orbital-spin-flavour

part must be a $[31]$ state

$$\psi_{[31]}^{osf}(q^4) = \tag{A.3}$$

which is obtained from the Young tabloid of the colour part by interchanging rows

and columns.

Total wave function of the q^4 configuration may be written in the general

form

$$\psi = \sum_{i,j=\lambda,\rho,\eta} a_{ij} \psi_{[211]_i}^c \psi_{[31]_j}^{osf} \tag{A.4}$$

The coefficients can be determined by operating the permutations of S_4 on the

general form, using the $[31]$ and $[211]$ representation matrices.

For example, applying the permutation (12) first by using

$$D^{[31]}(12) = \begin{pmatrix} 1 & 0 & 0 \\ 0 & 1 & 0 \\ 0 & 0 & -1 \end{pmatrix}, \quad D^{[211]}(12) = \begin{pmatrix} 1 & 0 & 0 \\ 0 & -1 & 0 \\ 0 & 0 & -1 \end{pmatrix} \tag{A.5}$$

One gets

$$\begin{aligned} (12)\psi &= +a_{\lambda\lambda}\psi_{[211]_\lambda}^c \psi_{[31]_\lambda}^{osf} - a_{\lambda\rho}\psi_{[211]_\lambda}^c \psi_{[31]_\rho}^{osf} + a_{\lambda\eta}\psi_{[211]_\lambda}^c \psi_{[31]_\eta}^{osf} \\ &\quad -a_{\rho\lambda}\Psi_{[211]_\rho}^c \psi_{[31]_\lambda}^{osf} + a_{\rho\rho}\psi_{[211]_\rho}^c \psi_{[31]_\rho}^{osf} - a_{\rho\eta}\psi_{[211]_\rho}^c \psi_{[31]_\eta}^{osf} \end{aligned}$$

$$-a_{\eta\lambda}\Psi^{c}_{[211]_\eta}\psi^{osf}_{[31]_\lambda} + a_{\eta\rho}\psi^{c}_{[211]_\eta}\psi^{osf}_{[31]_\rho} - a_{\eta\eta}\psi^{c}_{[211]_\eta}\psi^{osf}_{[31]_\eta}$$

An antisymmetric ψ requires $a_{\lambda\lambda} = a_{\lambda\eta} = a_{\rho\rho} = a_{\eta\rho} = 0$. Therefore, we have

$$\psi = a_{\lambda\rho}\psi^{c}_{[211]_\lambda}\psi^{osf}_{[31]_\rho} + a_{\rho\lambda}\psi^{c}_{[211]_\rho}\psi^{osf}_{[31]_\lambda} + a_{\rho\eta}\psi^{c}_{[211]_\rho}\psi^{osf}_{[31]_\eta}$$
$$+a_{\eta\lambda}\psi^{c}_{[211]_\eta}\psi^{osf}_{[31]_\lambda} + a_{\eta\eta}\psi^{c}_{[211]_\eta}\psi^{osf}_{[31]_\eta}$$

The action of the permutation (13) of S_4 on the above equation and the application of the antisymmetric restriction, $(13)\psi = -\psi$ lead to $a_{\eta\lambda} = a_{\rho\eta} = 0$ and $a_{\rho\lambda} = -a_{\lambda\rho}$, and hence

$$\psi = a_{\lambda\rho}\psi^{c}_{[211]_\lambda}\psi^{osf}_{[31]_\rho} - a_{\lambda\rho}\psi^{c}_{[211]_\rho}\psi^{osf}_{[31]_\lambda} + a_{\eta\eta}\psi^{c}_{[211]_\eta}\psi^{osf}_{[31]_\eta}$$

Applying the permutation (34) of S_4 to the above equation, we have

$$(34)\psi = -a_{\lambda\rho}\psi^{c}_{[211]_\lambda}\psi^{osf}_{[31]_\rho}$$
$$+ a_{\rho\lambda}\left(-\frac{1}{3}\psi^{c}_{[211]_\rho} + \frac{2\sqrt{2}}{3}\psi^{c}_{[211]_\eta}\right)\left(\frac{1}{3}\psi^{osf}_{[31]_\lambda} + \frac{2\sqrt{2}}{3}\psi^{osf}_{[31]_\eta}\right)$$
$$+ a_{\eta\eta}\left(\frac{2\sqrt{2}}{3}\psi^{c}_{[211]_\rho} + \frac{1}{3}\psi^{c}_{[211]_\eta}\right)\left(\frac{2\sqrt{2}}{3}\psi^{osf}_{[31]_\lambda} - \frac{1}{3}\psi^{osf}_{[31]_\eta}\right). \qquad (A.6)$$

Here we have used the [31] and [211] representation matrices for the permutation (34),

$$D^{[31]}(34) = \begin{pmatrix} 1/3 & 0 & 2\sqrt{2}/3 \\ 0 & 1 & 0 \\ 2\sqrt{2}/3 & 0 & -1/3 \end{pmatrix}, \quad D^{[211]}(34) = \begin{pmatrix} -1 & 0 & 0 \\ 0 & -1/3 & 2\sqrt{2}/3 \\ 0 & 2\sqrt{2}/3 & 1/3 \end{pmatrix} \quad (A.7)$$

$$D^{[31]}(34) = \begin{pmatrix} 1/3 & 0 & 2\sqrt{2}/3 \\ 0 & 1 & 0 \\ 2\sqrt{2}/3 & 0 & -1/3 \end{pmatrix}, \quad D^{[211]}(34) = \begin{pmatrix} -1 & 0 & 0 \\ 0 & -1/3 & 2\sqrt{2}/3 \\ 0 & 2\sqrt{2}/3 & 1/3 \end{pmatrix} \quad (A.8)$$

An antisymmetric ψ demands $a_{\lambda\rho} = a_{\eta\eta}$. Finally, we derive a fully antisymmetric wave function for the q^4 configuration

$$\psi = \frac{1}{\sqrt{3}}\left(\psi^{c}_{[211]_\lambda}\psi^{osf}_{[31]_\rho} - \psi^{c}_{[211]_\rho}\psi^{osf}_{[31]_\lambda} + \psi^{c}_{[211]_\eta}\psi^{osf}_{[31]_\eta}\right) \qquad (A.9)$$

The spatial-flavor-spin wave function of the q^4 cluster may be written in the general form

$$\Psi^{osf}_{[31]} = \sum_{i,j=S,A,\lambda,\rho,\eta} b_{ij} \Psi^o_{[X]_i} \Psi^{sf}_{[Y]_j} \tag{A.10}$$

Applying the permutations of S_4 on the general form leads to all the possible spatial-spin-flavor configurations:

The flavor-spin wave function of the q^4 cluster may be written in the general form

$$\Psi^{sf}_{[Z]} = \sum_{i,j=S,A,\lambda,\rho,\eta} c_{ij} \Phi^f_{[X]_i} \chi^s_{[Y]_j} \tag{A.11}$$

Applying the permutations of S_4 on the general form leads to all the possible spin-flavor configurations.

For the pentaquark states with isospin $I = 0$ and strangeness $S = 1$, the q^4 flavor-spin wave function of must be as follows:

$$\begin{array}{ccccc}
[31] & = & [22] & \otimes & [31] \\
SU_{sf}(6) & & SU_f(3) & & SU_s(2)
\end{array} \tag{A.12}$$

Again, the spin-flavor wave functions of various permutation symmetries take the general form,

$$\psi^{\text{sf}} = \sum_{i=\lambda,\rho} \sum_{j=\lambda,\rho,\eta} a_{ij} \, \phi_{[22]_i} \chi_{[31]_j} \tag{A.13}$$

a_{ij} can be determined by acting the permutations of S_4 on the general form. In this appendix we list explicitly the spatial-spin-flavor as well as spin-flavor wave functions for all the configurations in Tables 2.1 and 2.2. $O_{[X]}$, $F_{[X]}$, $S_{[X]}$, $FS_{[X]}$, and $OFS_{[X]}$ in the content below stand respectively for the spatial, flavor, spin, spin-flavor, and spatial-spin-flavor symmetries. $OFS_{[31]}$ and $FS_{[4]}$, $FS_{[31]}$, $FS_{[211]}$, $FS_{[22]}$, $FS_{[1111]}$ wave functions are listed separately in Tables A.1, A.2, A.3, A.4, A.5 and A.6.

Table A.1 Explicit $OFS_{[31]}$ wave functions in $O_{[X]}$ and $FS_{[X]}$ configurations.

$O_{[X]}\ FS_{[X]}$	$OFS_{[31]}$ Type	Explicit wave function
$O_{[4]}FS_{[31]}$	ρ	$\phi^{o}_{[4]_S}\phi^{sf}_{[31]_\rho}$
	λ	$\phi^{o}_{[4]_S}\phi^{sf}_{[31]_\lambda}$
	η	$\phi^{o}_{[4]_S}\phi^{sf}_{[31]_\eta}$
$O_{[1111]}FS_{[211]}$	ρ	$\phi^{o}_{[1111]_A}\phi^{sf}_{[211]_\rho}$
	λ	$\phi^{o}_{[1111]_A}\phi^{sf}_{[211]_\lambda}$
	η	$\phi^{o}_{[1111]_A}\phi^{sf}_{[211]_\eta}$
$O_{[22]}FS_{[31]}$	ρ	$\frac{1}{2}\phi^{o}_{[22]_\lambda}\phi^{sf}_{[31]_\rho} + \frac{1}{2}\phi^{o}_{[22]_\rho}\phi^{sf}_{[31]_\lambda} - \frac{1}{\sqrt{2}}\phi^{o}_{[22]_\rho}\phi^{sf}_{[31]_\eta}$
	λ	$-\frac{1}{2}\phi^{o}_{[22]_\lambda}\phi^{sf}_{[31]_\lambda} + \frac{1}{2}\phi^{o}_{[22]_\rho}\phi^{sf}_{[31]_\rho} - \frac{1}{\sqrt{2}}\phi^{o}_{[22]_\lambda}\phi^{sf}_{[31]_\eta}$
	η	$-\frac{1}{\sqrt{2}}\phi^{o}_{[22]_\lambda}\phi^{sf}_{[31]_\lambda} - \frac{1}{\sqrt{2}}\phi^{o}_{[22]_\rho}\phi^{sf}_{[31]_\rho}$
$O_{[22]}FS_{[211]}$	ρ	$\frac{1}{2}\phi^{o}_{[22]_\rho}\phi^{sf}_{[211]_\lambda} + \frac{1}{2}\phi^{o}_{[22]_\lambda}\phi^{sf}_{[211]_\rho} + \frac{1}{\sqrt{2}}\phi^{o}_{[22]_\lambda}\phi^{sf}_{[211]_\eta}$
	λ	$-\frac{1}{2}\phi^{o}_{[22]_\lambda}\phi^{sf}_{[211]_\lambda} + \frac{1}{2}\phi^{o}_{[22]_\rho}\phi^{sf}_{[211]_\rho} - \frac{1}{\sqrt{2}}\phi^{o}_{[22]_\rho}\phi^{sf}_{[211]_\eta}$
	η	$\frac{1}{\sqrt{2}}\phi^{o}_{[22]_\lambda}\phi^{sf}_{[211]_\lambda} + \frac{1}{\sqrt{2}}\phi^{o}_{[22]_\rho}\phi^{sf}_{[211]_\rho}$
$O_{[211]}FS_{[31]}$	ρ	$\frac{1}{\sqrt{2}}\phi^{o}_{[211]_\eta}\phi^{sf}_{[31]_\lambda} + \frac{1}{\sqrt{2}}\phi^{o}_{[211]_\rho}\phi^{sf}_{[31]_\eta}$
	λ	$\frac{1}{\sqrt{2}}\phi^{o}_{[211]_\lambda}\phi^{sf}_{[31]_\eta} - \frac{1}{\sqrt{2}}\phi^{o}_{[211]_\eta}\phi^{sf}_{[31]_\rho}$
	η	$-\frac{1}{\sqrt{2}}\phi^{o}_{[211]_\lambda}\phi^{sf}_{[31]_\lambda} - \frac{1}{\sqrt{2}}\phi^{o}_{[211]_\rho}\phi^{sf}_{[31]_\rho}$
$O_{[211]}FS_{[211]}$	ρ	$\frac{1}{\sqrt{3}}\phi^{o}_{[211]_\lambda}\phi^{sf}_{[211]_\lambda} + \frac{1}{\sqrt{3}}\phi^{o}_{[211]_\rho}\phi^{sf}_{[211]_\lambda} - \frac{1}{\sqrt{6}}\phi^{o}_{[211]_\eta}\phi^{sf}_{[211]_\lambda} - \frac{1}{\sqrt{6}}\phi^{o}_{[211]_\lambda}\phi^{sf}_{[211]_\eta}$
	λ	$\frac{1}{\sqrt{3}}\phi^{o}_{[211]_\rho}\phi^{sf}_{[211]_\rho} + \frac{1}{\sqrt{6}}\phi^{o}_{[211]_\eta}\phi^{sf}_{[211]_\rho} + \frac{1}{\sqrt{6}}\phi^{o}_{[211]_\rho}\phi^{sf}_{[211]_\eta} - \frac{1}{\sqrt{3}}\phi^{o}_{[211]_\lambda}\phi^{sf}_{[211]_\lambda}$
	η	$-\frac{1}{\sqrt{6}}\phi^{o}_{[211]_\lambda}\phi^{sf}_{[211]_\lambda} - \frac{1}{\sqrt{6}}\phi^{o}_{[211]_\rho}\phi^{sf}_{[211]_\rho} + \frac{2}{\sqrt{6}}\phi^{o}_{[211]_\eta}\phi^{sf}_{[211]_\eta}$
$O_{[211]}FS_{[22]}$	ρ	$\frac{1}{2}\phi^{o}_{[211]_\lambda}\phi^{sf}_{[22]_\rho} + \frac{1}{2}\phi^{o}_{[211]_\rho}\phi^{sf}_{[22]_\lambda} + \frac{1}{\sqrt{2}}\phi^{o}_{[211]_\eta}\phi^{sf}_{[22]_\lambda}$
	λ	$-\frac{1}{2}\phi^{o}_{[211]_\lambda}\phi^{sf}_{[22]_\lambda} + \frac{1}{2}\phi^{o}_{[211]_\rho}\phi^{sf}_{[22]_\rho} - \frac{1}{\sqrt{2}}\phi^{o}_{[211]_\eta}\phi^{sf}_{[22]_\rho}$
	η	$\frac{1}{\sqrt{2}}\phi^{o}_{[211]_\lambda}\phi^{sf}_{[22]_\lambda} + \frac{1}{\sqrt{2}}\phi^{o}_{[211]_\rho}\phi^{sf}_{[22]_\rho}$

Table A.1 (Continued)

$O_{[X]}\ FS_{[X]}$	$OFS_{[31]}$ Type	Explicit wave function
$O_{[31]}FS_{[4]}$	ρ	$\phi^o_{[31]_\rho}\phi^{sf}_{[4]_S}$
	λ	$\phi^o_{[31]_\lambda}\phi^{sf}_{[4]_S}$
	η	$\phi^o_{[31]_\eta}\phi^{sf}_{[4]_S}$
$O_{[31]}FS_{[31]}$	ρ	$\frac{1}{\sqrt{3}}\phi^o_{[31]_\lambda}\phi^{sf}_{[31]_\rho} + \frac{1}{\sqrt{3}}\phi^o_{[31]_\rho}\phi^{sf}_{[31]_\lambda} + \frac{1}{\sqrt{6}}\phi^o_{[31]_\eta}\phi^{sf}_{[31]_\rho} + \frac{1}{\sqrt{6}}\phi^o_{[31]_\rho}\phi^{sf}_{[31]_\eta}$
	λ	$-\frac{1}{\sqrt{3}}\phi^o_{[31]_\lambda}\phi^{sf}_{[31]_\lambda} + \frac{1}{\sqrt{3}}\phi^o_{[31]_\rho}\phi^{sf}_{[31]_\rho} + \frac{1}{\sqrt{6}}\phi^o_{[31]_\eta}\phi^{sf}_{[31]_\lambda} + \frac{1}{\sqrt{6}}\phi^o_{[31]_\lambda}\phi^{sf}_{[31]_\eta}$
	η	$\frac{1}{\sqrt{6}}\phi_{[31]_\lambda}\phi^{sf}_{[31]_\lambda} + \frac{1}{\sqrt{6}}\phi_{[31]_\rho}\phi^{sf}_{[31]_\rho} - \frac{2}{\sqrt{6}}\phi_{[31]_\eta}\phi^{sf}_{[31]_\eta}$
$O_{[31]}FS_{[211]}$	ρ	$\frac{1}{\sqrt{2}}\phi^o_{[31]_\lambda}\phi^{sf}_{[211]_\eta} + \frac{1}{\sqrt{2}}\phi^o_{[31]_\eta}\phi^{sf}_{[211]_\rho}$
	λ	$\frac{1}{\sqrt{2}}\phi^o_{[31]_\eta}\phi^{sf}_{[211]_\lambda} - \frac{1}{\sqrt{2}}\phi^o_{[31]_\rho}\phi^{sf}_{[211]_\eta}$
	η	$-\frac{1}{\sqrt{2}}\phi^o_{[31]_\lambda}\phi^{sf}_{[211]_\lambda} - \frac{1}{\sqrt{2}}\phi^o_{[31]_\rho}\phi^{sf}_{[211]_\rho}$
$O_{[31]}FS_{[22]}$	ρ	$\frac{1}{2}\phi^o_{[31]_\lambda}\phi^{sf}_{[22]_\rho} + \frac{1}{2}\phi^o_{[31]_\rho}\phi^{sf}_{[22]_\lambda} - \frac{1}{\sqrt{2}}\phi^o_{[31]_\eta}\phi^{sf}_{[22]_\rho}$
	λ	$-\frac{1}{2}\phi^o_{[31]_\lambda}\phi^{sf}_{[22]_\lambda} + \frac{1}{2}\phi^o_{[31]_\rho}\phi^{sf}_{[22]_\rho} - \frac{1}{\sqrt{2}}\phi^o_{[31]_\eta}\phi^{sf}_{[22]_\lambda}$
	η	$-\frac{1}{\sqrt{2}}\phi^o_{[31]_\lambda}\phi^{sf}_{[22]_\lambda} - \frac{1}{\sqrt{2}}\phi^o_{[31]_\rho}\phi^{sf}_{[22]_\rho}$

Table A.2 Explicit $FS_{[4]}$ wave functions in $F_{[X]}$ and $S_{[X]}$ configurations.

$F_{[X]}\ S_{[X]}$	$FS_{[4]}$ Type	Explicit wave function
$F_{[4]}S_{[4]}$	S	$\phi_{[4]_S}\chi_{[4]_S}$
$F_{[31]}S_{[31]}$	S	$\frac{1}{\sqrt{3}}\phi_{[31]_\lambda}\chi_{[31]_\lambda} + \frac{1}{\sqrt{3}}\phi_{[31]_\rho}\chi_{[31]_\rho} + \frac{1}{\sqrt{3}}\phi_{[31]_\eta}\chi_{[31]_\eta}$
$F_{[22]}S_{[22]}$	S	$\frac{1}{\sqrt{2}}\phi_{[22]_\lambda}\chi_{[22]_\lambda} + \frac{1}{\sqrt{2}}\phi_{[22]_\rho}\chi_{[22]_\rho}$

Table A.3 Explicit $FS_{[31]}$ wave functions in $F_{[X]}$ and $S_{[X]}$ configurations.

$F_{[X]}\ S_{[X]}$	$FS_{[31]}$ Type	Explicit wave function
$F_{[4]}S_{[31]}$	ρ	$\phi_{[4]_S}\chi_{[31]_\rho}$

Table A.3 (Continued)

$F_{[X]}\ S_{[X]}$	$FS_{[31]}$ Type	Explicit wave function
	λ	$\phi_{[4]_S}\chi_{[31]_\lambda}$
	η	$\phi_{[4]_S}\chi_{[31]_\eta}$
$F_{[31]}S_{[4]}$	ρ	$\phi_{[31]_\rho}\chi_{[4]_S}$
	λ	$\phi_{[31]_\lambda}\chi_{[4]_S}$
	η	$\phi_{[31]_\eta}\chi_{[4]_S}$
$F_{[31]}S_{[31]}$	ρ	$\frac{1}{\sqrt{3}}\phi_{[31]_\lambda}\chi_{[31]_\rho}\ +\ \frac{1}{\sqrt{3}}\phi_{[31]_\rho}\chi_{[31]_\lambda}\ +\ \frac{1}{\sqrt{6}}\phi_{[31]_\eta}\chi_{[31]_\rho}\ +$ $\frac{1}{\sqrt{6}}\phi_{[31]_\rho}\chi_{[31]_\eta}$
	λ	$-\frac{1}{\sqrt{3}}\phi_{[31]_\lambda}\chi_{[31]_\lambda}\ +\ \frac{1}{\sqrt{3}}\phi_{[31]_\rho}\chi_{[31]_\rho}\ +\ \frac{1}{\sqrt{6}}\phi_{[31]_\eta}\chi_{[31]_\lambda}\ +$ $\frac{1}{\sqrt{6}}\phi_{[31]_\lambda}\chi_{[31]_\eta}$
	η	$\frac{1}{\sqrt{6}}\phi_{[31]_\lambda}\chi_{[31]_\lambda}\ +\ \frac{1}{\sqrt{6}}\phi_{[31]_\rho}\chi_{[31]_\rho}\ -\ \frac{2}{\sqrt{6}}\phi_{[31]_\eta}\chi_{[31]_\eta}$
$F_{[31]}FS_{[22]}$	ρ	$\frac{1}{2}\phi_{[31]_\lambda}\chi_{[22]_\rho}+\frac{1}{2}\phi_{[31]_\rho}\chi_{[22]_\lambda}-\frac{1}{\sqrt{2}}\phi_{[31]_\eta}\chi_{[22]_\rho}$
	λ	$-\frac{1}{2}\phi_{[31]_\lambda}\chi_{[22]_\lambda}+\frac{1}{2}\phi_{[31]_\rho}\chi_{[22]_\rho}-\frac{1}{\sqrt{2}}\phi_{[31]_\eta}\chi_{[22]_\lambda}$
	η	$-\frac{1}{\sqrt{2}}\phi_{[31]_\lambda}\chi_{[22]_\lambda}-\frac{1}{\sqrt{2}}\phi_{[31]_\rho}\chi_{[22]_\rho}$
$F_{[211]}S_{[31]}$	ρ	$\frac{1}{\sqrt{2}}\phi_{[211]_\eta}\chi_{[31]_\lambda}+\frac{1}{\sqrt{2}}\phi_{[211]_\rho}\chi_{[31]_\eta}$
	λ	$\frac{1}{\sqrt{2}}\phi_{[211]_\lambda}\chi_{[31]_\eta}-\frac{1}{\sqrt{2}}\phi_{[211]_\eta}\chi_{[31]_\rho}$
	η	$-\frac{1}{\sqrt{2}}\phi_{[211]_\lambda}\chi_{[31]_\lambda}-\frac{1}{\sqrt{2}}\phi_{[211]_\rho}\chi_{[31]_\rho}$
$F_{[211]}S_{[22]}$	ρ	$\frac{1}{2}\phi_{[211]_\lambda}\chi_{[22]_\rho}+\frac{1}{2}\phi_{[211]_\rho}\chi_{[22]_\lambda}+\frac{1}{\sqrt{2}}\phi_{[211]_\eta}\chi_{[22]_\lambda}$
	λ	$-\frac{1}{2}\phi_{[211]_\lambda}\chi_{[22]_\lambda}+\frac{1}{2}\phi_{[211]_\rho}\chi_{[22]_\rho}-\frac{1}{\sqrt{2}}\phi_{[211]_\eta}\chi_{[22]_\rho}$
	η	$\frac{1}{\sqrt{2}}\phi_{[211]_\lambda}\chi_{[22]_\lambda}+\frac{1}{\sqrt{2}}\phi_{[211]_\rho}\chi_{[22]_\rho}$
$F_{[22]}S_{[31]}$	ρ	$\frac{1}{2}\phi_{[22]_\lambda}\chi_{[31]_\rho}+\frac{1}{2}\phi_{[22]_\rho}\chi_{[31]_\lambda}-\frac{1}{\sqrt{2}}\phi_{[22]_\rho}\chi_{[31]_\eta}$
	λ	$-\frac{1}{2}\phi_{[22]_\lambda}\chi_{[31]_\lambda}+\frac{1}{2}\phi_{[22]_\rho}\chi_{[31]_\rho}-\frac{1}{\sqrt{2}}\phi_{[22]_\lambda}\chi_{[31]_\eta}$
	η	$-\frac{1}{\sqrt{2}}\phi_{[22]_\lambda}\chi_{[31]_\lambda}-\frac{1}{\sqrt{2}}\phi_{[22]_\rho}\chi_{[31]_\rho}$

Table A.4 Explicit $FS_{[211]}$ wave functions in $F_{[X]}$ and $S_{[X]}$ configurations.

$F_{[X]}\ S_{[X]}$	$FS_{[211]}$ Type	Explicit wave function
$F_{[31]}S_{[31]}$	ρ	$\frac{1}{\sqrt{2}}\phi_{[31]_\eta}\chi_{[31]_\rho} - \frac{1}{\sqrt{2}}\phi_{[31]_\rho}\chi_{[31]_\eta}$
	λ	$\frac{1}{\sqrt{2}}\phi_{[31]_\eta}\chi_{[31]_\lambda} - \frac{1}{\sqrt{2}}\phi_{[31]_\lambda}\chi_{[31]_\eta}$
	η	$\frac{1}{\sqrt{2}}\phi_{[31]_\lambda}\chi_{[31]_\rho} - \frac{1}{\sqrt{2}}\phi_{[31]_\rho}\chi_{[31]_\lambda}$
$F_{[31]}S_{[22]}$	ρ	$\frac{1}{2}\phi_{[31]_\lambda}\chi_{[22]_\rho} + \frac{1}{2}\phi_{[31]_\rho}\chi_{[22]_\lambda} + \frac{1}{\sqrt{2}}\phi_{[31]_\eta}\chi_{[22]_\rho}$
	λ	$-\frac{1}{2}\phi_{[31]_\lambda}\chi_{[22]_\lambda} + \frac{1}{2}\phi_{[31]_\rho}\chi_{[22]_\rho} + \frac{1}{\sqrt{2}}\phi_{[31]_\eta}\chi_{[22]_\lambda}$
	η	$\frac{1}{\sqrt{2}}\phi_{[31]_\rho}\chi_{[22]_\lambda} - \frac{1}{\sqrt{2}}\phi_{[31]_\lambda}\chi_{[22]_\rho}$
$F_{[211]}S_{[4]}$	ρ	$\phi_{[211]_\rho}\chi_{[4]_S}$
	λ	$\phi_{[211]_\lambda}\chi_{[4]_S}$
	η	$\phi_{[211]_\eta}\chi_{[4]_S}$
$F_{[211]}S_{[31]}$	ρ	$\frac{1}{\sqrt{3}}\phi_{[211]_\lambda}\chi_{[31]_\rho} + \frac{1}{\sqrt{3}}\phi_{[211]_\rho}\chi_{[31]_\lambda} + \frac{1}{\sqrt{6}}\phi_{[211]_\eta}\chi_{[31]_\lambda} - \frac{1}{\sqrt{6}}\phi_{[211]_\rho}\chi_{[31]_\eta}$
	λ	$-\frac{1}{\sqrt{3}}\phi_{[211]_\lambda}\chi_{[31]_\lambda} + \frac{1}{\sqrt{3}}\phi_{[211]_\rho}\chi_{[31]_\rho} - \frac{1}{\sqrt{6}}\phi_{[211]_\eta}\chi_{[31]_\rho} - \frac{1}{\sqrt{6}}\phi_{[211]_\lambda}\chi_{[31]_\eta}$
	η	$\frac{1}{\sqrt{6}}\phi_{[211]_\lambda}\chi_{[31]_\rho} - \frac{1}{\sqrt{6}}\phi_{[211]_\rho}\chi_{[31]_\lambda} + \frac{2}{\sqrt{6}}\phi_{[211]_\eta}\chi_{[31]_\eta}$
$F_{[211]}FS_{[22]}$	ρ	$\frac{1}{2}\phi_{[211]_\lambda}\chi_{[22]_\rho} + \frac{1}{2}\phi_{[211]_\rho}\chi_{[22]_\lambda} - \frac{1}{\sqrt{2}}\phi_{[211]_\eta}\chi_{[22]_\lambda}$
	λ	$-\frac{1}{2}\phi_{[211]_\lambda}\chi_{[22]_\lambda} + \frac{1}{2}\phi_{[211]_\rho}\chi_{[22]_\rho} + \frac{1}{\sqrt{2}}\phi_{[211]_\eta}\chi_{[22]_\rho}$
	η	$-\frac{1}{\sqrt{2}}\phi_{[211]_\rho}\chi_{[22]_\lambda} + \frac{1}{\sqrt{2}}\phi_{[211]_\lambda}\chi_{[22]_\rho}$
$F_{[22]}S_{[31]}$	ρ	$\frac{1}{2}\phi_{[22]_\lambda}\chi_{[31]_\rho} + \frac{1}{2}\phi_{[22]_\rho}\chi_{[31]_\lambda} + \frac{1}{\sqrt{2}}\phi_{[22]_\rho}\chi_{[31]_\eta}$
	λ	$-\frac{1}{2}\phi_{[22]_\lambda}\chi_{[31]_\lambda} + \frac{1}{2}\phi_{[22]_\rho}\chi_{[31]_\rho} + \frac{1}{\sqrt{2}}\phi_{[22]_\lambda}\chi_{[31]_\eta}$
	η	$-\frac{1}{\sqrt{2}}\phi_{[22]_\rho}\chi_{[31]_\lambda} + \frac{1}{\sqrt{2}}\phi_{[22]_\lambda}\chi_{[31]_\rho}$

Table A.5 Explicit $FS_{[22]}$ wave functions in $F_{[X]}$ and $S_{[X]}$ configurations.

$F_{[X]}\ S_{[X]}$	$FS_{[22]}$ Type	Explicit wave function
$F_{[4]}S_{[22]}$	ρ	$\phi_{[4]_S}\chi_{[22]_\rho}$

Table A.5 (Continued)

$F_{[X]}\ S_{[X]}$	$FS_{[22]}$ Type	Explicit wave function
	λ	$\phi_{[4]_S}\chi_{[22]_\lambda}$
$F_{[31]}S_{[31]}$	ρ	$\frac{1}{\sqrt{3}}\phi_{[31]_\lambda}\chi_{[31]_\rho} + \frac{1}{\sqrt{3}}\phi_{[31]_\rho}\chi_{[31]_\lambda} - \frac{1}{\sqrt{6}}\phi_{[31]_\eta}\chi_{[31]_\rho} - \frac{1}{\sqrt{6}}\phi_{[31]_\rho}\chi_{[31]_\eta}$
	λ	$-\frac{1}{\sqrt{3}}\phi_{[31]_\lambda}\chi_{[31]_\lambda} + \frac{1}{\sqrt{3}}\phi_{[31]_\rho}\chi_{[31]_\rho} - \frac{1}{\sqrt{6}}\phi_{[31]_\eta}\chi_{[31]_\lambda} - \frac{1}{\sqrt{6}}\phi_{[31]_\lambda}\chi_{[31]_\eta}$
$F_{[211]}S_{[31]}$	ρ	$\frac{1}{\sqrt{3}}\phi_{[211]_\lambda}\chi_{[31]_\rho} + \frac{1}{\sqrt{3}}\phi_{[211]_\rho}\chi_{[31]_\lambda} - \frac{1}{\sqrt{6}}\phi_{[211]_\eta}\chi_{[31]_\lambda} + \frac{1}{\sqrt{6}}\phi_{[211]_\rho}\chi_{[31]_\eta}$
	λ	$-\frac{1}{\sqrt{3}}\phi_{[211]_\lambda}\chi_{[31]_\lambda} + \frac{1}{\sqrt{3}}\phi_{[211]_\rho}\chi_{[31]_\rho} + \frac{1}{\sqrt{6}}\phi_{[211]_\eta}\chi_{[31]_\rho} + \frac{1}{\sqrt{6}}\phi_{[211]_\lambda}\chi_{[31]_\eta}$
$F_{[22]}S_{[4]}$	ρ	$\phi_{[22]_\rho}\chi_{[4]_S}$
	λ	$\phi_{[22]_\lambda}\chi_{[4]_S}$
$F_{[22]}S_{[22]}$	ρ	$\frac{1}{\sqrt{2}}\phi_{[22]_\rho}\chi_{[22]_\lambda} + \frac{1}{\sqrt{2}}\phi_{[22]_\lambda}\chi_{[22]_\rho}$
	λ	$-\frac{1}{\sqrt{2}}\phi_{[22]_\lambda}\chi_{[22]_\lambda} + \frac{1}{\sqrt{2}}\phi_{[22]_\rho}\chi_{[22]_\rho}$

Table A.6 Explicit $FS_{[1111]}$ wave functions in $F_{[X]}$ and $S_{[X]}$ configurations.

$F_{[X]}\ S_{[X]}$	$FS_{[1111]}$ Type	Explicit wave function
$F_{[211]}S_{[31]}$	A	$-\frac{1}{\sqrt{3}}\phi_{[211]_\rho}\chi_{[31]_\lambda} + \frac{1}{\sqrt{3}}\phi_{[211]_\lambda}\chi_{[31]_\rho} + \frac{1}{\sqrt{3}}\phi_{[211]_\eta}\chi_{[31]_\eta}$
$F_{[22]}S_{[22]}$	A	$-\frac{1}{\sqrt{2}}\phi_{[22]_\rho}\chi_{[22]_\lambda} + \frac{1}{\sqrt{2}}\phi_{[22]_\lambda}\chi_{[22]_\rho}$

The hyperfine contributions $\Delta M^{OGE}(q^4\bar{q})$ in Eq. (A.14) show the detailed dependence of pentaquark hyperfine interaction on the color-spin-flavor wave function.

Table A.7 Expectation values of spin configuration [22] with pentaquark spin $s = 1/2$

$\vec{\sigma}_i \cdot \vec{\sigma}_j$	12	13	23	14	24	34	15	25	35	45
$\langle \vec{\sigma}_i^\rho \cdot \vec{\sigma}_j^\rho \rangle$	-3	0	0	0	0	-3	0	0	0	0
$\langle \vec{\sigma}_i^\rho \cdot \vec{\sigma}_j^\lambda \rangle$	0	$-\sqrt{3}$	$\sqrt{3}$	$\sqrt{3}$	$-\sqrt{3}$	0	0	0	0	0
$\langle \vec{\sigma}_i^\lambda \cdot \vec{\sigma}_j^\lambda \rangle$	1	-2	-2	-2	-2	1	0	0	0	0

$$\Delta M^{OGE}(q^4\bar{q}) = \langle \psi(q^4\bar{q}) | H_{OGE}(q^4\bar{q}) | \psi(q^4\bar{q}) \rangle$$

$$= -\frac{m_u^2}{3m_i m_j} C_G \left(\langle \psi^c_{[211]_\lambda} | \lambda_i^C \cdot \lambda_j^C | \psi^c_{[211]_\lambda} \rangle \langle \psi^{sf}_{[31]_\rho} | \vec{\sigma}_i \cdot \vec{\sigma}_j | \psi^{sf}_{[31]_\rho} \rangle \right.$$

$$-2\langle \psi^c_{[211]_\lambda} | \lambda_i^C \cdot \lambda_j^C | \psi^c_{[211]_\rho} \rangle \langle \psi^{sf}_{[31]_\lambda} | \vec{\sigma}_i \cdot \vec{\sigma}_j | \psi^{sf}_{[31]_\rho} \rangle$$

$$+2\langle \psi^c_{[211]_\lambda} | \lambda_i^C \cdot \lambda_j^C | \psi^c_{[211]_\eta} \rangle \langle \psi^{sf}_{[31]_\rho} | \vec{\sigma}_i \cdot \vec{\sigma}_j | \psi^{sf}_{[31]_\eta} \rangle$$

$$+\langle \psi^c_{[211]_\rho} | \lambda_i^C \cdot \lambda_j^C | \psi^c_{[211]_\rho} \rangle \langle \psi^{sf}_{[31]_\lambda} | \vec{\sigma}_i \cdot \vec{\sigma}_j | \psi^{sf}_{[31]_\lambda} \rangle$$

$$-2\langle \psi^c_{[211]_\rho} | \lambda_i^C \cdot \lambda_j^C | \psi^c_{[211]_\eta} \rangle \langle \psi^{sf}_{[31]_\lambda} | \vec{\sigma}_i \cdot \vec{\sigma}_j | \psi^{sf}_{[31]_\eta} \rangle$$

$$+\left. \langle \psi^c_{[211]_\eta} | \lambda_i^C \cdot \lambda_j^C | \psi^c_{[211]_\eta} \rangle \langle \psi^{sf}_{[31]_\eta} | \vec{\sigma}_i \cdot \vec{\sigma}_j | \psi^{sf}_{[31]_\eta} \rangle \right)$$

$$\text{(A.14)}$$

Where the expectation values $\langle \psi^c_{[211]_x} | \lambda_i^C \cdot \lambda_j^C | \psi^c_{[211]_y} \rangle$ for [211] color configuration and $\langle \psi^{sf}_{[31]_x} | \vec{\sigma}_i \cdot \vec{\sigma}_j | \psi^{sf}_{[31]_y} \rangle$ for different spin configurations are simplified as $\lambda_i^C \cdot \lambda_j^C$ and $\vec{\sigma}_i \cdot \vec{\sigma}_j$. The s quark mass m_s is different from u and d quark mass for the flavor correction, so as for the heavy quark masses m_c and m_b. The expectation values for each quark pair in pentaquark state for spin configuration [22] and [31] are listed in Tables A.7, A.8 and A.9.

Spin configuration [4] with total pentaquark spin 5/2 have all expectation values as 1 between every quark pair in pentaquark state, while all expectation values of the quark-antiquark pair change to -1 when total pentaquark spin equal 3/2.

Table A.8 Expectation values of spin configuration [31] with pentaquark spin $s = 1/2$

$\vec{\sigma}_i \cdot \vec{\sigma}_j$	12	13	23	14	24	34	15	25	35	45
$\langle \vec{\sigma}_i^{\rho} \cdot \vec{\sigma}_j^{\rho} \rangle$	-3	0	0	0	0	1	0	0	-2	-2
$\langle \vec{\sigma}_i^{\lambda} \cdot \vec{\sigma}_j^{\lambda} \rangle$	1	-2	-2	$\frac{2}{3}$	$\frac{2}{3}$	$-\frac{1}{3}$	$-\frac{4}{3}$	$-\frac{4}{3}$	$\frac{2}{3}$	-2
$\langle \sigma_i^{\eta} \cdot \sigma_j^{\eta} \rangle$	1	1	1	$-\frac{5}{3}$	$-\frac{5}{3}$	$-\frac{5}{3}$	$-\frac{5}{3}$	$-\frac{5}{3}$	$-\frac{5}{3}$	1
$\langle \vec{\sigma}_i^{\rho} \cdot \vec{\sigma}_j^{\lambda} \rangle$	0	$-\sqrt{3}$	$\sqrt{3}$	$-\frac{1}{\sqrt{3}}$	$\frac{1}{\sqrt{3}}$	0	$\frac{2}{\sqrt{3}}$	$-\frac{2}{\sqrt{3}}$	0	0
$\langle \vec{\sigma}_i^{\rho} \cdot \vec{\sigma}_j^{\eta} \rangle$	0	0	0	$-\frac{2\sqrt{6}}{3}$	$\frac{2\sqrt{6}}{3}$	0	$\frac{\sqrt{6}}{3}$	$-\frac{\sqrt{6}}{3}$	0	0
$\langle \vec{\sigma}_i^{\lambda} \cdot \vec{\sigma}_j^{\eta} \rangle$	0	0	0	$-\frac{2\sqrt{2}}{3}$	$-\frac{2\sqrt{2}}{3}$	$\frac{4\sqrt{2}}{3}$	$\frac{\sqrt{2}}{3}$	$\frac{\sqrt{2}}{3}$	$-\frac{2\sqrt{2}}{3}$	0

The expectation values for each quark pair in pentaquark state for color configuration [211] is listed in Table A.10.

Table A.9 Expectation values of spin configuration [31] with pentaquark spin $s = 3/2$

$\vec{\sigma}_i \cdot \vec{\sigma}_j$	12	13	23	14	24	34	15	25	35	45
$\langle \vec{\sigma}_i^\rho \cdot \vec{\sigma}_j^\rho \rangle$	-3	0	0	0	0	1	0	0	1	1
$\langle \vec{\sigma}_i^\lambda \cdot \vec{\sigma}_j^\lambda \rangle$	1	-2	-2	$\frac{2}{3}$	$\frac{2}{3}$	$-\frac{1}{3}$	$\frac{2}{3}$	$\frac{2}{3}$	$-\frac{1}{3}$	1
$\langle \sigma_i^\eta \cdot \sigma_j^\eta \rangle$	1	1	1	$-\frac{5}{3}$	$-\frac{5}{3}$	$-\frac{5}{3}$	$\frac{5}{6}$	$\frac{5}{6}$	$\frac{5}{6}$	$-\frac{1}{2}$
$\langle \vec{\sigma}_i^\rho \cdot \vec{\sigma}_j^\lambda \rangle$	0	$-\sqrt{3}$	$\sqrt{3}$	$-\frac{1}{\sqrt{3}}$	$\frac{1}{\sqrt{3}}$	0	$-\frac{1}{\sqrt{3}}$	$\frac{1}{\sqrt{3}}$	0	0
$\langle \vec{\sigma}_i^\rho \cdot \vec{\sigma}_j^\eta \rangle$	0	0	0	$-\frac{2\sqrt{6}}{3}$	$\frac{2\sqrt{6}}{3}$	0	$-\frac{\sqrt{6}}{6}$	$\frac{\sqrt{6}}{6}$	0	0
$\langle \vec{\sigma}_i^\lambda \cdot \vec{\sigma}_j^\eta \rangle$	0	0	0	$-\frac{2\sqrt{2}}{3}$	$-\frac{2\sqrt{2}}{3}$	$\frac{4\sqrt{2}}{3}$	$-\frac{\sqrt{2}}{6}$	$-\frac{\sqrt{2}}{6}$	$\frac{\sqrt{2}}{3}$	0

Table A.10 Expectation values of color configuration [211]

$\lambda_i \cdot \lambda_j$	12	13	23	14	24	34	15	25	35	45
$\langle \lambda_i^\rho \cdot \lambda_j^\rho \rangle$	$-\frac{8}{3}$	$\frac{1}{3}$	$\frac{1}{3}$	$-\frac{7}{3}$	$-\frac{7}{3}$	$-\frac{4}{3}$	$-\frac{2}{3}$	$-\frac{2}{3}$	$-\frac{14}{3}$	$\frac{2}{3}$
$\langle \lambda_i^\lambda \cdot \lambda_j^\lambda \rangle$	$\frac{4}{3}$	$-\frac{5}{3}$	$-\frac{5}{3}$	$-\frac{5}{3}$	$-\frac{5}{3}$	$-\frac{8}{3}$	$-\frac{10}{3}$	$-\frac{10}{3}$	$\frac{2}{3}$	$\frac{2}{3}$
$\langle \lambda_i^\eta \cdot \lambda_j^\eta \rangle$	$-\frac{8}{3}$	$-\frac{8}{3}$	$-\frac{8}{3}$	0	0	0	0	0	0	$-\frac{16}{3}$
$\langle \lambda_i^\rho \cdot \lambda_j^\lambda \rangle$	0	$-\sqrt{3}$	$\sqrt{3}$	$-\frac{1}{\sqrt{3}}$	$\frac{1}{\sqrt{3}}$	0	$\frac{4}{\sqrt{3}}$	$-\frac{4}{\sqrt{3}}$	0	0
$\langle \lambda_i^\rho \cdot \lambda_j^\eta \rangle$	0	0	0	$-\frac{2\sqrt{2}}{3}$	$-\frac{2\sqrt{2}}{3}$	$\frac{4\sqrt{2}}{3}$	$\frac{2\sqrt{2}}{3}$	$\frac{2\sqrt{2}}{3}$	$-\frac{4\sqrt{2}}{3}$	0
$\langle \lambda_i^\lambda \cdot \lambda_j^\eta \rangle$	0	0	0	$\frac{4}{\sqrt{6}}$	$-\frac{4}{\sqrt{6}}$	0	$-\frac{4}{\sqrt{6}}$	$\frac{4}{\sqrt{6}}$	0	0

APPENDIX B

q^3 AND $q^4\bar{q}$ FULL WAVE FUNCTION IN SU(3) FLAVOR SYMMETRY

B.1 q^3 Color-spin-flavor Wave Functions

In this Appendix the q^3 color-spatial-spin-flavor wave functions with the principle quantum number $N \leq 2$ are listed in Table B.1, where χ_i, Φ_j, and $\phi_{L'M'y}^{N'}$ are the spin, flavor, and spatial wave functions, respectively. And flavor singlet 20 supermultiplets are not discussed here. The $SU(3)_F$ singlet states are excluded since only nucleon and Δ resonances are discussed. The wave functions of baryon octet and decuplet states refer to group theory lecture notes in our group.

Out of the $3^3 \times 2^3 = 216$ baryonic supermultiplets, derived are 56 symmetric, 70 ρ-type, 70 λ-type, and 20 antisymmetric states listed as follows:

$$
\begin{aligned}
S: & & (\mathbf{10}, \mathbf{4}) + (\mathbf{8}, \mathbf{2}) &= \mathbf{56} \\
\lambda: & \ (\mathbf{10}, \mathbf{2}) + (\mathbf{8}, \mathbf{4}) + (\mathbf{8}, \mathbf{2}) + (\mathbf{1}, \mathbf{2}) &= \mathbf{70} \\
\rho: & \ (\mathbf{10}, \mathbf{2}) + (\mathbf{8}, \mathbf{4}) + (\mathbf{8}, \mathbf{2}) + (\mathbf{1}, \mathbf{2}) &= \mathbf{70} \\
A: & & (\mathbf{8}, \mathbf{2}) + (\mathbf{1}, \mathbf{4}) &= \mathbf{20}
\end{aligned}
\tag{B.1}
$$

Table B.1 Explicit q^3 orbital-spin-flavor wave functions.

	$SU(6)_{SF}$	l^P	$SU(6)_{SF} \times O(3)$ wave functions	
N	Rep.	O(3)	$SU(3)_F$ octet	$SU(3)_F$ decuplet
0	56	0^+	$J^P = \frac{1}{2}^+$	$J^P = \frac{3}{2}^+$
			$\frac{1}{\sqrt{2}}\phi^0_{00s}(\Phi_\lambda\chi_\rho + \Phi_\rho\chi_\lambda)$	$\phi^0_{00S}\Phi_S\chi_S$
1	70	1^-	$J^P = \frac{1}{2}^-, \frac{3}{2}^-$	$J^P = \frac{1}{2}^-, \frac{3}{2}^-$
			$\frac{1}{2}[\phi^1_{1m\rho}(\Phi_\lambda\chi_\rho + \Phi_\rho\chi_\lambda) +$	$\frac{1}{\sqrt{2}}\Phi_S(\phi^1_{1m\lambda}\chi_\lambda + \phi^1_{1m\rho}\chi_\rho)$
			$\phi^1_{1m\lambda}(\Phi_\rho\chi_\rho - \Phi_\lambda\chi_\lambda)]$	
			$J^P = \frac{1}{2}^-, \frac{3}{2}^-, \frac{5}{2}^-$	
			$\frac{1}{\sqrt{2}}\chi_S(\phi^1_{1m\lambda}\Phi_\lambda + \phi^1_{1m\rho}\Phi_\rho)$	
2	56	0^+	$J^P = \frac{1}{2}^+$	$J^P = \frac{3}{2}^+$
			$\frac{1}{\sqrt{2}}\phi^2_{00s}(\Phi_\lambda\chi_\rho + \Phi_\rho\chi_\lambda)$	$\Phi_S\phi^2_{00S}\chi_S$
	70	0^+	$J^P = \frac{1}{2}^+$	$J^P = \frac{1}{2}^+$
			$\frac{1}{2}[\phi^2_{00\rho}(\Phi_\lambda\chi_\rho + \Phi_\rho\chi_\lambda) +$	$\frac{1}{\sqrt{2}}\Phi_S(\phi^2_{00\lambda}\chi_\lambda + \phi^2_{00\rho}\chi_\rho)$
			$\phi^2_{00\lambda}(\Phi_\rho\chi_\rho - \Phi_\lambda\chi_\lambda)]$	
			$J^P = \frac{3}{2}^+$	
			$\frac{1}{\sqrt{2}}\chi_S(\phi^2_{00\lambda}\Phi_\lambda + \phi^2_{00\rho}\Phi_\rho)$	
2	56	2^+	$J^P = \frac{3}{2}^+, \frac{5}{2}^+$	$J^P = \frac{1}{2}^+, \frac{3}{2}^+, \frac{5}{2}^+, \frac{7}{2}^+$
			$\frac{1}{\sqrt{2}}\phi^2_{2mS}(\Phi_\rho\chi_\rho + \Phi_\lambda\chi_\lambda)$	$\phi^2_{2mS}\Phi_S\chi_S$
	70	2^+	$J^P = \frac{3}{2}^+, \frac{5}{2}^+$	$J^P = \frac{3}{2}^+, \frac{5}{2}^+$
			$\frac{1}{2}[\phi^2_{2m\rho}(\Phi_\lambda\chi_\rho + \Phi_\rho\chi_\lambda) +$	$\frac{1}{\sqrt{2}}\Phi_S(\phi^2_{2m\lambda}\chi_\lambda + \phi^2_{2m\rho}\chi_\rho)$
			$\phi^2_{2m\lambda}(\Phi_\rho\chi_\rho - \Phi_\lambda\chi_\lambda)]$	
			$J^P = \frac{1}{2}^+, \frac{3}{2}^+, \frac{5}{2}^+, \frac{7}{2}^+$	
			$\frac{1}{\sqrt{2}}\chi_S(\phi^2_{2m\lambda}\Phi_\lambda + \phi^2_{2m\rho}\Phi_\rho)$	

B.2 $q^4\bar{q}$ Color-spin-flavor Wave Functions

For q^4 systems, the projection operators according to Young tableaux of ρ, λ and η types, for example,

The projection operator of
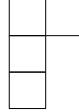
$$
\begin{aligned}
P_{[211]_\rho} = \;& 6 - 6(12) + 3(13) - 5(14) + 3(23) - 5(24) - 2(34) \\
& +2(12)(34) - 4(14)(23) - 4(13)(24) \\
& -3(123) + 5(124) - 3(132) - (134) + 5(142) - (143) - (234) - (243) \\
& (1234) + (1243) + 4(1324) + (1342) + 4(1423) + (1432),
\end{aligned}
$$

$$
\begin{aligned}
P_{[211]_\lambda} = \;& 2 + 2(12) - (13) - (14) - (23) - (24) - 2(34) \\
& -2(12)(34) \\
& -(123) - (124) - (132) + (134) - (142) + (143) + (234) + (243) \\
& +(1234) + (1243) + (1342) + (1432),
\end{aligned}
$$

$$
\begin{aligned}
P_{[211]_\eta} = \;& 3 - 3(12) - 3(13) + (14) - 3(23) + (24) + (34) \\
& -(12)(34) - (14)(23) - (13)(24) \\
& +3(123) - (124) + 3(132) - (134) - (142) - (143) - (234) - (243) \\
& +(1234) + (1243) + (1324) + (1342) + (1423) + (1432).
\end{aligned}
\tag{B.2}
$$

q^4 color wave functions can be derived by applying the λ-, ρ- and η-type projection operators of the S_4 $IR[211]$ in Yamanouchi basis,

$$
\left| \begin{array}{|c|c|} \hline 1 & 2 \\ \hline 3 \\ \hline 4 \\ \hline \end{array} , \begin{array}{|c|c|} \hline R & R \\ \hline G \\ \hline B \\ \hline \end{array} \right\rangle = P_{[211]_\lambda}(RRGB) \Longrightarrow \psi^c_{[211]_\lambda}(R) :
$$

$$
\frac{1}{\sqrt{16}} (2|RRGB\rangle - 2|RRBG\rangle - |GRRB\rangle - |RGRB\rangle - |BRGR\rangle
$$

$$
-|RBGR\rangle + |BRRG\rangle + |GRBR\rangle + |RBRG\rangle + |RGBR\rangle)
$$

$$
\left| \begin{array}{|c|c|} \hline 1 & 3 \\ \hline 2 \\ \hline 4 \\ \hline \end{array} , \begin{array}{|c|c|} \hline R & R \\ \hline G \\ \hline B \\ \hline \end{array} \right\rangle = P_{[211]_\rho}(RGRB) \Longrightarrow \psi^c_{[211]_\rho}(R) :
$$

$$\frac{1}{\sqrt{48}}(3|RGRB\rangle - 3|GRRB\rangle + 3|BRRG\rangle - 3|RBRG\rangle + 2|GBRR\rangle$$
$$-2|BGRR\rangle - |BRGR\rangle + |RBGR\rangle + |GRBR\rangle - |RGBR\rangle)$$

$$\left|\begin{array}{|c|c|}\hline 1 & 4 \\\hline 2 \\\hline 3 \\\hline\end{array}, \begin{array}{|c|}\hline R & R \\\hline G \\\hline B \\\hline\end{array}\right\rangle = P_{[211]_\eta}(RGBR) \Longrightarrow \psi^c_{[211]_\eta}(R):$$
$$\frac{1}{\sqrt{6}}(|RGBR\rangle + |GBRR\rangle + |BRGR\rangle - |RBGR\rangle - |GRBR\rangle - |BGRR\rangle)$$

The singlet color wave function $\Psi^c_{[211]_j}$ $(j = \lambda, \rho, \eta)$ of pentaquarks is given by

$$\Psi^c_{[211]_j} = \frac{1}{\sqrt{3}}\left(\psi^c_{[211]_j}(R)\,\bar{R} + \psi^c_{[211]_j}(G)\,\bar{G} + \psi^c_{[211]_j}(B)\,\bar{B}\right).$$

For the flavor wave function of q^4, for example, isospin and isospin projection as $I = 1, Iz = 1$, for $\begin{array}{|c|c|c|}\hline u & u & u \\\hline d \\\hline\end{array}$

$$P_{[31]_\lambda}(uudu) \implies \phi_{[31]_\lambda}(1,1) = \frac{1}{\sqrt{6}}\,|\,2uudu - duuu - uduu\,\rangle$$
$$P_{[31]_\rho}(uduu) \implies \phi_{[31]_\rho}(1,1) = \frac{1}{\sqrt{2}}\,|\,uduu - duuu\,\rangle$$
$$P_{[31]_\eta}(uuud) \implies \phi_{[31]_\eta}(1,1) = \frac{1}{2\sqrt{3}}\,|\,3uuud - duuu - uduu - uudu\,\rangle \quad\text{(B.3)}$$

The isospin of pentaquark state $I = \frac{3}{2}$,

$$\phi(q^4\bar{q})_{[31]_\lambda}(\frac{3}{2},\frac{3}{2}) = \phi(Iq^4 = 1, m_{q^4} = 1)_{[31]_\lambda}\phi(I\bar{q} = 1/2, Iz\bar{q} = 1/2)$$
$$= \frac{1}{\sqrt{6}}\,|\,2uudu\bar{u} - duuu\bar{u} - uduu\bar{u}\,\rangle$$
$$\phi(q^4\bar{q})_{[31]_\rho}(\frac{3}{2},\frac{3}{2}) = \phi(Iq^4 = 1, m_{q^4} = 1)_{[31]_\rho}\phi(I\bar{q} = 1/2, Iz\bar{q} = 1/2)$$
$$= \frac{1}{\sqrt{2}}\,|\,uduu\bar{u} - duuu\bar{u}\,\rangle$$
$$\phi(q^4\bar{q})_{[31]_\eta}(\frac{3}{2},\frac{3}{2}) = \phi(Iq^4 = 1, m_{q^4} = 1)_{[31]_\eta}\phi(I\bar{q} = 1/2, Iz\bar{q} = 1/2)$$
$$= \frac{1}{2\sqrt{3}}\,|\,3uuud\bar{u} - duuu\bar{u} - uduu\bar{u} - uudu\bar{u}\,\rangle \quad\text{(B.4)}$$

To be noticed, for flavor configuration [211], there is no possible choices for non-strange q^4 states.

For the flavor wave function of q^4, for example, $S = 1, m_s = 1$, for $\boxed{\uparrow\,\uparrow\,\uparrow}$ $\boxed{\downarrow}$
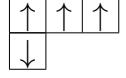
$$P_{[31]_\lambda}(\uparrow\uparrow\downarrow\uparrow) \implies \chi_{[31]_\lambda}(1,1) = \frac{1}{\sqrt{6}} \mid 2\uparrow\uparrow\downarrow\uparrow - \downarrow\uparrow\uparrow\uparrow - \uparrow\downarrow\uparrow\uparrow \rangle$$

$$P_{[31]_\rho}(\uparrow\downarrow\uparrow\uparrow) \implies \chi_{[31]_\rho}(1,1) = \frac{1}{\sqrt{2}} \mid \uparrow\downarrow\uparrow\uparrow - \downarrow\uparrow\uparrow\uparrow \rangle$$

$$P_{[31]_\eta}(\uparrow\uparrow\uparrow\downarrow) \implies \chi_{[31]_\eta}(1,1) = \frac{1}{2\sqrt{3}} \mid 3\uparrow\uparrow\uparrow\downarrow - \downarrow\uparrow\uparrow\uparrow - \uparrow\downarrow\uparrow\uparrow - \uparrow\uparrow\downarrow\uparrow \rangle \text{(B.5)}$$

The spin of pentaquark state in $q^4\bar{q}$ configuration is the coupling of the q^4 spin with the antiquark spin with corresponding Clebsch-Gordan coefficients. The pentaquark states of a certain spin and the same q^4 and antiquark spins but different spin projection m_s have the same expectation values. In this work all the spins take the maximum spin projections.

$$\chi(q^4\bar{s})_{[31]}(1/2, 1/2) = -\sqrt{\frac{2}{3}}\, \chi_{[31]}(s_{q^4} = 1, m_{q^4} = 1)\chi_{\bar{q}}(-1/2)$$

$$+\sqrt{\frac{1}{3}}\, \chi_{[31]}(s_{q^4} = 1, m_{q^4} = 0)\chi_{\bar{q}}(1/2) \qquad \text{(B.6)}$$

For hidden heavy pentaquark states, the $q^3Q\bar{Q}$ ($q^3c\bar{c}$,$q^3b\bar{b}$) color singlet young tabloid construction is,

$$\boxed{}\ (q^4\bar{q}) \quad = \quad \boxed{}\ (q^3) \quad \otimes \quad \boxed{}\ (Q\bar{Q})$$

the $q^3Q\bar{Q}$ ($q^3c\bar{c}$,$q^3b\bar{b}$) hidden color octet young tabloid construction is

$$\boxed{}\ (q^4\bar{q}) \quad = \quad \boxed{}\ (q^3) \quad \otimes \quad \boxed{}\ (Q\bar{Q})$$

The construction of the $q^3Q\bar{Q}$ pentaquark state follows the rule that $q^3Q\bar{Q}$ state must be a color singlet and the $q^3Q\bar{Q}$ wave function should be antisymmetric under any permutation between identical quarks. Requiring the $q^3Q\bar{Q}$

pentaquark to be a color singlet demands that the color part of the q^3 and $Q\bar{Q}$ must form a $[222]_1$ singlet state, there are two possible color configurations: the color part of the q^3 is a $[111]$ singlet and the $Q\bar{Q}$ is also a singlet and the color part of the q^3 is a $[21]$ octet and $Q\bar{Q}$ is also an octet. The pentaquark state in the $q^3 Q\bar{Q}$ system with the q^3 color singlet configuration corresponds to the hadronic molecular pentaquark state which is not confined in our Hamiltonian. And the $q^3 Q\bar{Q}$ system in the compact pentaquark picture takes the q^3 color octet configuration. Requiring the wave function of the three-quark configuration to be antisymmetric, the spatial-spin-flavor part of q^3 is required to be $[21]$ state by conjugation, and directly couples with the spatial-spin-flavor part of $Q\bar{Q}$. First we study the total antisymmetric wave function for the q^3 color octet configuration,

$$\psi_{[3]_A} = \frac{1}{\sqrt{2}} \left(\psi_{[21]_\lambda}^c \psi_{[21]_\rho}^{osf} - \psi_{[21]_\rho}^c \psi_{[21]_\lambda}^{osf} \right) \tag{B.7}$$

with

$$\psi_{[21]_{\rho,\lambda}}^{osf} = \sum_{i,j=S,\rho,\lambda} b_{ij} \psi_{[X]_i}^o \psi_{[Y]_j}^{sf},$$

$$\psi_{[Y]}^{sf} = \sum_{i,j=S,\rho,\lambda} c_{ij} \psi_{[x]_i}^s \psi_{[y]_j}^f,$$

$$\psi_{[X]_i}^s = \{\psi_{[3]_S}^s, \psi_{[21]_{\rho,\lambda}}^s\},$$

$$\psi_{[Y]_j}^f = \{\psi_{[3]_S}^f, \psi_{[111]_A}^f, \psi_{[21]_{\rho,\lambda}}^f\} \tag{B.8}$$

The total color wave function for $q^3 Q\bar{Q}$ pentaquark state takes the form,

$$\Psi_{[21]_{j=\rho,\lambda}}^c = \frac{1}{\sqrt{8}} \sum_i^8 \psi_{[21]_j^i}^c (q^3) \psi_{[21]_j^i}^c (Q\bar{Q}) \tag{B.9}$$

where the ρ and λ stand for the types of $[21]_8$ color octet configuration in Eq. (B.7). The detailed color wave function for both color singlet and color octet states for the q^3 and $Q\bar{Q}$ are listed in Table B.2.

The spin-flavor wave function of hidden heavy pentaquark states are the direct product of spin and flavor parts of q^3 and $Q\bar{Q}$ quark-antiquark pair. And the detailed will not be specified here.

Table B.2 $q^3 Q\bar{Q}$ color wave functions.

color list	q^3 color WF ρ type	$q\bar{q}$	q^3 color WF λ type
color singlet	$\frac{1}{\sqrt{6}}(RGB - GRB + GBR - BGR + BRG - RBG)$	$\frac{1}{\sqrt{3}}(R\bar{R} + G\bar{G} + B\bar{B})$	-
color octet 1	$\frac{1}{\sqrt{2}}(RGR - GRR)$	$B\bar{R}$	$\frac{1}{\sqrt{6}}(2RRG - RGR - GRR)$
color octet 2	$\frac{1}{\sqrt{2}}(RGG - GRG)$	$B\bar{G}$	$\frac{1}{\sqrt{6}}(RGG + GRG - 2GGR)$
color octet 3	$\frac{1}{\sqrt{2}}(RBR - BRR)$	$-G\bar{R}$	$\frac{1}{\sqrt{6}}(2RRB - RBR - BRR)$
color octet 4	$\frac{1}{2}(RBG + GBR - BRG - BGR)$	$\frac{1}{\sqrt{2}}(R\bar{R} - G\bar{G})$	$\frac{1}{\sqrt{12}}(2RGB + 2GRB - GBR - RBG - BRG - BGR)$
color octet 5	$\frac{1}{\sqrt{2}}(GBG - BGG)$	$R\bar{G}$	$\frac{1}{\sqrt{6}}(2GGB - GBG - BGG)$
color octet 6	$\frac{1}{\sqrt{12}}(2RGB - 2GRB - GBR + BGR - BRG + RBG)$	$\frac{1}{\sqrt{6}}(2B\bar{B} - R\bar{R} - G\bar{G})$	$\frac{1}{2}(RBG + BRG - BGR - GBR)$
color octet 7	$\frac{1}{\sqrt{2}}(RBB - BRB)$	$-G\bar{B}$	$\frac{1}{\sqrt{6}}(RBB + BRB - 2BBR)$
color octet 8	$\frac{1}{\sqrt{2}}(GBB - BGB)$	$R\bar{B}$	$\frac{1}{\sqrt{6}}(GBB + BGB - 2BBG)$

APPENDIX C

SPATIAL WAVE FUNCTION

In this appendix the spatial wave function of q^3 and $q^4\bar{q}$ in the harmonic oscillator basis are displayed, all the principle quantum number N stands for the real harmonic oscillation band which means the physical state since all functions fulfill the permutation symmetry of corresponding configuration. For $L = 0$, 56 multiplets till $N = 40$ states are showed below, while 70 multiplets is till N=20. And $L = 1$, 70 multiplets is for N=19 and $L = 2$, 56 multiplets show N=20.

For q^3 permutation symmetry, ρ and λ type spatial wave function is listed below. The total principle quantum number is N is written as:

$$N = 2n_\rho + l_\rho + 2n_\lambda + l_\lambda \tag{C.1}$$

$C_{n_\rho,l_\rho,n_\lambda,l_\lambda}$ is the normalization factor.

Table C.1 Normalized q^3 spatial wave functions with quantum number, $N = 2n$ and $L = M = 0$, 56 multiplet

NLM	$C_{n_\rho,l_\rho,n_\lambda,l_\lambda}(n_\rho, l_\rho, n_\lambda, l_\lambda)$
$000_{[3]_S}$	$(0,0,0,0)$
$200_{[3]_S}$	$\frac{1}{\sqrt{2}}(1,0,0,0),\ \frac{1}{\sqrt{2}}(0,0,1,0)$
$400_{[3]_S}$	$\frac{\sqrt{5}}{4}(2,0,0,0),\ \sqrt{\frac{3}{8}}(1,0,1,0),\ \frac{\sqrt{5}}{4}(0,0,2,0)$
$600_{[3]_S}$	$\frac{\sqrt{14}}{8}(3,0,0,0),\ \frac{\sqrt{18}}{8}(2,0,1,0),\ \frac{\sqrt{18}}{8}(1,0,2,0),\ \frac{\sqrt{14}}{8}(0,0,3,0)$
$800_{[3]_S}$	$\frac{\sqrt{42}}{16}(4,0,0,0),\ \frac{\sqrt{14}}{8}(3,0,1,0),\ \frac{\sqrt{15}}{8}(2,0,2,0)\ ,\ \frac{\sqrt{14}}{8}(1,0,3,0),$ $\frac{\sqrt{42}}{16}(0,0,4,0)$
$1000_{[3]_S}$	$\frac{\sqrt{33}}{16}(5,0,0,0),\ \frac{\sqrt{45}}{16}(4,0,1,0),\ \frac{\sqrt{50}}{16}(3,0,2,0),\ \frac{\sqrt{50}}{16}(2,0,3,0),$

Table C.1 (Continued)

NLM	$C_{n_\rho,l_\rho,n_\lambda,l_\lambda}(n_\rho, l_\rho, n_\lambda, l_\lambda)$
	$\frac{\sqrt{45}}{16}(1,0,4,0),\ \frac{\sqrt{33}}{16}(0,0,5,0)$
$1200_{[3]_S}$	$\frac{\sqrt{429}}{64}(6,0,0,0),\ \frac{\sqrt{594}}{64}(5,0,1,0),\ \frac{\sqrt{675}}{64}(4,0,2,0),\ \frac{\sqrt{175}}{32}(3,0,3,0),$
	$\frac{\sqrt{675}}{64}(2,0,4,0),\ \frac{\sqrt{594}}{64}(1,0,5,0),\ \frac{\sqrt{429}}{64}(0,0,6,0)$
$1400_{[3_S}$	$\frac{\sqrt{1430}}{128}(7,0,0,0),\ \frac{\sqrt{2002}}{128}(6,0,1,0),\ \frac{\sqrt{2310}}{128}(5,0,2,0),\ \frac{\sqrt{2450}}{128}(4,0,3,0),$
	$\frac{\sqrt{2450}}{128}(3,0,4,0),\ \frac{\sqrt{2310}}{128}(2,0,5,0),\ \frac{\sqrt{2002}}{128}(1,0,6,0),\ \frac{\sqrt{1430}}{128}(0,0,7,0)$
$1600_{[3]_S}$	$\frac{\sqrt{4862}}{256}(8,0,0,0),\ \frac{\sqrt{429}}{64}(7,0,1,0),\ \frac{\sqrt{2002}}{128}(6,0,2,0),\ \frac{\sqrt{539}}{64}(5,0,3,0),$
	$\frac{\sqrt{2205}}{128}(4,0,4,0),\ \frac{\sqrt{539}}{64}(3,0,5,0),\ \frac{\sqrt{2002}}{128}(2,0,6,0),\ \frac{\sqrt{429}}{64}(1,0,7,0),$
	$\frac{\sqrt{4862}}{256}(0,0,8,0)$
$1800_{[3]_S}$	$\frac{\sqrt{4199}}{256}(9,0,0,0),\ \frac{\sqrt{5967}}{256}(8,0,1,0),\ \frac{\sqrt{1755}}{128}(7,0,2,0),\ \frac{\sqrt{1911}}{128}(6,0,3,0),$
	$\frac{\sqrt{7938}}{256}(5,0,4,0),\ \frac{\sqrt{7938}}{256}(4,0,5,0),\ \frac{\sqrt{1911}}{128}(3,0,6,0),\ \frac{\sqrt{1755}}{128}(2,0,7,0),$
	$\frac{\sqrt{5967}}{256}(1,0,8,0),\ \frac{\sqrt{4199}}{256}(0,0,9,0)$
$2000_{[3]_S}$	$\frac{\sqrt{58786}}{1024}(10,0,0,0),\ \frac{\sqrt{20995}}{512}(9,0,1,0),\ \frac{\sqrt{99450}}{1024}(8,0,2,0),\ \frac{\sqrt{6825}}{256}(7,0,3,0),$
	$\frac{\sqrt{28665}}{512}(6,0,4,0),\ \frac{\sqrt{29106}}{512}(5,0,5,0),\ \frac{\sqrt{28665}}{512}(4,0,6,0),\ \frac{\sqrt{6825}}{256}(3,0,7,0),$
	$\frac{\sqrt{99450}}{1024}(2,0,8,0),\ \frac{\sqrt{20995}}{512}(1,0,9,0),\ \frac{\sqrt{58786}}{1024}(0,0,10,0)$
$2200_{[3]_S}$	$\frac{\sqrt{52003}}{1024}(11,0,0,0),\ \frac{\sqrt{74613}}{1024}(10,0,1,0),\ \frac{\sqrt{88825}}{1024}(9,0,2,0),\ \frac{\sqrt{98175}}{1024}(8,0,3,0),$
	$\frac{\sqrt{103950}}{1024}(7,0,4,0),\ \frac{\sqrt{106722}}{1024}(6,0,5,0),\ \frac{\sqrt{106722}}{1024}(5,0,6,0),\ \frac{\sqrt{103950}}{1024}(4,0,7,0),$
	$\frac{\sqrt{98175}}{1024}(3,0,8,0),\ \frac{\sqrt{88825}}{1024}(2,0,9,0),\ \frac{\sqrt{74613}}{1024}(1,0,10,0),\ \frac{\sqrt{52003}}{1024}(0,0,11,0)$

Table C.2 Normalized q^3 spatial wave functions with quantum number, $N = 2n$ and $L = M = 0$, 70 multiplet

NLM	$C_{n_\rho,l_\rho,n_\lambda,l_\lambda}(n_\rho, l_\rho, n_\lambda, l_\lambda)$
$200_{[21]_\rho}$	$(0,1,0,1)$
$200_{[21]_\lambda}$	$\frac{1}{\sqrt{2}}(1,0,0,0),\ -\frac{1}{\sqrt{2}}(0,0,1,0)$
$400_{[21]_\rho}$	$\frac{1}{\sqrt{2}}(1,1,0,1),\ \frac{1}{\sqrt{2}}(0,1,1,1)$

Table C.2 (Continued)

NLM	$C_{n_\rho,l_\rho,n_\lambda,l_\lambda}(n_\rho, l_\rho, n_\lambda, l_\lambda)$
$400_{[21]_\lambda}$	$\frac{1}{\sqrt{2}}(2,0,0,0),\ -\frac{1}{\sqrt{2}}(0,0,2,0)$
$600_{[21]_\rho}$	$\frac{\sqrt{42}}{12}(2,1,0,1),\ \frac{\sqrt{15}}{6}(1,1,1,1),\ \frac{\sqrt{42}}{12}(0,1,2,1)$
$600_{[21]_\lambda}$	$\frac{\sqrt{7}}{4}(3,0,0,0),\ \frac{1}{4}(2,0,1,0),\ -\frac{1}{4}(1,0,2,0),\ -\frac{\sqrt{7}}{4}(0,0,3,0)$
$800_{[21]_\rho}$	$\frac{\sqrt{3}}{4}(3,1,0,1),\ \frac{\sqrt{5}}{4}(2,1,1,1),\ \frac{\sqrt{5}}{4}(1,1,2,1),\ \frac{\sqrt{3}}{4}(0,1,3,1)$
$800_{[21]_\lambda}$	$\frac{\sqrt{6}}{4}(4,0,0,0),\ \frac{\sqrt{2}}{4}(3,0,1,0),\ -\frac{\sqrt{2}}{4}(1,0,2,0),\ -\frac{\sqrt{6}}{4}(1,0,3,0)$
$1000_{[21]_\rho}$	$\frac{\sqrt{33}}{16}(4,1,0,1),\ \frac{\sqrt{15}}{8}(3,1,1,1),\ \frac{\sqrt{70}}{16}(2,1,2,1)\ ,\ \frac{\sqrt{15}}{8}(1,1,3,1),$ $\frac{\sqrt{33}}{16}(0,1,4,1)$
$1000_{[21]_\lambda}$	$\frac{\sqrt{330}}{32}(5,0,0,0),\ \frac{9\sqrt{2}}{32}(4,0,1,0),\ \frac{\sqrt{5}}{16}(3,0,2,0)\ ,\ -\frac{\sqrt{5}}{16}(2,0,3,0),$ $-\frac{9\sqrt{2}}{32}(1,0,4,0),\ -\frac{\sqrt{330}}{32}(0,0,5,0)$
$1200_{[21]_\rho}$	$\frac{\sqrt{858}}{96}(5,1,0,1),\ \frac{5\sqrt{66}}{96}(4,1,1,1),\ \frac{5\sqrt{21}}{48}(3,1,2,1),\ \frac{5\sqrt{21}}{48}(2,1,3,1),$ $\frac{5\sqrt{66}}{96}(1,1,4,1),\ \frac{\sqrt{858}}{96}(0,1,5,1)$
$1200_{[21]_\lambda}$	$\frac{\sqrt{286}}{32}(6,0,0,0),\ \frac{\sqrt{11}}{8}(5,0,1,0),\ \frac{5\sqrt{2}}{32}(4,0,2,0),\ -\frac{5\sqrt{2}}{32}(2,0,4,0),$ $-\frac{\sqrt{11}}{8}(1,0,5,0),\ -\frac{\sqrt{286}}{32}(0,0,6,0)$
$1400_{[21]_\rho}$	$\frac{\sqrt{286}}{64}(6,1,0,1),\ \frac{\sqrt{143}}{32}(5,1,1,1),\ \frac{\sqrt{770}}{64}(4,1,2,1),\ \frac{\sqrt{210}}{32}(3,1,3,1),$ $\frac{\sqrt{770}}{64}(2,1,4,1),\ \frac{\sqrt{143}}{32}(1,1,5,1),\ \frac{\sqrt{286}}{64}(0,1,6,1)$
$1400_{[21]_\lambda}$	$\frac{\sqrt{1001}}{64}(7,0,0,0),\ \frac{\sqrt{715}}{64}(6,0,1,0),\ \frac{3\sqrt{33}}{64}(5,0,2,0),\ \frac{\sqrt{35}}{64}(4,0,3,0),$ $-\frac{\sqrt{35}}{64}(3,0,4,0),\ -\frac{3\sqrt{33}}{64}(2,0,5,0),\ -\frac{\sqrt{715}}{64}(1,0,6,0),\ -\frac{\sqrt{1001}}{64}(0,0,7,0)$
$1600_{[21]_\rho}$	$\frac{\sqrt{221}}{64}(7,1,0,1),\ \frac{\sqrt{455}}{64}(6,1,1,1),\ \frac{7\sqrt{13}}{64}(5,1,2,1),\ \frac{\sqrt{2450}}{128}(4,1,3,1),$ $\frac{\sqrt{2450}}{128}(3,1,4,1),\ \frac{7\sqrt{13}}{64}(2,1,5,1),\ \frac{\sqrt{455}}{64}(1,1,6,1),\ \frac{\sqrt{221}}{64}(0,1,7,1)$
$1600_{[21]_\lambda}$	$\frac{\sqrt{221}}{32}(8,0,0,0),\ \frac{3\sqrt{78}}{64}(7,0,1,0),\ \frac{\sqrt{91}}{32}(6,0,2,0),\ \frac{7\sqrt{2}}{64}(5,0,3,0),$ $-\frac{7\sqrt{2}}{64}(3,0,5,0),\ -\frac{\sqrt{91}}{32}(2,0,6,0),\ -\frac{3\sqrt{78}}{64}(1,0,7,0),\ -\frac{\sqrt{221}}{32}(0,0,8,0)$
$1800_{[21]_\rho}$	$\frac{\sqrt{25194}}{768}(8,1,0,1),\ \frac{\sqrt{3315}}{192}(7,1,1,1),\ \frac{7\sqrt{390}}{384}(6,1,2,1),\ \frac{7\sqrt{13}}{64}(5,1,3,1),$ $\frac{7\sqrt{55}}{128}(4,1,4,1),\ \frac{7\sqrt{13}}{64}(3,1,5,1),\ \frac{7\sqrt{390}}{384}(2,1,6,1),\ \frac{\sqrt{3315}}{192}(1,1,7,1),$ $\frac{\sqrt{25194}}{768}(0,1,8,1)$

Table C.2 **(Continued)**

NLM	$C_{n_\rho, l_\rho, n_\lambda, l_\lambda}(n_\rho, l_\rho, n_\lambda, l_\lambda)$
$1800_{[21]_\lambda}$	$\frac{\sqrt{12597}}{256}(9,0,0,0)$, $\frac{7\sqrt{221}}{256}(8,0,1,0)$, $\frac{5\sqrt{65}}{128}(7,0,2,0)$, $\frac{7\sqrt{13}}{128}(6,0,3,0)$, $\frac{7\sqrt{6}}{256}(5,0,4,0)$, $-\frac{7\sqrt{6}}{256}(4,0,5,0)$, $-\frac{7\sqrt{13}}{128}(3,0,6,0)$, $-\frac{5\sqrt{65}}{128}(2,0,7,0)$, $-\frac{7\sqrt{221}}{256}(1,0,8,0)$, $-\frac{\sqrt{12597}}{256}(0,0,9,0)$
$2000_{[21]_\rho}$	$\frac{\sqrt{2261}}{256}(9,1,0,1)$, $\frac{\sqrt{4845}}{256}(8,1,1,1)$, $\frac{\sqrt{1785}}{128}(7,1,2,1)$, $\frac{21\sqrt{5}}{128}(6,1,3,1)$, $\frac{21\sqrt{22}}{256}(5,1,4,1)$, $\frac{21\sqrt{22}}{256}(4,1,5,1)$, $\frac{21\sqrt{5}}{128}(3,1,6,1)$, $\frac{\sqrt{1785}}{128}(2,1,7,1)$, $\frac{\sqrt{4845}}{256}(1,1,8,1)$, $\frac{\sqrt{2261}}{256}(0,1,9,1)$
$2000_{[21]_\lambda}$	$\frac{\sqrt{11305}}{256}(10,0,0,0)$, $\frac{\sqrt{646}}{64}(9,0,1,0)$, $\frac{9\sqrt{85}}{256}(8,0,2,0)$, $\frac{\sqrt{210}}{64}(7,0,3,0)$, $\frac{21\sqrt{2}}{256}(6,0,4,0)$, $-\frac{21\sqrt{2}}{256}(4,0,6,0)$, $-\frac{\sqrt{210}}{64}(3,0,7,0)$, $-\frac{9\sqrt{85}}{256}(2,0,8,0)$, $-\frac{\sqrt{646}}{64}(1,0,9,0)$, $-\frac{\sqrt{11305}}{256}(0,0,10,0)$

Table C.3 Normalized q^3 spatial wave functions with quantum number, $N = 2n + 1$ and $L = M = 1$, 70 multiplet

NLM	$C_{n_\rho, l_\rho, n_\lambda, l_\lambda}(n_\rho, l_\rho, n_\lambda, l_\lambda)$
$111_{[21]_\rho}$	$(0,1,0,0)$
$111_{[21]_\lambda}$	$(0,0,0,1)$
$311_{[21]_\rho}$	$\frac{\sqrt{10}}{4}(1,1,0,0)$, $\frac{\sqrt{6}}{4}(0,1,1,0)$
$311_{[21]_\lambda}$	$\frac{\sqrt{10}}{4}(0,0,1,1)$, $\frac{\sqrt{6}}{4}(1,0,0,1)$
$511_{[21]_\rho}$	$\frac{\sqrt{7}}{4}(2,1,0,0)$, $\frac{\sqrt{6}}{4}(1,1,1,0)$, $\frac{\sqrt{3}}{4}(0,1,2,0)$
$511_{[21]_\lambda}$	$\frac{\sqrt{7}}{4}(0,0,2,1)$, $\frac{\sqrt{6}}{4}(1,0,1,1)$, $\frac{\sqrt{3}}{4}(2,0,0,1)$
$711_{[21]_\rho}$	$\frac{\sqrt{21}}{8}(3,1,0,0)$, $\frac{\sqrt{21}}{8}(2,1,1,0)$, $\frac{\sqrt{15}}{8}(1,1,2,0)$, $\frac{\sqrt{7}}{8}(0,1,3,0)$
$711_{[21]_\lambda}$	$\frac{\sqrt{21}}{8}(0,0,3,1)$, $\frac{\sqrt{21}}{8}(1,0,2,1)$, $\frac{\sqrt{15}}{8}(2,0,1,1)$, $\frac{\sqrt{7}}{8}(3,0,0,1)$
$911_{[21]_\rho}$	$\frac{\sqrt{66}}{16}(4,1,0,0)$, $\frac{\sqrt{18}}{8}(3,1,1,0)$, $\frac{\sqrt{15}}{8}(2,1,2,0)$, $\frac{\sqrt{10}}{8}(1,1,3,0)$, $\frac{\sqrt{18}}{16}(0,1,4,0)$
$911_{[21]_\lambda}$	$\frac{\sqrt{66}}{16}(0,0,4,1)$, $\frac{\sqrt{18}}{8}(1,0,3,1)$, $\frac{\sqrt{15}}{8}(2,0,2,1)$, $\frac{\sqrt{10}}{8}(3,0,1,1)$,

Table C.3 (Continued)

NLM	$C_{n_\rho, l_\rho, n_\lambda, l_\lambda}(n_\rho, l_\rho, n_\lambda, l_\lambda)$
	$\frac{\sqrt{18}}{16}(4,0,0,1)$
$1111_{[21]\rho}$	$\frac{\sqrt{858}}{64}(5,1,0,0)$, $\frac{3\sqrt{110}}{64}(4,1,1,0)$, $\frac{15}{32}(3,1,2,0)$, $\frac{5\sqrt{7}}{32}(2,1,3,0)$,
	$\frac{15\sqrt{2}}{64}(1,1,4,0)$, $\frac{3\sqrt{22}}{64}(0,1,5,0)$
$1111_{[21]\lambda}$	$\frac{\sqrt{858}}{64}(0,0,5,1)$, $\frac{3\sqrt{110}}{64}(1,0,4,1)$, $\frac{15}{32}(2,0,3,1)$, $\frac{5\sqrt{7}}{32}(3,0,2,1)$,
	$\frac{15\sqrt{2}}{64}(4,0,1,1)$, $\frac{3\sqrt{22}}{64}(5,0,0,1)$
$1311_{[21]\rho}$	$\frac{\sqrt{715}}{64}(6,1,0,0)$, $\frac{\sqrt{858}}{64}(5,1,1,0)$, $\frac{5\sqrt{33}}{64}(4,1,2,0)$, $\frac{5\sqrt{7}}{32}(3,1,3,0)$,
	$\frac{5\sqrt{21}}{64}(2,1,4,0)$, $\frac{\sqrt{330}}{64}(1,1,5,0)$, $\frac{\sqrt{143}}{64}(0,1,6,0)$
$1311_{[21]\lambda}$	$\frac{\sqrt{715}}{64}(0,0,6,1)$, $\frac{\sqrt{858}}{64}(1,0,5,1)$, $\frac{5\sqrt{33}}{64}(2,0,4,1)$, $\frac{5\sqrt{7}}{32}(3,0,3,1)$,
	$\frac{5\sqrt{21}}{64}(4,0,2,1)$, $\frac{\sqrt{330}}{64}(5,0,1,1)$, $\frac{\sqrt{143}}{64}(6,0,0,1)$
$1511_{[21]\rho}$	$\frac{\sqrt{2431}}{128}(7,1,0,0)$, $\frac{\sqrt{3003}}{128}(6,1,1,0)$, $\frac{\sqrt{3003}}{128}(5,1,2,0)$, $\frac{7\sqrt{55}}{128}(4,1,3,0)$,
	$\frac{21\sqrt{5}}{128}(3,1,4,0)$, $\frac{7\sqrt{33}}{128}(2,1,5,0)$, $\frac{\sqrt{1001}}{128}(1,1,6,0)$, $\frac{\sqrt{429}}{128}(0,1,7,0)$
$1511_{[21]\lambda}$	$\frac{\sqrt{2431}}{128}(0,0,7,1)$, $\frac{\sqrt{3003}}{128}(1,0,6,1)$, $\frac{\sqrt{3003}}{128}(2,0,5,1)$, $\frac{7\sqrt{55}}{128}(3,0,4,1)$,
	$\frac{21\sqrt{5}}{128}(4,0,3,1)$, $\frac{7\sqrt{33}}{128}(5,0,2,1)$, $\frac{\sqrt{1001}}{128}(6,0,1,1)$, $\frac{\sqrt{429}}{128}(7,0,0,1)$
$1711_{[21]\rho}$	$\frac{\sqrt{8398}}{256}(8,1,0,0)$, $\frac{\sqrt{663}}{64}(7,1,1,0)$, $\frac{\sqrt{2730}}{128}(6,1,2,0)$, $\frac{7\sqrt{13}}{64}(5,1,3,0)$,
	$\frac{21\sqrt{5}}{128}(4,1,4,0)$, $\frac{21}{64}(3,1,5,0)$, $\frac{7\sqrt{26}}{128}(2,1,6,0)$, $\frac{\sqrt{195}}{64}(1,1,7,0)$,
	$\frac{\sqrt{1326}}{256}(0,1,8,0)$
$1711_{[21]\lambda}$	$\frac{\sqrt{8398}}{256}(0,0,8,1)$, $\frac{\sqrt{663}}{64}(1,0,7,1)$, $\frac{\sqrt{2730}}{128}(2,0,6,1)$, $\frac{7\sqrt{13}}{64}(3,0,5,1)$,
	$\frac{21\sqrt{5}}{128}(4,0,4,1)$, $\frac{21}{64}(5,0,3,1)$, $\frac{7\sqrt{26}}{128}(6,0,2,1)$, $\frac{\sqrt{195}}{64}(7,0,1,1)$,
	$\frac{\sqrt{1326}}{256}(8,0,0,1)$
$1911_{[21]\rho}$	$\frac{\sqrt{29393}}{512}(9,1,0,0)$, $\frac{3\sqrt{4199}}{512}(8,1,1,0)$, $\frac{3\sqrt{1105}}{256}(7,1,2,0)$, $\frac{7\sqrt{195}}{256}(6,1,3,0)$,
	$\frac{21\sqrt{78}}{512}(5,1,4,0)$, $\frac{21\sqrt{66}}{512}(4,1,5,0)$, $\frac{21\sqrt{13}}{256}(3,1,6,0)$, $\frac{3\sqrt{455}}{256}(2,1,7,0)$,
	$\frac{3\sqrt{1105}}{512}(1,1,8,0)$, $\frac{\sqrt{4199}}{512}(0,1,9,0)$
$1911_{[21]\lambda}$	$\frac{\sqrt{29393}}{512}(0,0,9,1)$, $\frac{3\sqrt{4199}}{512}(1,0,8,1)$, $\frac{3\sqrt{1105}}{256}(2,0,7,1)$, $\frac{7\sqrt{195}}{256}(3,0,6,1)$,
	$\frac{21\sqrt{78}}{512}(4,0,5,1)$, $\frac{21\sqrt{66}}{512}(5,0,4,1)$, $\frac{21\sqrt{13}}{256}(6,0,3,1)$, $\frac{3\sqrt{455}}{256}(7,0,2,1)$,

Table C.3 (Continued)

NLM	$C_{n_\rho,l_\rho,n_\lambda,l_\lambda}(n_\rho, l_\rho, n_\lambda, l_\lambda)$
	$\frac{3\sqrt{1105}}{512}(8,0,1,1),\ \frac{\sqrt{4199}}{512}(9,0,0,1)$

Table C.4 Normalized q^3 spatial wave functions with quantum number, $N = 2n + 2$ and $L = M = 2$, 56 multiplet

NLM	$C_{n_\rho,l_\rho,n_\lambda,l_\lambda}(n_\rho, l_\rho, n_\lambda, l_\lambda)$
$222[3]_S$	$\frac{1}{\sqrt{2}}(0,2,0,0),\ \frac{1}{\sqrt{2}}(0,0,0,2)$
$422[3]_S$	$\frac{\sqrt{35}}{10}(1,2,0,0),\ \frac{\sqrt{15}}{10}(0,2,1,0),\ \frac{\sqrt{15}}{10}(1,0,0,2),\ \frac{\sqrt{35}}{10}(0,0,1,2)$
$622[3]_S$	$\frac{\sqrt{105}}{20}(2,2,0,0),\ \frac{\sqrt{18}}{8}(1,2,1,0),\ \frac{\sqrt{18}}{8}(0,2,2,0),\ \frac{\sqrt{14}}{8}(2,0,0,2),$ $\frac{\sqrt{675}}{64}(1,0,1,2),\ \frac{\sqrt{594}}{64}(0,0,2,2)$
$822[3]_S$	$\frac{\sqrt{330}}{40}(3,2,0,0),\ \frac{\sqrt{270}}{40}(2,2,1,0),\ \frac{\sqrt{6}}{8}(1,2,2,0),\ \frac{\sqrt{2}}{8}(0,2,3,0),$ $\frac{\sqrt{2}}{8}(3,0,0,2),\ \frac{\sqrt{6}}{8}(2,0,1,2),\ \frac{\sqrt{270}}{40}(1,0,2,2),\ \frac{\sqrt{330}}{40}(0,0,3,2)$
$1022[3]_S$	$\frac{\sqrt{4290}}{160}(4,2,0,0),\ \frac{\sqrt{990}}{80}(3,2,1,0),\ \frac{\sqrt{27}}{16}(2,2,2,0),\ \frac{\sqrt{14}}{16}(1,2,3,0),$ $\frac{\sqrt{18}}{32}(0,2,4,0),\ \frac{\sqrt{18}}{32}(4,0,0,2),\ \frac{\sqrt{14}}{16}(3,0,1,2),\ \frac{\sqrt{27}}{16}(2,0,2,2),$ $\frac{\sqrt{990}}{80}(1,0,3,2),\ \frac{\sqrt{4290}}{160}(0,0,4,2)$
$1222[3]_S$	$\frac{\sqrt{143}}{32}(5,2,0,0),\ \frac{\sqrt{143}}{32}(4,2,1,0),\ \frac{\sqrt{110}}{32}(3,2,2,0),\ \frac{\sqrt{70}}{32}(2,2,3,0),$ $\frac{\sqrt{35}}{32}(1,2,4,0),\ \frac{\sqrt{11}}{32}(0,2,5,0),\ \frac{\sqrt{11}}{32}(5,0,0,2),\ \frac{\sqrt{35}}{32}(4,0,1,2),$ $\frac{\sqrt{70}}{32}(3,0,2,2),\ \frac{\sqrt{110}}{32}(2,0,3,2),\ \frac{\sqrt{143}}{32}(1,0,4,2),\ \frac{\sqrt{143}}{32}(0,0,5,2)$
$1422[3]_S$	$\frac{\sqrt{12155}}{320}(6,2,0,0),\ \frac{\sqrt{12870}}{320}(5,2,1,0),\ \frac{\sqrt{429}}{64}(4,2,2,0),\ \frac{\sqrt{77}}{32}(3,2,3,0),$ $\frac{\sqrt{189}}{64}(2,2,4,0),\ \frac{\sqrt{2310}}{320}(1,2,5,0),\ \frac{\sqrt{715}}{320}(0,2,6,0),\ \frac{\sqrt{715}}{320}(6,0,0,2),$ $\frac{\sqrt{2310}}{320}(5,0,1,2),\ \frac{\sqrt{189}}{64}(4,0,2,2),\ \frac{\sqrt{77}}{32}(3,0,3,2),\ \frac{\sqrt{429}}{64}(2,0,4,2),$ $\frac{\sqrt{12870}}{320}(1,0,5,2),\ \frac{\sqrt{12155}}{320}(0,0,6,2)$
$1622[3]_S$	$\frac{\sqrt{41990}}{640}(7,2,0,0),\ \frac{\sqrt{46410}}{640}(6,2,1,0),\ \frac{\sqrt{1638}}{128}(5,2,2,0),\ \frac{\sqrt{1274}}{128}(4,2,3,0),$ $\frac{\sqrt{882}}{128}(3,2,4,0),\ \frac{\sqrt{13230}}{640}(2,2,5,0),\ \frac{\sqrt{6370}}{640}(1,2,6,0),\ \frac{\sqrt{78}}{128}(0,2,7,0),$ $\frac{\sqrt{78}}{128}(7,0,0,2),\ \frac{\sqrt{6370}}{640}(6,0,1,2),\ \frac{\sqrt{13230}}{640}(5,0,2,2),\ \frac{\sqrt{882}}{128}(4,0,3,2),$

Table C.4   (Continued)

NLM	$C_{n_\rho,l_\rho,n_\lambda,l_\lambda}(n_\rho, l_\rho, n_\lambda, l_\lambda)$
	$\frac{\sqrt{1274}}{128}(3,0,4,2)$, $\frac{\sqrt{1638}}{128}(2,0,5,2)$, $\frac{\sqrt{46410}}{640}(1,0,6,2)$, $\frac{\sqrt{41990}}{640}(0,0,7,2)$
$1822[3]_S$	$\frac{\sqrt{146965}}{1280}(8,2,0,0)$, $\frac{\sqrt{41990}}{640}(7,2,1,0)$, $\frac{\sqrt{1547}}{128}(6,2,2,0)$, $\frac{\sqrt{1274}}{128}(5,2,3,0)$,
	$\frac{\sqrt{3822}}{256}(4,2,4,0)$, $\frac{\sqrt{16170}}{640}(3,2,5,0)$, $\frac{\sqrt{9555}}{640}(2,2,6,0)$, $\frac{\sqrt{182}}{128}(1,2,7,0)$,
	$\frac{\sqrt{221}}{256}(0,2,8,0)$, $\frac{\sqrt{221}}{256}(8,0,0,2)$, $\frac{\sqrt{182}}{128}(7,0,1,2)$, $\frac{\sqrt{9555}}{640}(6,0,2,2)$,
	$\frac{\sqrt{16170}}{640}(5,0,3,2)$, $\frac{\sqrt{3822}}{256}(4,0,4,2)$, $\frac{\sqrt{1274}}{128}(3,0,5,2)$, $\frac{\sqrt{1547}}{128}(2,0,6,2)$,
	$\frac{\sqrt{41990}}{640}(1,0,7,2)$, $\frac{\sqrt{146965}}{1280}(0,0,8,2)$
$2022[3]_S$	$\frac{\sqrt{520030}}{2560}(9,2,0,0)$, $\frac{\sqrt{610470}}{2560}(8,2,1,0)$, $\frac{\sqrt{5814}}{256}(7,2,2,0)$, $\frac{\sqrt{4998}}{256}(6,2,3,0)$,
	$\frac{63}{256}(5,2,4,0)$, $\frac{\sqrt{72765}}{1280}(4,2,5,0)$, $\frac{\sqrt{48510}}{1280}(3,2,6,0)$, $\frac{\sqrt{1134}}{256}(2,2,7,0)$,
	$\frac{\sqrt{2142}}{512}(1,2,8,0)$, $\frac{\sqrt{646}}{512}(0,2,9,0)$, $\frac{\sqrt{646}}{512}(9,0,0,2)$, $\frac{\sqrt{2142}}{512}(8,0,1,2)$,
	$\frac{\sqrt{1134}}{256}(7,0,2,2)$, $\frac{\sqrt{48510}}{1280}(6,0,3,2)$, $\frac{\sqrt{72765}}{1280}(5,0,4,2)$, $\frac{63}{256}(4,0,5,2)$,
	$\frac{\sqrt{4998}}{256}(3,0,6,2)$, $\frac{\sqrt{5814}}{256}(2,0,7,2)$, $\frac{\sqrt{610470}}{2560}(1,0,8,2)$, $\frac{\sqrt{520030}}{2560}(0,0,9,2)$

Table C.5 Normalized q^3 spatial wave functions with quantum number, $N = 2n + 2$ and $L = M = 2$, 70 multiplet

NLM	$C_{n_\rho,l_\rho,n_\lambda,l_\lambda}(n_\rho, l_\rho, n_\lambda, l_\lambda)$
$222_{[21]\rho}$	$(0,1,0,1)$
$222_{[21]\lambda}$	$\frac{1}{\sqrt{2}}(0,2,0,0)$, $-\frac{1}{\sqrt{2}}(0,2,0,0)$
$422_{[21]\rho}$	$\frac{1}{\sqrt{2}}(1,1,0,1)$, $\frac{1}{\sqrt{2}}(0,1,1,1)$
$422_{[21]\lambda}$	$\frac{\sqrt{35}}{10}(1,2,0,0)$, $\frac{\sqrt{15}}{10}(0,2,1,0)$, $-\frac{\sqrt{15}}{10}(1,0,0,2)$, $-\frac{\sqrt{35}}{10}(0,0,1,2)$
$622_{[21]\rho}$	$\frac{\sqrt{42}}{12}(2,1,0,1)$, $\frac{\sqrt{15}}{6}(1,1,1,1)$, $\frac{\sqrt{42}}{12}(0,1,2,1)$
$622_{[21]\lambda}$	$\frac{\sqrt{105}}{20}(2,2,0,0)$, $\frac{\sqrt{70}}{20}(1,2,1,0)$, $\frac{1}{4}(0,2,2,0)$, $-\frac{1}{4}(2,0,0,2)$,
	$-\frac{\sqrt{70}}{20}(1,0,1,2)$, $-\frac{\sqrt{105}}{20}(0,0,2,2)$
$822_{[21]\rho}$	$\frac{\sqrt{3}}{4}(3,1,0,1)$, $\frac{\sqrt{5}}{4}(2,1,1,1)$, $\frac{\sqrt{5}}{4}(1,1,2,1)$, $\frac{\sqrt{3}}{4}(0,1,3,1)$
$822_{[21]\lambda}$	$\frac{\sqrt{330}}{40}(3,2,0,0)$, $\frac{\sqrt{21}}{8}(2,2,1,0)$, $\frac{\sqrt{15}}{8}(1,2,2,0)$, $\frac{\sqrt{7}}{8}(0,2,3,0)$,

Table C.5 (Continued)

NLM	$C_{n_\rho,l_\rho,n_\lambda,l_\lambda}(n_\rho, l_\rho, n_\lambda, l_\lambda)$
	$\frac{\sqrt{330}}{40}(3,0,0,2),\ \frac{7\sqrt{33}}{128}(2,0,1,2),\ \frac{\sqrt{1001}}{128}(1,0,2,2),\ \frac{-\sqrt{330}}{40}(0,0,3,2)$

NLM	
$1022_{[21]\rho}$	$\frac{\sqrt{33}}{16}(4,1,0,1),\ \frac{\sqrt{15}}{8}(3,1,1,1),\ \frac{\sqrt{70}}{16}(2,1,2,1),\ \frac{\sqrt{15}}{8}(1,1,3,1),$
	$\frac{\sqrt{33}}{16}(0,1,4,1)$
$1022_{[21]\lambda}$	$\frac{\sqrt{4290}}{160}(4,2,0,0),\ \frac{\sqrt{990}}{80}(3,2,1,0),\ \frac{\sqrt{27}}{16}(2,2,2,0),\ \frac{\sqrt{14}}{16}(1,2,3,0),$
	$\frac{\sqrt{18}}{32}(0,2,4,0),\ -\frac{\sqrt{18}}{32}(4,0,0,2),\ -\frac{\sqrt{14}}{16}(3,0,1,2),\ -\frac{\sqrt{27}}{16}(2,0,2,2),$
	$-\frac{\sqrt{990}}{80}(1,0,3,2),\ -\frac{\sqrt{4290}}{160}(0,0,4,2)$
$1222_{[21]\rho}$	$\frac{\sqrt{858}}{96}(5,1,0,1),\ \frac{\sqrt{1650}}{96}(4,1,1,1),\ \frac{\sqrt{525}}{48}(3,1,2,1),\ \frac{\sqrt{525}}{48}(2,1,3,1),$
	$\frac{\sqrt{1650}}{96}(1,1,4,1),\ \frac{\sqrt{858}}{96}(0,1,5,1)$
$1222_{[21]\lambda}$	$\frac{\sqrt{143}}{32}(5,2,0,0),\ \frac{\sqrt{143}}{32}(4,2,1,0),\ \frac{\sqrt{110}}{32}(3,2,2,0),\ \frac{\sqrt{70}}{32}(2,2,3,0),$
	$\frac{\sqrt{35}}{32}(1,2,4,0),\ \frac{\sqrt{11}}{32}(0,2,5,0),\ -\frac{\sqrt{11}}{32}(5,0,0,2),\ -\frac{\sqrt{35}}{32}(4,0,1,2),$
	$-\frac{\sqrt{70}}{32}(3,0,2,2),\ -\frac{\sqrt{110}}{32}(2,0,3,2),\ -\frac{\sqrt{143}}{32}(1,0,4,2),\ -\frac{\sqrt{143}}{32}(0,0,5,2)$
$1422_{[21]\rho}$	$\frac{\sqrt{286}}{64}(6,1,0,1),\ \frac{\sqrt{143}}{32}(5,1,1,1),\ \frac{\sqrt{770}}{64}(4,1,2,1),\ \frac{\sqrt{210}}{32}(3,1,3,1),$
	$\frac{\sqrt{770}}{64}(2,1,4,1),\ \frac{\sqrt{143}}{32}(1,1,5,1),\ \frac{\sqrt{286}}{64}(0,1,6,1)$
$1422_{[21]\lambda}$	$\frac{\sqrt{12155}}{320}(6,2,0,0),\ \frac{\sqrt{12870}}{320}(5,2,1,0),\ \frac{\sqrt{429}}{64}(4,2,2,0),\ \frac{\sqrt{77}}{32}(3,2,3,0),$
	$\frac{\sqrt{189}}{64}(2,2,4,0),\ \frac{\sqrt{2310}}{320}(1,2,5,0),\ \frac{\sqrt{715}}{320}(0,2,6,0),\ -\frac{\sqrt{715}}{320}(6,0,0,2),$
	$-\frac{\sqrt{2310}}{320}(5,0,1,2),\ -\frac{\sqrt{189}}{64}(4,0,2,2),\ -\frac{\sqrt{77}}{32}(3,0,3,2),\ -\frac{\sqrt{429}}{64}(2,0,4,2),$
	$-\frac{\sqrt{12870}}{320}(1,0,5,2),\ -\frac{\sqrt{12155}}{320}(0,0,6,2)$
$1622_{[21]\rho}$	$\frac{\sqrt{221}}{64}(7,1,0,1),\ \frac{\sqrt{637}}{64}(6,1,1,1),\ \frac{\sqrt{735}}{64}(5,1,2,1),\ \frac{\sqrt{455}}{64}(4,1,3,1),$
	$\frac{\sqrt{455}}{64}(3,1,4,1),\ \frac{\sqrt{735}}{64}(2,1,5,1),\ \frac{\sqrt{637}}{64}(1,1,6,1),\ \frac{\sqrt{221}}{64}(0,1,7,1)$
$1622_{[21]\lambda}$	$\frac{\sqrt{41990}}{640}(7,2,0,0),\ \frac{\sqrt{46410}}{640}(6,2,1,0),\ \frac{\sqrt{1638}}{128}(5,2,2,0),\ \frac{\sqrt{1274}}{128}(4,2,3,0),$
	$\frac{\sqrt{882}}{128}(3,2,4,0),\ \frac{\sqrt{13230}}{640}(2,2,5,0),\ \frac{\sqrt{6370}}{640}(1,2,6,0),\ \frac{\sqrt{78}}{128}(0,2,7,0),$
	$-\frac{\sqrt{78}}{128}(7,0,0,2),\ -\frac{\sqrt{6370}}{640}(6,0,1,2),\ -\frac{\sqrt{13230}}{640}(5,0,2,2),$
	$-\frac{\sqrt{882}}{128}(4,0,3,2),\ -\frac{\sqrt{1274}}{128}(3,0,4,2),\ -\frac{\sqrt{1638}}{128}(2,0,5,2),$

Table C.5 **(Continued)**

NLM	$C_{n_\rho,l_\rho,n_\lambda,l_\lambda}(n_\rho,l_\rho,n_\lambda,l_\lambda)$
	$-\frac{\sqrt{46410}}{640}(1,0,6,2),\ -\frac{\sqrt{41990}}{640}(0,0,7,2)$
$1822_{[21]\rho}$	$\frac{\sqrt{25194}}{768}(8,1,0,1),\ \frac{\sqrt{3315}}{192}(7,1,1,1),\ \frac{\sqrt{19110}}{384}(6,1,2,1),\ \frac{\sqrt{637}}{64}(5,1,3,1),$
	$\frac{\sqrt{2695}}{128}(4,1,4,1),\ \frac{\sqrt{637}}{64}(3,1,5,1),\ \frac{\sqrt{19110}}{384}(2,1,6,1),\ \frac{\sqrt{3315}}{192}(1,1,7,1),$
	$\frac{\sqrt{25194}}{768}(0,1,8,1)$
$1822_{[21]\lambda}$	$\frac{\sqrt{146965}}{1280}(8,2,0,0),\ \frac{\sqrt{41990}}{640}(7,2,1,0),\ \frac{\sqrt{1547}}{128}(6,2,2,0),\ \frac{\sqrt{1274}}{128}(5,2,3,0),$
	$\frac{\sqrt{3822}}{256}(4,2,4,0),\ \frac{\sqrt{16170}}{640}(3,2,5,0),\ \frac{\sqrt{9555}}{640}(2,2,6,0),\ \frac{\sqrt{182}}{128}(1,2,7,0),$
	$\frac{\sqrt{221}}{256}(0,2,8,0),\ -\frac{\sqrt{221}}{256}(8,0,0,2),\ -\frac{\sqrt{182}}{128}(7,0,1,2),\ -\frac{\sqrt{9555}}{640}(6,0,2,2),$
	$-\frac{\sqrt{16170}}{640}(5,0,3,2),\ -\frac{\sqrt{3822}}{256}(4,0,4,2),\ -\frac{\sqrt{1274}}{128}(3,0,5,2),$
	$-\frac{\sqrt{1547}}{128}(2,0,6,2),\ -\frac{\sqrt{41990}}{640}(1,0,7,2),\ -\frac{\sqrt{146965}}{1280}(0,0,8,2)$
$2022_{[21]\rho}$	$\frac{\sqrt{2261}}{256}(9,1,0,1),\ \frac{\sqrt{4845}}{256}(8,1,1,1),\ \frac{\sqrt{1785}}{128}(7,1,2,1),\ \frac{\sqrt{2205}}{128}(6,1,3,1),$
	$\frac{\sqrt{9702}}{256}(5,1,4,1),\ \frac{\sqrt{9702}}{256}(4,1,5,1),\ \frac{\sqrt{2205}}{128}(3,1,6,1),\ \frac{\sqrt{1785}}{128}(2,1,7,1),$
	$\frac{\sqrt{4845}}{256}(1,1,8,1),\ \frac{\sqrt{2261}}{256}(0,1,9,1)$
$2022_{[21]\lambda}$	$\frac{\sqrt{520030}}{2560}(9,2,0,0),\ \frac{\sqrt{610470}}{2560}(8,2,1,0),\ \frac{\sqrt{5814}}{256}(7,2,2,0),\ \frac{\sqrt{4998}}{256}(6,2,3,0),$
	$\frac{63}{256}(5,2,4,0),\ \frac{\sqrt{72765}}{1280}(4,2,5,0),\ \frac{\sqrt{48510}}{1280}(3,2,6,0),\ \frac{\sqrt{1134}}{256}(2,2,7,0),$
	$\frac{\sqrt{2142}}{512}(1,2,8,0),\ \frac{\sqrt{646}}{512}(0,2,9,0),\ -\frac{\sqrt{646}}{512}(9,0,0,2),\ -\frac{\sqrt{2142}}{512}(8,0,1,2),$
	$-\frac{\sqrt{1134}}{256}(7,0,2,2),\ -\frac{\sqrt{48510}}{1280}(6,0,3,2),\ -\frac{\sqrt{72765}}{1280}(5,0,4,2),$
	$-\frac{63}{256}(4,0,5,2),\ -\frac{\sqrt{4998}}{256}(3,0,6,2),\ -\frac{\sqrt{5814}}{256}(2,0,7,2),$
	$-\frac{\sqrt{610470}}{2560}(1,0,8,2),\ -\frac{\sqrt{520030}}{2560}(0,0,9,2)$

Table C.6 Normalized q^3 spatial wave functions with quantum number, $N = 2n + 1$ and $L = M = 1$, 20 multiplet

NLM	$C_{n_\rho,l_\rho,n_\lambda,l_\lambda}(n_\rho,l_\rho,n_\lambda,l_\lambda)$
$211_{[111]A}$	$(0,1,0,1)$
$411_{[111]A}$	$\frac{1}{\sqrt{2}}(1,1,0,1),\ \frac{1}{\sqrt{2}}(0,1,1,1)$

Table C.6 (Continued)

NLM	$C_{n_\rho,l_\rho,n_\lambda,l_\lambda}(n_\rho, l_\rho, n_\lambda, l_\lambda)$
$611_{[111]A}$	$\frac{\sqrt{42}}{12}(2,1,0,1),\ \frac{\sqrt{15}}{6}(1,1,1,1),\ \frac{\sqrt{42}}{12}(0,1,2,1)$
$811_{[111]A}$	$\frac{\sqrt{3}}{4}(3,1,0,1),\ \frac{\sqrt{5}}{4}(2,1,1,1),\ \frac{\sqrt{5}}{4}(1,1,2,1),\ \frac{\sqrt{3}}{4}(0,1,3,1)$
$1011_{[111]A}$	$\frac{\sqrt{33}}{16}(4,1,0,1),\ \frac{\sqrt{15}}{8}(3,1,1,1),\ \frac{\sqrt{70}}{16}(2,1,2,1)\ ,\ \frac{\sqrt{15}}{8}(1,1,3,1),$ $\frac{\sqrt{33}}{16}(0,1,4,1)$
$1211_{[111]A}$	$\frac{\sqrt{858}}{96}(5,1,0,1),\ \frac{5\sqrt{66}}{96}(4,1,1,1),\ \frac{5\sqrt{21}}{48}(3,1,2,1),\ \frac{5\sqrt{21}}{48}(2,1,3,1),$ $\frac{5\sqrt{66}}{96}(1,1,4,1),\ \frac{\sqrt{858}}{96}(0,1,5,1)$
$1411_{[111]A}$	$\frac{\sqrt{286}}{64}(6,1,0,1),\ \frac{\sqrt{143}}{32}(5,1,1,1),\ \frac{\sqrt{770}}{64}(4,1,2,1),\ \frac{\sqrt{210}}{32}(3,1,3,1),$ $\frac{\sqrt{770}}{64}(2,1,4,1),\ \frac{\sqrt{143}}{32}(1,1,5,1),\ \frac{\sqrt{286}}{64}(0,1,6,1)$
$1611_{[111]A}$	$\frac{\sqrt{221}}{64}(7,1,0,1),\ \frac{\sqrt{455}}{64}(6,1,1,1),\ \frac{7\sqrt{13}}{64}(5,1,2,1),\ \frac{\sqrt{2450}}{128}(4,1,3,1),$ $\frac{\sqrt{2450}}{128}(3,1,4,1),\ \frac{7\sqrt{13}}{64}(2,1,5,1),\ \frac{\sqrt{455}}{64}(1,1,6,1),\ \frac{\sqrt{221}}{64}(0,1,7,1)$
$1811_{[111]A}$	$\frac{\sqrt{25194}}{768}(8,1,0,1),\ \frac{\sqrt{3315}}{192}(7,1,1,1),\ \frac{7\sqrt{390}}{384}(6,1,2,1),\ \frac{7\sqrt{13}}{64}(5,1,3,1),$ $\frac{7\sqrt{55}}{128}(4,1,4,1),\ \frac{7\sqrt{13}}{64}(3,1,5,1),\ \frac{7\sqrt{390}}{384}(2,1,6,1),\ \frac{\sqrt{3315}}{192}(1,1,7,1),$ $\frac{\sqrt{25194}}{768}(0,1,8,1)$
$2011_{[111]A}$	$\frac{\sqrt{2261}}{256}(9,1,0,1),\ \frac{\sqrt{4845}}{256}(8,1,1,1),\ \frac{\sqrt{1785}}{128}(7,1,2,1),\ \frac{21\sqrt{5}}{128}(6,1,3,1),$ $\frac{21\sqrt{22}}{256}(5,1,4,1),\ \frac{21\sqrt{22}}{256}(4,1,5,1),\ \frac{21\sqrt{5}}{128}(3,1,6,1),\ \frac{\sqrt{1785}}{128}(2,1,7,1),$ $\frac{\sqrt{4845}}{256}(1,1,8,1),\ \frac{\sqrt{2261}}{256}(0,1,9,1)$

In this part the spatial wave functions of the q^4 subsystem of pentaquarks with the permutation symmetries $[4]_S$ are listed in Table C.7 up to $N' = 22$, where l_ρ, l_λ, l_η and are L' are limited to 0 and 1 only. Note that we have set $M' = 0$ and used the abbreviation,

$$\sum_{\{n_i,l_i,m_i\}} C_{n_\rho,l_\rho,m_\rho,n_\lambda,l_\lambda,m_\lambda,n_\eta,l_\eta,m_\eta} \psi_{n_\rho l_\rho m_\rho}(\vec{\rho})\psi_{n_\lambda l_\lambda m_\lambda}(\vec{\lambda})\psi_{n_\eta l_\eta m_\eta}(\vec{\eta})$$
$$\equiv \sum_{\{n_i,l_i\}} C_{n_\rho,l_\rho,n_\lambda,l_\lambda,n_\eta,l_\eta}\ \psi(n_\rho, l_\rho, n_\lambda, l_\lambda, n_\eta, l_\eta)$$

$$\equiv \sum_{\{n_i, l_i\}} C_{n_\rho, l_\rho, n_\lambda, l_\lambda, n_\eta, l_\eta} (n_\rho, l_\rho, n_\lambda, l_\lambda, n_\eta, l_\eta)$$

$$(C.2)$$

Table C.7 Normalized pentaquark (q^4 symmetry) spatial wave functions with quantum number, $N' = 2n$ and $L' = M' = 0$

NLM	$C_{n_\rho, l_\rho, n_\lambda, l_\lambda, n_\eta, l_\eta}(n_\rho, l_\rho, n_\lambda, l_\lambda, n_\eta, l_\eta)$
$000_{[4]S}$	$(0,0,0,0,0,0)$
$200_{[4]S}$	$\frac{1}{\sqrt{3}}(1,0,0,0,0,0)$, $\frac{1}{\sqrt{3}}(0,0,1,0,0,0)$, $\frac{1}{\sqrt{3}}(0,0,0,0,1,0)$
$200_{[31]\rho}$	$\frac{1}{\sqrt{3}}(0,1,0,0,0,1)$, $\sqrt{\frac{2}{3}}(0,1,0,1,0,0)$
$200_{[31]\lambda}$	$\frac{1}{\sqrt{3}}(0,0,0,1,0,1)$, $-\frac{1}{\sqrt{3}}(0,0,1,0,0,0)$, $\frac{1}{\sqrt{3}}(1,0,0,0,0,0)$
$200_{[31]\eta}$	$-\sqrt{\frac{2}{3}}(0,0,0,0,1,0)$, $\frac{1}{\sqrt{6}}(0,0,1,0,0,0)$, $\frac{1}{\sqrt{6}}(1,0,0,0,0,0)$
$200_{[22]\rho}$	$-\frac{1}{\sqrt{3}}(0,1,0,1,0,0)$, $\sqrt{\frac{2}{3}}(0,1,0,0,0,1)$
$200_{[22]\lambda}$	$\sqrt{\frac{2}{3}}(0,0,0,1,0,1)$, $\frac{1}{\sqrt{6}}(0,0,1,0,0,0)$, $-\frac{1}{\sqrt{6}}(1,0,0,0,0,0)$
$400_{[4]S}$	$\sqrt{\frac{5}{33}}(2,0,0,0,0,0)$, $\sqrt{\frac{5}{33}}(0,0,2,0,0,0)$, $\sqrt{\frac{5}{33}}(0,0,0,0,2,0)$, $\sqrt{\frac{2}{11}}(1,0,1,0,0,0)$, $\sqrt{\frac{2}{11}}(1,0,0,0,1,0)$, $\sqrt{\frac{2}{11}}(0,0,1,0,1,0)$
$400_{[31]\rho}$	$\sqrt{\frac{5}{39}}(0,1,0,0,1,1)$, $\sqrt{\frac{2}{13}}(0,1,0,1,1,0)$, $\frac{1}{\sqrt{13}}(0,1,1,0,0,1)$, $\sqrt{\frac{10}{39}}(0,1,1,1,0,0)$, $\sqrt{\frac{5}{39}}(1,1,0,0,0,1)$, $\sqrt{\frac{10}{39}}(1,1,0,1,0,0)$
$400_{[31]\lambda}$	$\sqrt{\frac{5}{39}}(0,0,0,1,1,1)$, $-\frac{1}{\sqrt{13}}(0,0,1,0,1,0)$, $\sqrt{\frac{5}{39}}(0,0,1,1,0,1)$, $-\sqrt{\frac{10}{39}}(0,0,2,0,0,0)$, $\frac{1}{\sqrt{13}}(1,0,0,0,1,0)$, $\frac{1}{\sqrt{13}}(1,0,0,1,0,1)$, $\sqrt{\frac{10}{39}}(2,0,0,0,0,0)$
$400_{[31]\eta}$	$-\sqrt{\frac{20}{39}}(0,0,0,0,2,0)$, $-\frac{1}{\sqrt{26}}(0,0,1,0,1,0)$, $\sqrt{\frac{5}{39}}(0,0,2,0,0,0)$, $-\frac{1}{\sqrt{26}}(1,0,0,0,1,0)$, $\sqrt{\frac{2}{13}}(1,0,1,0,0,0)$, $\sqrt{\frac{5}{39}}(2,0,0,0,0,0)$
$400_{[22]\rho}$	$\sqrt{\frac{10}{39}}(0,1,0,0,1,1)$, $-\frac{1}{\sqrt{13}}(0,1,0,1,1,0)$, $\sqrt{\frac{2}{13}}(0,1,1,0,0,1)$, $-\sqrt{\frac{5}{39}}(0,1,1,1,0,0)$, $\sqrt{\frac{10}{39}}(1,1,0,0,0,1)$, $-\sqrt{\frac{5}{39}}(1,1,0,1,0,0)$
$400_{[22]\lambda}$	$\sqrt{\frac{10}{39}}(0,0,0,1,1,1)$, $\frac{1}{\sqrt{26}}(0,0,1,0,1,0)$, $\sqrt{\frac{10}{39}}(0,0,1,1,0,1)$, $\sqrt{\frac{5}{39}}(0,0,2,0,0,0)$, $-\frac{1}{\sqrt{26}}(1,0,0,0,1,0)$, $\sqrt{\frac{2}{13}}(1,0,0,1,0,1)$

Table C.7 (Continued)

NLM	$C_{n_\rho, l_\rho, n_\lambda, l_\lambda, n_\eta, l_\eta}(n_\rho, l_\rho, n_\lambda, l_\lambda, n_\eta, l_\eta)$
	$\sqrt{\frac{5}{39}}(2,0,0,0,0,0)$
$600_{[4]S}$	$\sqrt{\frac{35}{429}}(3,0,0,0,0,0)$, $\sqrt{\frac{35}{429}}(0,0,3,0,0,0)$, $\sqrt{\frac{35}{429}}(0,0,0,0,3,0)$, $\sqrt{\frac{15}{143}}(2,0,1,0,0,0)$, $\sqrt{\frac{15}{143}}(2,0,0,0,1,0)$, $\sqrt{\frac{15}{143}}(1,0,2,0,0,0)$, $\sqrt{\frac{15}{143}}(0,0,2,0,1,0)$, $\sqrt{\frac{15}{143}}(1,0,0,0,2,0)$, $\sqrt{\frac{15}{143}}(0,0,1,0,2,0)$, $\sqrt{\frac{18}{143}}(1,0,1,0,1,0)$
$600_{[31]\rho}$	$\sqrt{\frac{7}{117}}(0,1,0,0,2,1)$, $\sqrt{\frac{2}{39}}(0,1,0,1,2,0)$, $\sqrt{\frac{2}{39}}(0,1,1,0,1,1)$, $\frac{2}{\sqrt{39}}(0,1,1,1,1,0)$, $\frac{1}{\sqrt{39}}(0,1,2,0,0,1)$, $\sqrt{\frac{14}{117}}(0,1,2,1,0,0)$, $\sqrt{\frac{10}{117}}(1,1,0,0,1,1)$, $\frac{2}{\sqrt{39}}(1,1,0,1,1,0)$, $\sqrt{\frac{2}{39}}(1,1,1,0,0,1)$, $\sqrt{\frac{20}{117}}(1,1,1,1,0,0)$, $\sqrt{\frac{7}{117}}(2,1,0,0,0,1)$, $\sqrt{\frac{14}{117}}(2,1,0,1,0,0)$
$600_{[31]\lambda}$	$\sqrt{\frac{7}{117}}(0,0,0,1,2,1)$, $\frac{1}{\sqrt{39}}(0,0,1,0,2,0)$, $\sqrt{\frac{10}{117}}(0,0,1,1,1,1)$, $-\frac{2}{\sqrt{39}}(0,0,2,0,1,0)$, $\sqrt{\frac{7}{117}}(0,0,2,1,0,1)$, $-\sqrt{\frac{7}{39}}(0,0,3,0,0,0)$, $\frac{1}{\sqrt{39}}(1,0,0,0,2,0)$, $\sqrt{\frac{2}{39}}(1,0,0,1,1,1)$, $\sqrt{\frac{2}{39}}(1,0,1,1,0,1)$, $-\frac{1}{\sqrt{39}}(1,0,2,0,0,0)$, $\frac{2}{\sqrt{39}}(2,0,0,0,1,0)$, $\frac{1}{\sqrt{39}}(2,0,0,1,0,1)$, $\frac{1}{\sqrt{39}}(2,0,1,0,0,0)$, $\sqrt{\frac{7}{39}}(3,0,0,0,0,0)$
$600_{[31]\eta}$	$-\sqrt{\frac{14}{39}}(0,0,0,0,3,0)$, $-\sqrt{\frac{3}{26}}(0,0,1,0,2,0)$, $\sqrt{\frac{7}{78}}(0,0,3,0,0,0)$, $-\frac{3}{\sqrt{26}}(1,0,0,0,2,0)$, $\frac{3}{\sqrt{26}}(1,0,2,0,0,0)$, $\sqrt{\frac{3}{26}}(2,0,1,0,0,0)$, $\sqrt{\frac{7}{78}}(3,0,0,0,0,0)$
$600_{[22]\rho}$	$\sqrt{\frac{14}{117}}(0,1,0,0,2,1)$, $-\frac{1}{\sqrt{39}}(0,1,0,1,2,0)$, $\frac{2}{39}(0,1,1,0,1,1)$, $-\sqrt{\frac{2}{39}}(0,1,1,1,1,0)$, $\sqrt{\frac{2}{39}}(0,1,2,0,0,1)$, $-\sqrt{\frac{7}{117}}(0,1,2,1,0,0)$, $\sqrt{\frac{20}{117}}(1,1,0,0,1,1)$, $-\sqrt{\frac{2}{39}}(1,1,0,1,1,0)$, $\frac{2}{\sqrt{39}}(1,1,1,0,0,1)$, $-\sqrt{\frac{10}{117}}(1,1,1,1,0,0)$, $\sqrt{\frac{14}{117}}(2,1,0,0,0,1)$, $-\sqrt{\frac{7}{117}}(2,1,0,1,0,0)$
$600_{[22]\lambda}$	$\sqrt{\frac{14}{117}}(0,0,0,1,2,1)$, $\frac{1}{\sqrt{78}}(0,0,1,0,2,0)$, $\sqrt{\frac{20}{117}}(0,0,1,1,1,1)$, $\sqrt{\frac{2}{39}}(0,0,2,0,1,0)$, $\sqrt{\frac{14}{117}}(0,0,2,1,0,1)$, $\sqrt{\frac{7}{78}}(0,0,3,0,0,0)$, $-\frac{1}{\sqrt{78}}(1,0,0,0,2,0)$, $\frac{2}{\sqrt{39}}(1,0,0,1,1,1)$, $\frac{2}{\sqrt{39}}(1,0,1,1,0,1)$,

Table C.7 (Continued)

NLM	$C_{n_\rho,l_\rho,n_\lambda,l_\lambda,n_\eta,l_\eta}(n_\rho, l_\rho, n_\lambda, l_\lambda, n_\eta, l_\eta)$
	$\frac{1}{\sqrt{78}}(1,0,2,0,0,0),\ -\sqrt{\frac{2}{39}}(2,0,0,0,1,0),\ \sqrt{\frac{2}{39}}(2,0,0,1,0,1),$
	$-\frac{1}{\sqrt{78}}(2,0,1,0,0,0),\ -\sqrt{\frac{7}{78}}(3,0,0,0,0,0)$
$800_{[4]S}$	$\sqrt{\frac{7}{143}}(4,0,0,0,0,0),\ \sqrt{\frac{7}{143}}(0,0,4,0,0,0),\ \sqrt{\frac{7}{143}}(0,0,0,0,4,0),$
	$\sqrt{\frac{28}{429}}(3,0,1,0,0,0),\ \sqrt{\frac{28}{429}}(3,0,0,0,1,0),\ \sqrt{\frac{28}{429}}(1,0,3,0,0,0),$
	$\sqrt{\frac{28}{429}}(0,0,3,0,1,0),\ \sqrt{\frac{28}{429}}(1,0,0,0,3,0),\ \sqrt{\frac{28}{429}}(0,0,1,0,3,0),$
	$\sqrt{\frac{10}{143}}(0,0,2,0,2,0),\ \sqrt{\frac{10}{143}}(2,0,0,0,2,0),\ \sqrt{\frac{10}{143}}(2,0,2,0,0,0),$
	$\sqrt{\frac{12}{143}}(2,0,1,0,1,0),\ \sqrt{\frac{12}{143}}(1,0,2,0,1,0),\ \sqrt{\frac{12}{143}}(1,0,1,0,2,0)$
$800_{[31]\rho}$	$\sqrt{\frac{7}{221}}(0,1,0,0,3,1),\ \sqrt{\frac{14}{663}}(0,1,0,1,3,0),\ \sqrt{\frac{7}{221}}(0,1,1,0,2,1),$
	$\sqrt{\frac{10}{221}}(0,1,1,1,2,0),\ \sqrt{\frac{5}{221}}(0,1,2,0,1,1),\ \sqrt{\frac{14}{221}}(0,1,2,1,1,0),$
	$\sqrt{\frac{7}{663}}(0,1,3,0,0,1),\ \sqrt{\frac{14}{221}}(0,1,3,1,0,0),\ \sqrt{\frac{35}{663}}(1,1,0,0,2,1),$
	$\sqrt{\frac{10}{221}}(1,1,0,1,2,0),\ \sqrt{\frac{10}{221}}(1,1,1,0,1,1),\ \sqrt{\frac{20}{221}}(1,1,1,1,1,0),$
	$\sqrt{\frac{5}{221}}(1,1,2,0,0,1),\ \sqrt{\frac{70}{663}}(1,1,2,1,0,0),\ \sqrt{\frac{35}{663}}(2,1,0,0,1,1),$
	$\sqrt{\frac{14}{221}}(2,1,1,0,0,1),\ \sqrt{\frac{7}{221}}(2,1,1,0,0,1),\ \sqrt{\frac{70}{663}}(2,1,1,1,0,0),$
	$\sqrt{\frac{7}{221}}(3,1,0,0,0,1),\ \sqrt{\frac{14}{221}}(3,1,0,1,0,0)$
$800_{[31]\lambda}$	$\sqrt{\frac{7}{221}}(0,0,0,1,3,1),\ \sqrt{\frac{7}{663}}(0,0,1,0,3,0),\ \sqrt{\frac{35}{663}}(0,0,1,1,2,1),$
	$-\sqrt{\frac{10}{221}}(0,0,2,0,2,0),\ \sqrt{\frac{35}{663}}(0,0,2,1,1,1),\ -\sqrt{\frac{21}{221}}(0,0,3,0,1,0),$
	$\sqrt{\frac{7}{221}}(0,0,3,1,0,1),\ -\sqrt{\frac{28}{221}}(0,0,4,0,0,0),\ \sqrt{\frac{7}{663}}(1,0,0,0,3,0),$
	$\sqrt{\frac{7}{221}}(1,0,0,1,2,1),\ \sqrt{\frac{10}{221}}(1,0,1,1,1,1),\ -\sqrt{\frac{3}{221}}(1,0,2,0,1,0),$
	$\sqrt{\frac{7}{221}}(1,0,2,1,0,1),\ \sqrt{\frac{28}{663}}(1,0,3,0,0,0),\ \sqrt{\frac{10}{221}}(2,0,0,0,2,0),$
	$\sqrt{\frac{5}{221}}(2,0,0,1,1,1),\ \sqrt{\frac{3}{221}}(2,0,1,0,1,0),\ \sqrt{\frac{5}{221}}(2,0,1,1,0,1),$
	$\sqrt{\frac{21}{221}}(3,0,0,0,1,0),\ \sqrt{\frac{7}{663}}(3,0,0,1,0,1),\ \sqrt{\frac{28}{663}}(3,0,1,0,0,0),$
	$\sqrt{\frac{28}{221}}(4,0,0,0,0,0)$
$800_{[31]\eta}$	$-\sqrt{\frac{56}{221}}(0,0,0,0,4,0),\ -\sqrt{\frac{175}{1326}}(0,0,1,0,3,0),\ -\sqrt{\frac{5}{221}}(0,0,2,0,2,0),$
	$\sqrt{\frac{7}{1326}}(0,0,3,0,1,0),\ \sqrt{\frac{14}{221}}(0,0,4,0,0,0),\ -\sqrt{\frac{175}{1326}}(1,0,0,0,3,0),$

Table C.7 (Continued)

NLM	$C_{n_\rho,l_\rho,n_\lambda,l_\lambda,n_\eta,l_\eta}(n_\rho,l_\rho,n_\lambda,l_\lambda,n_\eta,l_\eta)$
	$-\sqrt{\frac{6}{221}}(1,0,1,0,2,0),\ \sqrt{\frac{3}{442}}(1,0,2,0,1,0),\ \sqrt{\frac{56}{663}}(1,0,3,0,0,0),$
	$-\sqrt{\frac{5}{221}}(2,0,0,0,2,0),\ \sqrt{\frac{3}{442}}(2,0,1,0,1,0),\ \sqrt{\frac{20}{221}}(2,0,2,0,0,0),$
	$\sqrt{\frac{7}{1326}}(3,0,0,0,1,0),\ \sqrt{\frac{56}{663}}(3,0,1,0,0,0),\ \sqrt{\frac{14}{221}}(4,0,0,0,0,0)$
$800_{[22]\rho}$	$\sqrt{\frac{14}{221}}(0,1,0,0,3,1),\ -\sqrt{\frac{7}{663}}(0,1,0,1,3,0),\ \sqrt{\frac{14}{221}}(0,1,1,0,2,1),$
	$-\sqrt{\frac{5}{221}}(0,1,1,1,2,0),\ \sqrt{\frac{10}{221}}(0,1,2,0,1,1),\ -\sqrt{\frac{7}{221}}(0,1,2,1,1,0),$
	$\sqrt{\frac{14}{663}}(0,1,3,0,0,1),\ -\sqrt{\frac{7}{221}}(0,1,3,1,0,0),\ \sqrt{\frac{70}{663}}(1,1,0,0,2,1),$
	$-\sqrt{\frac{5}{221}}(1,1,0,1,2,0),\ \sqrt{\frac{20}{221}}(1,1,1,0,1,1),\ -\sqrt{\frac{10}{221}}(1,1,1,1,1,0),$
	$\sqrt{\frac{10}{221}}(1,1,2,0,0,1),\ -\sqrt{\frac{35}{663}}(1,1,2,1,0,0),\ \sqrt{\frac{70}{663}}(2,1,0,0,1,1),$
	$-\sqrt{\frac{7}{221}}(2,1,1,0,0,1),\ \sqrt{\frac{14}{221}}(2,1,1,0,0,1),\ -\sqrt{\frac{35}{663}}(2,1,1,1,0,0),$
	$\sqrt{\frac{14}{221}}(3,1,0,0,0,1),\ -\sqrt{\frac{7}{221}}(3,1,0,1,0,0)$
$800_{[22]\lambda}$	$\sqrt{\frac{14}{221}}(0,0,0,1,3,1),\ \sqrt{\frac{7}{1326}}(0,0,1,0,3,0),\ \sqrt{\frac{70}{663}}(0,0,1,1,2,1),$
	$\sqrt{\frac{5}{221}}(0,0,2,0,2,0),\ \sqrt{\frac{70}{663}}(0,0,2,1,1,1),\ \sqrt{\frac{21}{442}}(0,0,3,0,1,0),$
	$\sqrt{\frac{14}{221}}(0,0,3,1,0,1),\ \sqrt{\frac{14}{221}}(0,0,4,0,0,0),\ -\sqrt{\frac{7}{1326}}(1,0,0,0,3,0),$
	$\sqrt{\frac{14}{221}}(1,0,0,1,2,1),\ \sqrt{\frac{20}{221}}(1,0,1,1,1,1),\ \sqrt{\frac{3}{442}}(1,0,2,0,1,0),$
	$\sqrt{\frac{14}{221}}(1,0,2,1,0,1),\ \sqrt{\frac{14}{663}}(1,0,3,0,0,0),\ -\sqrt{\frac{5}{221}}(2,0,0,0,2,0),$
	$\sqrt{\frac{10}{221}}(2,0,0,1,1,1),\ -\sqrt{\frac{3}{442}}(2,0,1,0,1,0),\ \sqrt{\frac{10}{221}}(2,0,1,1,0,1),$
	$-\sqrt{\frac{21}{442}}(3,0,0,0,1,0),\ \sqrt{\frac{14}{663}}(3,0,0,1,0,1),\ -\sqrt{\frac{14}{663}}(3,0,1,0,0,0),$
	$-\sqrt{\frac{14}{221}}(4,0,0,0,0,0)$
$1000_{[4]S}$	$\sqrt{\frac{7}{221}}(5,0,0,0,0,0),\ \sqrt{\frac{7}{221}}(0,0,5,0,0,0),\ \sqrt{\frac{7}{221}}(0,0,0,0,5,0),$
	$\sqrt{\frac{105}{2431}}(4,0,1,0,0,0),\ \sqrt{\frac{105}{2431}}(4,0,0,0,1,0),\ \sqrt{\frac{105}{2431}}(1,0,4,0,0,0),$
	$\sqrt{\frac{105}{2431}}(0,0,4,0,1,0),\ \sqrt{\frac{105}{2431}}(1,0,0,0,4,0),\ \sqrt{\frac{105}{2431}}(0,0,1,0,4,0),$
	$\sqrt{\frac{350}{7293}}(3,0,2,0,0,0),\ \sqrt{\frac{350}{7293}}(3,0,0,0,2,0),\ \sqrt{\frac{350}{7293}}(2,0,3,0,0,0),$
	$\sqrt{\frac{350}{7293}}(0,0,3,0,2,0),\ \sqrt{\frac{350}{7293}}(2,0,0,0,3,0),\ \sqrt{\frac{350}{7293}}(0,0,2,0,3,0),$
	$\sqrt{\frac{150}{2431}}(1,0,2,0,2,0),\ \sqrt{\frac{150}{2431}}(2,0,1,0,2,0),\ \sqrt{\frac{150}{2431}}(2,0,2,0,1,0),$

Table C.7 (Continued)

NLM	$C_{n_\rho,l_\rho,n_\lambda,l_\lambda,n_\eta,l_\eta}(n_\rho,l_\rho,n_\lambda,l_\lambda,n_\eta,l_\eta)$
	$\sqrt{\frac{12}{143}}(3,0,1,0,1,0),\ \sqrt{\frac{12}{143}}(1,0,3,0,1,0),\ \sqrt{\frac{12}{143}}(1,0,1,0,3,0)$

$1000_{[31]\rho}$

$\sqrt{\frac{77}{4199}}(0,1,0,0,4,1),\ \sqrt{\frac{42}{4199}}(0,1,0,1,4,0),\ \sqrt{\frac{84}{4199}}(0,1,1,0,3,1),$

$\sqrt{\frac{280}{12597}}(0,1,1,1,3,0),\ \sqrt{\frac{70}{4199}}(0,1,2,0,2,1),\ \sqrt{\frac{140}{4199}}(0,1,2,1,2,0),$

$\sqrt{\frac{140}{12597}}(0,1,3,0,1,1),\ \sqrt{\frac{168}{4199}}(0,1,3,1,1,0),\ \sqrt{\frac{21}{4199}}(0,1,4,0,0,1),$

$\sqrt{\frac{154}{4199}}(0,1,4,1,0,0),\ \sqrt{\frac{140}{4199}}(1,1,0,0,3,1),\ \sqrt{\frac{280}{12597}}(1,1,0,1,3,0),$

$\sqrt{\frac{140}{4199}}(1,1,1,0,2,1),\ \sqrt{\frac{200}{4199}}(1,1,1,1,2,0),\ \frac{10}{\sqrt{4199}}(1,1,2,0,1,1),$

$\sqrt{\frac{280}{12597}}(1,1,2,1,1,0),\ \sqrt{\frac{140}{4199}}(1,1,3,0,0,1),\ \sqrt{\frac{280}{4199}}(1,1,3,1,0,0),$

$\sqrt{\frac{490}{12597}}(2,1,0,0,2,1),\ \sqrt{\frac{140}{4199}}(2,1,0,1,2,0),\ \sqrt{\frac{140}{4199}}(2,1,1,0,1,1),$

$\sqrt{\frac{280}{4199}}(2,1,1,1,1,0),\ \sqrt{\frac{70}{4199}}(2,1,2,0,0,1),\ \sqrt{\frac{980}{12597}}(2,1,2,1,0,0),$

$\sqrt{\frac{140}{4199}}(3,1,0,0,1,1),\ \sqrt{\frac{168}{4199}}(3,1,0,1,1,0),\ \sqrt{\frac{84}{4199}}(3,1,1,0,0,1),$

$\sqrt{\frac{280}{4199}}(3,1,1,1,0,0),\ \sqrt{\frac{77}{4199}}(4,1,0,0,0,1),\ \sqrt{\frac{154}{4199}}(4,1,0,1,0,0)$

$1000_{[31]\lambda}$

$\sqrt{\frac{77}{4199}}(0,0,0,1,4,1),\ -\sqrt{\frac{21}{4199}}(0,0,1,0,4,0),\ \sqrt{\frac{140}{4199}}(0,0,1,1,3,1),$

$-\sqrt{\frac{280}{12597}}(0,0,2,0,3,0),\ \sqrt{\frac{490}{12597}}(0,0,2,1,2,1),\ -\sqrt{\frac{210}{4199}}(0,0,3,0,2,0),$

$\sqrt{\frac{140}{4199}}(0,0,3,1,1,1),\ -\sqrt{\frac{336}{4199}}(0,0,4,0,1,0),\ \sqrt{\frac{77}{4199}}(0,0,4,1,0,1),$

$-\sqrt{\frac{385}{4199}}(0,0,5,0,0,0),\ \sqrt{\frac{21}{4199}}(1,0,0,0,4,0),\ \sqrt{\frac{84}{4199}}(1,0,0,1,3,1),$

$\sqrt{\frac{140}{4199}}(1,0,1,1,2,1),\ -\sqrt{\frac{30}{4199}}(1,0,2,0,2,0),\ \frac{140}{\sqrt{4199}}(1,1,2,1,1,1),$

$-\sqrt{\frac{112}{4199}}(1,0,3,0,1,0),\ \sqrt{\frac{84}{4199}}(1,0,3,1,0,1),\ -\sqrt{\frac{189}{4199}}(1,0,4,0,0,0),$

$\sqrt{\frac{280}{12597}}(2,0,0,0,3,0),\ \sqrt{\frac{70}{4199}}(2,0,0,1,2,1),\ \sqrt{\frac{30}{4199}}(2,0,1,1,1,1),$

$\frac{10}{\sqrt{4199}}(2,0,1,1,1,1),\ \sqrt{\frac{70}{4199}}(2,0,2,1,0,1),\ -\sqrt{\frac{70}{12597}}(2,0,3,0,0,0),$

$\sqrt{\frac{210}{4199}}(3,0,0,0,2,0),\ \sqrt{\frac{140}{12597}}(3,0,0,1,1,1),\ \sqrt{\frac{112}{4199}}(3,0,1,0,1,0),$

$\sqrt{\frac{140}{12597}}(3,0,1,1,0,1),\ \sqrt{\frac{70}{12597}}(3,0,2,0,0,0),\ \sqrt{\frac{336}{4199}}(4,0,0,0,1,0),$

$\sqrt{\frac{21}{4199}}(4,0,0,1,0,1),\ \sqrt{\frac{189}{4199}}(4,0,1,0,0,0),\ \sqrt{\frac{385}{4199}}(5,0,0,0,0,0)$

$1000_{[31]\eta}$

$-\sqrt{\frac{770}{4199}}(0,0,0,0,5,0),\ -\sqrt{\frac{1029}{8398}}(0,0,1,0,4,0),\ -\sqrt{\frac{560}{12597}}(0,0,2,0,3,0),$

$-\sqrt{\frac{35}{12597}}(0,0,3,0,2,0),\ \sqrt{\frac{42}{4199}}(0,0,4,0,1,0),\ \sqrt{\frac{385}{8398}}(0,0,5,0,0,0),$

Table C.7 (Continued)

NLM	$C_{n_\rho,l_\rho,n_\lambda,l_\lambda,n_\eta,l_\eta}(n_\rho,l_\rho,n_\lambda,l_\lambda,n_\eta,l_\eta)$
	$-\sqrt{\frac{1029}{8398}}(1,0,0,0,4,0),\ -\sqrt{\frac{224}{4199}}(1,0,1,0,3,0),\ -\sqrt{\frac{15}{4199}}(1,0,2,0,2,0),$
	$\sqrt{\frac{56}{4199}}(1,0,3,0,1,0),\ \sqrt{\frac{525}{8398}}(1,0,4,0,0,0),\ -\sqrt{\frac{560}{12597}}(2,0,0,0,3,0),$
	$-\sqrt{\frac{15}{4199}}(2,0,1,0,2,0),\ \sqrt{\frac{60}{4199}}(2,0,2,0,1,0),\ \sqrt{\frac{875}{12597}}(2,0,3,0,0,0),$
	$-\sqrt{\frac{35}{12597}}(3,0,0,0,2,0),\ \sqrt{\frac{56}{4199}}(3,0,1,0,1,0),\ \sqrt{\frac{875}{12597}}(3,0,2,0,0,0),$
	$\sqrt{\frac{42}{4199}}(4,0,0,0,1,0),\ \sqrt{\frac{525}{8398}}(4,0,1,0,0,0),\ \sqrt{\frac{385}{8398}}(5,0,0,0,0,0)$
$1000_{[22]\rho}$	$\sqrt{\frac{154}{4199}}(0,1,0,0,4,1),\ -\sqrt{\frac{21}{4199}}(0,1,0,1,4,0),\ \sqrt{\frac{168}{4199}}(0,1,1,0,3,1),$
	$-\sqrt{\frac{140}{12597}}(0,1,1,1,3,0),\ \sqrt{\frac{140}{4199}}(0,1,2,0,2,1),\ -\sqrt{\frac{70}{4199}}(0,1,2,1,2,0),$
	$\sqrt{\frac{280}{12597}}(0,1,3,0,1,1),\ -\sqrt{\frac{84}{4199}}(0,1,3,1,1,0),\ \sqrt{\frac{42}{4199}}(0,1,4,0,0,1),$
	$-\sqrt{\frac{77}{4199}}(0,1,4,1,0,0),\ \sqrt{\frac{70}{4199}}(1,1,0,0,3,1),\ -\sqrt{\frac{140}{12597}}(1,1,0,1,3,0),$
	$\sqrt{\frac{280}{4199}}(1,1,1,0,2,1),\ -\frac{10}{\sqrt{4199}}(1,1,1,1,2,0),\ \sqrt{\frac{200}{4199}}(1,1,2,0,1,1),$
	$-\sqrt{\frac{140}{12597}}(1,1,2,1,1,0),\ \sqrt{\frac{280}{4199}}(1,1,3,0,0,1),\ -\sqrt{\frac{140}{4199}}(1,1,3,1,0,0),$
	$\sqrt{\frac{980}{12597}}(2,1,0,0,2,1),\ -\sqrt{\frac{70}{4199}}(2,1,0,1,2,0),\ \sqrt{\frac{280}{4199}}(2,1,1,0,1,1),$
	$-\sqrt{\frac{140}{4199}}(2,1,1,1,1,0),\ \sqrt{\frac{140}{4199}}(2,1,2,0,0,1),\ -\sqrt{\frac{490}{12597}}(2,1,2,1,0,0),$
	$\sqrt{\frac{280}{4199}}(3,1,0,0,1,1),\ -\sqrt{\frac{84}{4199}}(3,1,0,1,1,0),\ \sqrt{\frac{168}{4199}}(3,1,1,0,0,1),$
	$-\sqrt{\frac{140}{4199}}(3,1,1,1,0,0),\ \sqrt{\frac{154}{4199}}(4,1,0,0,0,1),\ -\sqrt{\frac{77}{4199}}(4,1,0,1,0,0)$
$1000_{[22]\lambda}$	$\sqrt{\frac{154}{4199}}(0,0,0,1,4,1),\ \sqrt{\frac{21}{8398}}(0,0,1,0,4,0),\ \sqrt{\frac{280}{4199}}(0,0,1,1,3,1),$
	$\sqrt{\frac{140}{12597}}(0,0,2,0,3,0),\ \sqrt{\frac{980}{12597}}(0,0,2,1,2,1),\ \sqrt{\frac{105}{4199}}(0,0,3,0,2,0),$
	$\sqrt{\frac{280}{4199}}(0,0,3,1,1,1),\ \sqrt{\frac{168}{4199}}(0,0,4,0,1,0),\ \sqrt{\frac{154}{4199}}(0,0,4,1,0,1),$
	$\sqrt{\frac{385}{8398}}(0,0,5,0,0,0),\ -\sqrt{\frac{21}{8398}}(1,0,0,0,4,0),\ \sqrt{\frac{168}{4199}}(1,0,0,1,3,1),$
	$\sqrt{\frac{280}{4199}}(1,0,1,1,2,1),\ \sqrt{\frac{15}{4199}}(1,0,2,0,2,0),\ \frac{280}{\sqrt{4199}}(1,1,2,1,1,1),$
	$\sqrt{\frac{56}{4199}}(1,0,3,0,1,0),\ \sqrt{\frac{168}{4199}}(1,0,3,1,0,1),\ \sqrt{\frac{189}{8398}}(1,0,4,0,0,0),$
	$-\sqrt{\frac{140}{12597}}(2,0,0,0,3,0),\ \sqrt{\frac{140}{4199}}(2,0,0,1,2,1),\ -\sqrt{\frac{15}{4199}}(2,0,1,1,1,1),$
	$\sqrt{\frac{200}{4199}}(2,0,1,1,1,1),\ \sqrt{\frac{140}{4199}}(2,0,2,1,0,1),\ \sqrt{\frac{35}{12597}}(2,0,3,0,0,0),$
	$-\sqrt{\frac{105}{4199}}(3,0,0,0,2,0),\ \sqrt{\frac{280}{12597}}(3,0,0,1,1,1),\ -\sqrt{\frac{56}{4199}}(3,0,1,0,1,0),$

Table C.7 (Continued)

NLM	$C_{n_\rho, l_\rho, n_\lambda, l_\lambda, n_\eta, l_\eta}(n_\rho, l_\rho, n_\lambda, l_\lambda, n_\eta, l_\eta)$
	$\sqrt{\frac{280}{12597}}(3,0,1,1,0,1),\ -\sqrt{\frac{35}{12597}}(3,0,2,0,0,0),\ -\sqrt{\frac{168}{4199}}(4,0,0,0,1,0),$
	$\sqrt{\frac{42}{4199}}(4,0,0,1,0,1),\ -\sqrt{\frac{189}{8398}}(4,0,1,0,0,0),\ -\sqrt{\frac{385}{8398}}(5,0,0,0,0,0)$
$1200_{[4]S}$	$\sqrt{\frac{7}{323}}(6,0,0,0,0,0),\ \sqrt{\frac{7}{323}}(0,0,6,0,0,0),\ \sqrt{\frac{7}{323}}(0,0,0,0,6,0),$
	$\sqrt{\frac{126}{4199}}(5,0,1,0,0,0),\ \sqrt{\frac{126}{4199}}(5,0,0,0,1,0),\ \sqrt{\frac{126}{4199}}(1,0,5,0,0,0),$
	$\sqrt{\frac{126}{4199}}(0,0,5,0,1,0),\ \sqrt{\frac{126}{4199}}(1,0,0,0,5,0),\ \sqrt{\frac{126}{4199}}(0,0,1,0,5,0),$
	$\sqrt{\frac{1575}{46189}}(4,0,2,0,0,0),\ \sqrt{\frac{1575}{46189}}(4,0,0,0,2,0),\ \sqrt{\frac{1575}{46189}}(2,0,4,0,0,0),$
	$\sqrt{\frac{1575}{46189}}(0,0,4,0,2,0),\ \sqrt{\frac{1575}{46189}}(2,0,0,0,4,0),\ \sqrt{\frac{1575}{46189}}(0,0,2,0,4,0),$
	$\frac{70}{\sqrt{138567}}(0,0,3,0,3,0),\ \frac{70}{\sqrt{138567}}(3,0,0,0,3,0),\ \frac{70}{\sqrt{138567}}(3,0,3,0,0,0),$
	$\sqrt{\frac{2100}{46189}}(3,0,1,0,2,0),\ \sqrt{\frac{2100}{46189}}(3,0,2,0,1,0),\ \sqrt{\frac{2100}{46189}}(1,0,3,0,2,0),$
	$\sqrt{\frac{2100}{46189}}(2,0,3,0,1,0),\ \sqrt{\frac{2100}{46189}}(1,0,2,0,3,0),\ \sqrt{\frac{2100}{46189}}(2,0,1,0,3,0),$
	$\sqrt{\frac{1890}{46189}}(4,0,1,0,1,0),\ \sqrt{\frac{1890}{46189}}(1,0,4,0,1,0),\ \sqrt{\frac{1890}{46189}}(1,0,1,0,4,0),$
	$\sqrt{\frac{2250}{46189}}(2,0,2,0,2,0)$
$1400_{[4]S}$	$\sqrt{\frac{5}{323}}(7,0,0,0,0,0),\ \sqrt{\frac{5}{323}}(0,0,7,0,0,0),\ \sqrt{\frac{5}{323}}(0,0,0,0,7,0),$
	$\sqrt{\frac{7}{323}}(6,0,1,0,0,0),\ \sqrt{\frac{7}{323}}(6,0,0,0,1,0),\ \sqrt{\frac{7}{323}}(1,0,6,0,0,0),$
	$\sqrt{\frac{7}{323}}(0,0,6,0,1,0),\ \sqrt{\frac{7}{323}}(1,0,0,0,6,0),\ \sqrt{\frac{7}{323}}(0,0,1,0,6,0),$
	$\sqrt{\frac{105}{4199}}(5,0,2,0,0,0),\ \sqrt{\frac{105}{4199}}(5,0,0,0,2,0),\ \sqrt{\frac{105}{4199}}(2,0,5,0,0,0),$
	$\sqrt{\frac{105}{4199}}(0,0,5,0,2,0),\ \sqrt{\frac{105}{4199}}(2,0,0,0,5,0),\ \sqrt{\frac{105}{4199}}(0,0,2,0,5,0),$
	$\sqrt{\frac{126}{4199}}(5,0,1,0,1,0),\ \sqrt{\frac{126}{4199}}(1,0,5,0,1,0),\ \sqrt{\frac{126}{4199}}(1,0,1,0,5,0),$
	$\frac{35}{\sqrt{46189}}(0,0,4,0,3,0),\ \frac{35}{\sqrt{46189}}(0,0,3,0,4,0),\ \frac{35}{\sqrt{46189}}(4,0,0,0,3,0),$
	$\frac{35}{\sqrt{46189}}(3,0,0,0,4,0),\ \frac{35}{\sqrt{46189}}(4,0,3,0,0,0),\ \frac{35}{\sqrt{46189}}(3,0,4,0,0,0),$
	$\sqrt{\frac{1575}{46189}}(4,0,1,0,2,0),\ \sqrt{\frac{1575}{46189}}(4,0,2,0,1,0),\ \sqrt{\frac{1575}{46189}}(1,0,4,0,2,0),$
	$\sqrt{\frac{1575}{46189}}(2,0,4,0,1,0),\ \sqrt{\frac{1575}{46189}}(1,0,2,0,4,0),\ \sqrt{\frac{1575}{46189}}(2,0,1,0,4,0),$
	$\frac{70}{\sqrt{138567}}(1,0,3,0,3,0),\ \frac{70}{\sqrt{138567}}(3,0,1,0,3,0),\ \frac{70}{\sqrt{138567}}(3,0,3,0,1,0),$
	$\sqrt{\frac{1750}{46189}}(3,0,2,0,2,0),\ \sqrt{\frac{1750}{46189}}(2,0,3,0,2,0),\ \sqrt{\frac{1750}{46189}}(2,0,2,0,3,0)$

Table C.7 (Continued)

NLM	$C_{n_\rho,l_\rho,n_\lambda,l_\lambda,n_\eta,l_\eta}(n_\rho, l_\rho, n_\lambda, l_\lambda, n_\eta, l_\eta)$
$1600_{[4]S}$	$\sqrt{\frac{5}{437}}(8,0,0,0,0,0),\ \sqrt{\frac{5}{437}}(0,0,8,0,0,0),\ \sqrt{\frac{5}{437}}(0,0,0,0,8,0),$
	$\sqrt{\frac{120}{7429}}(7,0,1,0,0,0),\ \sqrt{\frac{120}{7429}}(7,0,0,0,1,0),\ \sqrt{\frac{120}{7429}}(1,0,7,0,0,0),$
	$\sqrt{\frac{120}{7429}}(0,0,7,0,1,0),\ \sqrt{\frac{120}{7429}}(1,0,0,0,7,0),\ \sqrt{\frac{120}{7429}}(0,0,1,0,7,0),$
	$\sqrt{\frac{140}{7429}}(6,0,2,0,0,0),\ \sqrt{\frac{140}{7429}}(6,0,0,0,2,0),\ \sqrt{\frac{140}{7429}}(2,0,6,0,0,0),$
	$\sqrt{\frac{140}{7429}}(0,0,6,0,2,0),\ \sqrt{\frac{140}{7429}}(2,0,0,0,6,0),\ \sqrt{\frac{140}{7429}}(0,0,2,0,6,0),$
	$\sqrt{\frac{168}{7429}}(6,0,1,0,1,0),\ \sqrt{\frac{168}{7429}}(1,0,6,0,1,0),\ \sqrt{\frac{168}{7429}}(1,0,1,0,6,0),$
	$\sqrt{\frac{1960}{96577}}(0,0,5,0,3,0),\ \sqrt{\frac{1960}{96577}}(0,0,3,0,5,0),\ \sqrt{\frac{1960}{96577}}(5,0,0,0,3,0),$
	$\sqrt{\frac{1960}{96577}}(3,0,0,0,5,0),\ \sqrt{\frac{1960}{96577}}(5,0,3,0,0,0),\ \sqrt{\frac{1960}{96577}}(3,0,5,0,0,0),$
	$\sqrt{\frac{2520}{96577}}(5,0,1,0,2,0),\ \sqrt{\frac{2520}{96577}}(5,0,2,0,1,0),\ \sqrt{\frac{2520}{96577}}(1,0,5,0,2,0),$
	$\sqrt{\frac{2520}{96577}}(2,0,5,0,1,0),\ \sqrt{\frac{2520}{96577}}(1,0,2,0,5,0),\ \sqrt{\frac{2520}{96577}}(2,0,1,0,5,0),$
	$\sqrt{\frac{22050}{1062347}}(0,0,4,0,4,0),\ \sqrt{\frac{22050}{1062347}}(4,0,0,0,4,0),\ \sqrt{\frac{22050}{1062347}}(4,0,4,0,0,0),$
	$\sqrt{\frac{29400}{1062347}}(4,0,1,0,3,0),\ \sqrt{\frac{29400}{1062347}}(4,0,3,0,1,0),\ \sqrt{\frac{29400}{1062347}}(1,0,4,0,3,0),$
	$\sqrt{\frac{29400}{1062347}}(3,0,4,0,1,0),\ \sqrt{\frac{29400}{1062347}}(1,0,3,0,4,0),\ \sqrt{\frac{29400}{1062347}}(3,0,1,0,4,0),$
	$\sqrt{\frac{31500}{1062347}}(4,0,2,0,2,0),\ \sqrt{\frac{31500}{1062347}}(2,0,4,0,2,0),\ \sqrt{\frac{31500}{1062347}}(2,0,2,0,4,0),$
	$\sqrt{\frac{98000}{3187041}}(2,0,3,0,3,0),\ \sqrt{\frac{98000}{3187041}}(3,0,2,0,3,0),\ \sqrt{\frac{98000}{3187041}}(3,0,3,0,2,0)$
$1800_{[4]S}$	$\frac{1}{\sqrt{105}}(9,0,0,0,0,0),\ \frac{1}{\sqrt{105}}(0,0,9,0,0,0),\ \frac{1}{\sqrt{105}}(0,0,0,0,9,0),$
	$\sqrt{\frac{27}{2185}}(8,0,1,0,0,0),\ \sqrt{\frac{27}{2185}}(8,0,0,0,1,0),\ \sqrt{\frac{27}{2185}}(1,0,8,0,0,0),$
	$\sqrt{\frac{27}{2185}}(0,0,8,0,1,0),\ \sqrt{\frac{27}{2185}}(1,0,0,0,8,0),\ \sqrt{\frac{27}{2185}}(0,0,1,0,8,0),$
	$\sqrt{\frac{108}{7429}}(7,0,2,0,0,0),\ \sqrt{\frac{108}{7429}}(7,0,0,0,2,0),\ \sqrt{\frac{108}{7429}}(2,0,7,0,0,0),$
	$\sqrt{\frac{108}{7429}}(0,0,7,0,2,0),\ \sqrt{\frac{108}{7429}}(2,0,0,0,7,0),\ \sqrt{\frac{108}{7429}}(0,0,2,0,7,0),$
	$\sqrt{\frac{648}{37145}}(7,0,1,0,1,0),\ \sqrt{\frac{648}{37145}}(1,0,7,0,1,0),\ \sqrt{\frac{648}{37145}}(1,0,1,0,7,0),$
	$\sqrt{\frac{588}{37145}}(0,0,6,0,3,0),\ \sqrt{\frac{588}{37145}}(0,0,3,0,6,0),\ \sqrt{\frac{588}{37145}}(6,0,0,0,3,0),$
	$\sqrt{\frac{588}{37145}}(3,0,0,0,6,0),\ \sqrt{\frac{588}{37145}}(6,0,3,0,0,0),\ \sqrt{\frac{588}{37145}}(3,0,6,0,0,0),$
	$\sqrt{\frac{756}{37145}}(6,0,1,0,2,0),\ \sqrt{\frac{756}{37145}}(6,0,2,0,1,0),\ \sqrt{\frac{756}{37145}}(1,0,6,0,2,0),$

Table C.7 **(Continued)**

NLM	$C_{n_\rho,l_\rho,n_\lambda,l_\lambda,n_\eta,l_\eta}(n_\rho,l_\rho,n_\lambda,l_\lambda,n_\eta,l_\eta)$
	$\sqrt{\frac{756}{37145}}(2,0,6,0,1,0),\ \sqrt{\frac{756}{37145}}(1,0,2,0,6,0),\ \sqrt{\frac{756}{37145}}(2,0,1,0,6,0),$
	$\sqrt{\frac{7938}{482885}}(0,0,5,0,4,0),\ \sqrt{\frac{7938}{482885}}(0,0,4,0,5,0),\ \sqrt{\frac{7938}{482885}}(5,0,0,0,4,0),$
	$\sqrt{\frac{7938}{482885}}(4,0,0,0,5,0),\ \sqrt{\frac{7938}{482885}}(5,0,4,0,0,0),\ \sqrt{\frac{7938}{482885}}(4,0,5,0,0,0),$
	$\sqrt{\frac{10584}{482885}}(5,0,1,0,3,0),\ \sqrt{\frac{10584}{482885}}(5,0,3,0,1,0),\ \sqrt{\frac{10584}{482885}}(1,0,5,0,3,0),$
	$\sqrt{\frac{10584}{482885}}(3,0,5,0,1,0),\ \sqrt{\frac{10584}{482885}}(1,0,3,0,5,0),\ \sqrt{\frac{10584}{482885}}(3,0,1,0,5,0),$
	$\sqrt{\frac{2268}{96577}}(5,0,2,0,2,0),\ \sqrt{\frac{2268}{96577}}(2,0,5,0,2,0),\ \sqrt{\frac{2268}{96577}}(2,0,2,0,5,0),$
	$\sqrt{\frac{23814}{1062347}}(1,0,4,0,4,0),\ \sqrt{\frac{23814}{1062347}}(4,0,1,0,4,0),\ \sqrt{\frac{23814}{1062347}}(4,0,4,0,1,0),$
	$\sqrt{\frac{26460}{1062347}}(4,0,2,0,3,0),\ \sqrt{\frac{26460}{1062347}}(4,0,3,0,2,0),\ \sqrt{\frac{26460}{1062347}}(2,0,4,0,3,0),$
	$\sqrt{\frac{26460}{1062347}}(3,0,4,0,2,0),\ \sqrt{\frac{26460}{1062347}}(2,0,3,0,4,0),\ \sqrt{\frac{26460}{1062347}}(3,0,2,0,4,0),$
	$\sqrt{\frac{2250}{46189}}(3,0,3,0,3,0)$
$2000_{[4]S}$	$\sqrt{\frac{7}{1035}}(10,0,0,0,0,0),\ \sqrt{\frac{7}{1035}}(0,0,10,0,0,0),\ \sqrt{\frac{7}{1035}}(0,0,0,0,10,0),$
	$\sqrt{\frac{2}{207}}(9,0,1,0,0,0),\ \sqrt{\frac{2}{207}}(9,0,0,0,1,0),\ \sqrt{\frac{2}{207}}(1,0,9,0,0,0),$
	$\sqrt{\frac{2}{207}}(0,0,9,0,1,0),\ \sqrt{\frac{2}{207}}(1,0,0,0,9,0),\ \sqrt{\frac{2}{207}}(0,0,1,0,9,0),$
	$\sqrt{\frac{5}{437}}(8,0,2,0,0,0),\ \sqrt{\frac{5}{437}}(8,0,0,0,2,0),\ \sqrt{\frac{5}{437}}(2,0,8,0,0,0),$
	$\sqrt{\frac{5}{437}}(0,0,8,0,2,0),\ \sqrt{\frac{5}{437}}(2,0,0,0,8,0),\ \sqrt{\frac{5}{437}}(0,0,2,0,8,0),$
	$\sqrt{\frac{6}{437}}(8,0,1,0,1,0),\ \sqrt{\frac{6}{437}}(1,0,8,0,1,0),\ \sqrt{\frac{6}{437}}(1,0,1,0,8,0),$
	$\sqrt{\frac{280}{22287}}(0,0,7,0,3,0),\ \sqrt{\frac{280}{22287}}(0,0,3,0,7,0),\ \sqrt{\frac{280}{22287}}(7,0,0,0,3,0),$
	$\sqrt{\frac{280}{22287}}(3,0,0,0,7,0),\ \sqrt{\frac{280}{22287}}(7,0,3,0,0,0),\ \sqrt{\frac{280}{22287}}(3,0,7,0,0,0),$
	$\sqrt{\frac{120}{7429}}(7,0,1,0,2,0),\ \sqrt{\frac{120}{7429}}(7,0,2,0,1,0),\ \sqrt{\frac{120}{7429}}(1,0,7,0,2,0),$
	$\sqrt{\frac{120}{7429}}(2,0,7,0,1,0),\ \sqrt{\frac{120}{7429}}(1,0,2,0,7,0),\ \sqrt{\frac{120}{7429}}(2,0,1,0,7,0),$
	$\sqrt{\frac{56}{7429}}(0,0,6,0,4,0),\ \sqrt{\frac{56}{7429}}(0,0,4,0,6,0),\ \sqrt{\frac{56}{7429}}(6,0,0,0,4,0),$
	$\sqrt{\frac{56}{7429}}(4,0,0,0,6,0),\ \sqrt{\frac{56}{7429}}(6,0,4,0,0,0),\ \sqrt{\frac{56}{7429}}(4,0,6,0,0,0),$
	$\sqrt{\frac{392}{22287}}(6,0,1,0,3,0),\ \sqrt{\frac{392}{22287}}(6,0,3,0,1,0),\ \sqrt{\frac{392}{22287}}(1,0,6,0,3,0),$
	$\sqrt{\frac{392}{22287}}(3,0,6,0,1,0),\ \sqrt{\frac{392}{22287}}(1,0,3,0,6,0),\ \sqrt{\frac{392}{22287}}(3,0,1,0,6,0),$

Table C.7 **(Continued)**

NLM	$C_{n_\rho,l_\rho,n_\lambda,l_\lambda,n_\eta,l_\eta}(n_\rho,l_\rho,n_\lambda,l_\lambda,n_\eta,l_\eta)$
	$\sqrt{\frac{140}{7429}}(6,0,2,0,2,0)$, $\sqrt{\frac{140}{7429}}(2,0,6,0,2,0)$, $\sqrt{\frac{140}{7429}}(2,0,2,0,6,0)$,
	$\sqrt{\frac{6468}{482885}}(0,0,5,0,5,0)$, $\sqrt{\frac{6468}{482885}}(5,0,0,0,5,0)$, $\sqrt{\frac{6468}{482885}}(5,0,5,0,0,0)$,
	$\frac{42}{\sqrt{96577}}(5,0,1,0,4,0)$, $\frac{42}{\sqrt{96577}}(5,0,4,0,1,0)$, $\frac{42}{\sqrt{96577}}(1,0,5,0,4,0)$,
	$\frac{42}{\sqrt{96577}}(4,0,5,0,1,0)$, $\frac{42}{\sqrt{96577}}(1,0,4,0,5,0)$, $\frac{42}{\sqrt{96577}}(4,0,1,0,5,0)$,
	$\sqrt{\frac{1960}{96577}}(5,0,2,0,3,0)$, $\sqrt{\frac{1960}{96577}}(5,0,3,0,2,0)$, $\sqrt{\frac{1960}{96577}}(2,0,5,0,3,0)$,
	$\sqrt{\frac{1960}{96577}}(3,0,5,0,2,0)$, $\sqrt{\frac{1960}{96577}}(2,0,3,0,5,0)$, $\sqrt{\frac{1960}{96577}}(3,0,2,0,5,0)$,
	$\sqrt{\frac{22050}{1062347}}(2,0,4,0,4,0)$, $\sqrt{\frac{22050}{1062347}}(4,0,2,0,4,0)$, $\sqrt{\frac{22050}{1062347}}(4,0,4,0,2,0)$,
	$\sqrt{\frac{68600}{3187041}}(4,0,3,0,3,0)$, $\sqrt{\frac{68600}{3187041}}(3,0,4,0,3,0)$, $\sqrt{\frac{68600}{3187041}}(3,0,3,0,4,0)$
$2200_{[4]S}$	$\sqrt{\frac{7}{1305}}(11,0,0,0,0,0)$, $\sqrt{\frac{7}{1305}}(0,0,11,0,0,0)$, $\sqrt{\frac{7}{1305}}(0,0,0,0,11,0)$,
	$\sqrt{\frac{77}{10005}}(10,0,1,0,0,0)$, $\sqrt{\frac{77}{10005}}(10,0,0,0,1,0)$, $\sqrt{\frac{77}{10005}}(1,0,10,0,0,0)$,
	$\sqrt{\frac{77}{10005}}(0,0,10,0,1,0)$, $\sqrt{\frac{77}{10005}}(1,0,0,0,10,0)$, $\sqrt{\frac{77}{10005}}(0,0,1,0,10,0)$,
	$\sqrt{\frac{55}{6003}}(9,0,2,0,0,0)$, $\sqrt{\frac{55}{6003}}(9,0,0,0,2,0)$, $\sqrt{\frac{55}{6003}}(2,0,9,0,0,0)$,
	$\sqrt{\frac{55}{6003}}(0,0,9,0,2,0)$, $\sqrt{\frac{55}{6003}}(2,0,0,0,9,0)$, $\sqrt{\frac{55}{6003}}(0,0,2,0,9,0)$,
	$\sqrt{\frac{22}{2001}}(9,0,1,0,1,0)$, $\sqrt{\frac{22}{2001}}(1,0,9,0,1,0)$, $\sqrt{\frac{22}{2001}}(1,0,1,0,9,0)$,
	$\sqrt{\frac{385}{38019}}(0,0,8,0,3,0)$, $\sqrt{\frac{385}{38019}}(0,0,3,0,8,0)$, $\sqrt{\frac{385}{38019}}(8,0,0,0,3,0)$,
	$\sqrt{\frac{385}{38019}}(3,0,0,0,8,0)$, $\sqrt{\frac{385}{38019}}(8,0,3,0,0,0)$, $\sqrt{\frac{385}{38019}}(3,0,8,0,0,0)$,
	$\sqrt{\frac{165}{12673}}(8,0,1,0,2,0)$, $\sqrt{\frac{165}{12673}}(8,0,2,0,1,0)$, $\sqrt{\frac{165}{12673}}(1,0,8,0,2,0)$,
	$\sqrt{\frac{165}{12673}}(2,0,8,0,1,0)$, $\sqrt{\frac{165}{12673}}(1,0,2,0,8,0)$, $\sqrt{\frac{165}{12673}}(2,0,1,0,8,0)$,
	$\sqrt{\frac{2310}{215441}}(0,0,7,0,4,0)$, $\sqrt{\frac{2310}{215441}}(0,0,4,0,7,0)$, $\sqrt{\frac{2310}{215441}}(7,0,0,0,4,0)$,
	$\sqrt{\frac{2310}{215441}}(4,0,0,0,7,0)$, $\sqrt{\frac{2310}{215441}}(7,0,4,0,0,0)$, $\sqrt{\frac{2310}{215441}}(4,0,7,0,0,0)$,
	$\sqrt{\frac{3080}{215441}}(7,0,1,0,3,0)$, $\sqrt{\frac{3080}{215441}}(7,0,3,0,1,0)$, $\sqrt{\frac{3080}{215441}}(1,0,7,0,3,0)$,
	$\sqrt{\frac{3080}{215441}}(3,0,7,0,1,0)$, $\sqrt{\frac{3080}{215441}}(1,0,3,0,7,0)$, $\sqrt{\frac{3080}{215441}}(3,0,1,0,7,0)$,
	$\sqrt{\frac{3300}{215441}}(7,0,2,0,2,0)$, $\sqrt{\frac{3300}{215441}}(2,0,7,0,2,0)$, $\sqrt{\frac{3300}{215441}}(2,0,2,0,7,0)$,
	$\sqrt{\frac{11858}{1077205}}(0,0,5,0,6,0)$, $\sqrt{\frac{11858}{1077205}}(0,0,6,0,5,0)$, $\sqrt{\frac{11858}{1077205}}(5,0,0,0,6,0)$,

Table C.7 (Continued)

NLM	$C_{n_\rho,l_\rho,n_\lambda,l_\lambda,n_\eta,l_\eta}(n_\rho, l_\rho, n_\lambda, l_\lambda, n_\eta, l_\eta)$
	$\sqrt{\frac{11858}{1077205}}(6,0,0,0,5,0),\ \sqrt{\frac{11858}{1077205}}(5,0,6,0,0,0),\ \sqrt{\frac{11858}{1077205}}(6,0,5,0,0,0),$
	$\sqrt{\frac{3234}{215441}}(6,0,1,0,4,0),\ \sqrt{\frac{3234}{215441}}(6,0,4,0,1,0),\ \sqrt{\frac{3234}{215441}}(1,0,6,0,4,0),$
	$\sqrt{\frac{3234}{215441}}(4,0,6,0,1,0),\ \sqrt{\frac{3234}{215441}}(1,0,4,0,6,0),\ \sqrt{\frac{3234}{215441}}(4,0,1,0,6,0),$
	$\sqrt{\frac{10780}{646323}}(6,0,2,0,3,0),\ \sqrt{\frac{10780}{646323}}(6,0,3,0,2,0),\ \sqrt{\frac{10780}{646323}}(2,0,6,0,3,0),$
	$\sqrt{\frac{10780}{646323}}(3,0,6,0,2,0),\ \sqrt{\frac{10780}{646323}}(2,0,3,0,6,0),\ \sqrt{\frac{10780}{646323}}(3,0,2,0,6,0),$
	$\frac{462}{\sqrt{14003665}}(1,0,5,0,5,0),\ \frac{462}{\sqrt{14003665}}(5,0,1,0,5,0),\ \frac{462}{\sqrt{14003665}}(5,0,5,0,1,0),$
	$\sqrt{\frac{48510}{2800733}}(5,0,2,0,4,0),\ \sqrt{\frac{48510}{2800733}}(5,0,4,0,2,0),\ \sqrt{\frac{48510}{2800733}}(2,0,5,0,4,0),$
	$\sqrt{\frac{48510}{2800733}}(4,0,5,0,2,0),\ \sqrt{\frac{48510}{2800733}}(2,0,4,0,5,0),\ \sqrt{\frac{48510}{2800733}}(4,0,2,0,5,0),$
	$\sqrt{\frac{150920}{8402199}}(5,0,3,0,3,0),\ \sqrt{\frac{150920}{8402199}}(3,0,5,0,3,0),\ \sqrt{\frac{150920}{8402199}}(3,0,3,0,5,0),$
	$\sqrt{\frac{51450}{2800733}}(3,0,4,0,4,0),\ \sqrt{\frac{51450}{2800733}}(4,0,3,0,4,0),\ \sqrt{\frac{51450}{2800733}}(4,0,4,0,3,0)$

Table C.8 Normalized pentaquark (q^4 symmetry) spatial wave functions with quantum number, $N' = 2n + 1$ and $L' = M' = 1$

NLM	$C_{n_\rho,l_\rho,n_\lambda,l_\lambda,n_\eta,l_\eta}(n_\rho, l_\rho, n_\lambda, l_\lambda, n_\eta, l_\eta)$
$110_{[31]\rho}$	$(0,1,0,0,0,0)$
$110_{[31]\lambda}$	$(0,0,0,1,0,0)$
$110_{[31]\eta}$	$(0,0,0,0,0,1)$
$310_{[31]\rho}$	$\sqrt{\frac{5}{33}}(1,1,0,0,0,0),\ \frac{1}{\sqrt{11}}(0,1,1,0,0,0),\ \frac{1}{\sqrt{11}}(0,1,0,0,1,0)$
$310_{[31]\lambda}$	$\sqrt{\frac{5}{33}}(0,0,1,1,0,0),\ \frac{1}{\sqrt{11}}(1,0,0,1,0,0),\ \frac{1}{\sqrt{11}}(0,0,0,1,1,0)$
$310_{[31]\eta}$	$\sqrt{\frac{5}{33}}(0,0,0,0,1,1),\ \frac{1}{\sqrt{11}}(1,0,0,0,0,1),\ \frac{1}{\sqrt{11}}(0,0,1,0,0,1)$
$510_{[31]\rho}$	$\sqrt{\frac{35}{429}}(2,1,0,0,0,0),\ \sqrt{\frac{5}{143}}(0,1,2,0,0,0),\ \sqrt{\frac{5}{143}}(0,1,0,0,2,0),$
	$\sqrt{\frac{10}{143}}(1,1,1,0,0,0),\ \sqrt{\frac{10}{143}}(1,1,0,0,1,0),\ \sqrt{\frac{6}{143}}(0,1,1,0,1,0)$
$510_{[31]\lambda}$	$\sqrt{\frac{35}{429}}(0,0,2,1,0,0),\ \sqrt{\frac{5}{143}}(2,0,0,1,0,0),\ \sqrt{\frac{5}{143}}(0,0,0,1,2,0),$
	$\sqrt{\frac{10}{143}}(1,0,1,1,0,0),\ \sqrt{\frac{10}{143}}(0,0,1,1,1,0),\ \sqrt{\frac{6}{143}}(1,0,0,1,1,0)$

Table C.8   (Continued)

NLM	$C_{n_\rho,l_\rho,n_\lambda,l_\lambda,n_\eta,l_\eta}(n_\rho, l_\rho, n_\lambda, l_\lambda, n_\eta, l_\eta)$
$510_{[31]\eta}$	$\sqrt{\frac{35}{429}}(0,0,0,0,2,1),\ \sqrt{\frac{5}{143}}(0,0,2,0,0,1),\ \sqrt{\frac{5}{143}}(2,0,0,0,0,1),$
	$\sqrt{\frac{10}{143}}(1,0,0,0,1,1),\ \sqrt{\frac{10}{143}}(0,0,1,0,1,1),\ \sqrt{\frac{6}{143}}(1,0,1,0,0,1)$
$710_{[31]\rho}$	$\sqrt{\frac{7}{429}}(0,1,3,0,0,0),\ \sqrt{\frac{3}{143}}(0,1,2,0,1,0),\ \sqrt{\frac{3}{143}}(0,1,1,0,2,0),$
	$\sqrt{\frac{5}{143}}(1,1,2,0,0,0),\ \sqrt{\frac{7}{429}}(0,1,0,0,3,0),\ \sqrt{\frac{6}{143}}(1,1,1,0,1,0),$
	$\sqrt{\frac{5}{143}}(1,1,0,0,2,0),\ \sqrt{\frac{7}{143}}(2,1,1,0,0,0),\ \sqrt{\frac{7}{143}}(2,1,0,0,1,0),$
	$\sqrt{\frac{7}{143}}(3,1,0,0,0,0)$
$710_{[31]\lambda}$	$\sqrt{\frac{7}{429}}(3,0,0,1,0,0),\ \sqrt{\frac{3}{143}}(2,0,0,1,1,0),\ \sqrt{\frac{3}{143}}(1,0,0,1,2,0),$
	$\sqrt{\frac{5}{143}}(2,0,1,1,0,0),\ \sqrt{\frac{7}{429}}(0,0,0,1,3,0),\ \sqrt{\frac{6}{143}}(1,0,1,1,1,0),$
	$\sqrt{\frac{5}{143}}(0,0,1,1,2,0),\ \sqrt{\frac{7}{143}}(1,0,2,1,0,0),\ \sqrt{\frac{7}{143}}(0,0,2,1,1,0),$
	$\sqrt{\frac{7}{143}}(0,0,3,1,0,0)$
$710_{[31]\eta}$	$\sqrt{\frac{7}{429}}(3,0,0,0,0,1),\ \sqrt{\frac{3}{143}}(2,0,1,0,0,1),\ \sqrt{\frac{3}{143}}(1,0,2,0,0,1),$
	$\sqrt{\frac{5}{143}}(2,0,0,0,1,1),\ \sqrt{\frac{7}{429}}(0,0,3,0,0,1),\ \sqrt{\frac{6}{143}}(1,0,1,0,1,1),$
	$\sqrt{\frac{5}{143}}(0,0,2,0,1,1),\ \sqrt{\frac{7}{143}}(1,0,0,0,2,1),\ \sqrt{\frac{7}{143}}(0,0,1,0,2,1),$
	$\sqrt{\frac{7}{143}}(0,0,0,0,3,1)$
$910_{[31]\rho}$	$\sqrt{\frac{21}{2431}}(0,1,0,0,4,0),\ \sqrt{\frac{28}{2431}}(0,1,1,0,3,0),\ \sqrt{\frac{30}{2431}}(0,1,2,0,2,0),$
	$\sqrt{\frac{28}{2431}}(0,1,3,0,1,0),\ \sqrt{\frac{21}{2431}}(0,1,4,0,0,0),\ \sqrt{\frac{140}{7293}}(1,1,0,0,3,0),$
	$\sqrt{\frac{60}{2431}}(1,1,1,0,2,0),\ \sqrt{\frac{60}{2431}}(1,1,2,0,1,0),\ \sqrt{\frac{140}{7293}}(1,1,3,0,0,0),$
	$\sqrt{\frac{70}{2431}}(2,1,0,0,2,0),\ \sqrt{\frac{84}{2431}}(2,1,1,0,1,0),\ \sqrt{\frac{70}{2431}}(2,1,2,0,0,0),$
	$\sqrt{\frac{84}{2431}}(3,1,0,0,1,0),\ \sqrt{\frac{84}{2431}}(3,1,1,0,0,0),\ \sqrt{\frac{7}{221}}(4,1,0,0,0,0)$
$910_{[31]\lambda}$	$\sqrt{\frac{21}{2431}}(0,0,0,1,4,0),\ \sqrt{\frac{28}{2431}}(1,0,0,1,3,0),\ \sqrt{\frac{30}{2431}}(2,0,0,1,2,0),$
	$\sqrt{\frac{28}{2431}}(3,0,0,1,1,0),\ \sqrt{\frac{21}{2431}}(4,0,0,1,0,0),\ \sqrt{\frac{140}{7293}}(0,0,1,1,3,0),$
	$\sqrt{\frac{60}{2431}}(1,0,1,1,2,0),\ \sqrt{\frac{60}{2431}}(2,0,1,1,1,0),\ \sqrt{\frac{140}{7293}}(3,0,1,1,0,0),$
	$\sqrt{\frac{70}{2431}}(0,0,2,1,2,0),\ \sqrt{\frac{84}{2431}}(1,0,2,1,1,0),\ \sqrt{\frac{70}{2431}}(2,0,2,1,0,0),$
	$\sqrt{\frac{84}{2431}}(0,0,3,1,1,0),\ \sqrt{\frac{84}{2431}}(1,0,3,1,0,0),\ \sqrt{\frac{7}{221}}(0,0,4,1,0,0)$

Table C.8 (Continued)

NLM	$C_{n_\rho,l_\rho,n_\lambda,l_\lambda,n_\eta,l_\eta}(n_\rho,l_\rho,n_\lambda,l_\lambda,n_\eta,l_\eta)$
$910_{[31]\eta}$	$\sqrt{\frac{21}{2431}}(0,0,4,0,0,1),\ \sqrt{\frac{28}{2431}}(1,0,3,0,0,1),\ \sqrt{\frac{30}{2431}}(2,0,2,0,0,1),$
	$\sqrt{\frac{28}{2431}}(3,0,1,0,0,1),\ \sqrt{\frac{21}{2431}}(4,0,0,0,0,1),\ \sqrt{\frac{140}{7293}}(0,0,3,0,1,1),$
	$\sqrt{\frac{60}{2431}}(1,0,2,0,1,1),\ \sqrt{\frac{60}{2431}}(2,0,1,0,1,1),\ \sqrt{\frac{140}{7293}}(3,0,0,0,1,1),$
	$\sqrt{\frac{70}{2431}}(2,0,0,0,2,1),\ \sqrt{\frac{84}{2431}}(1,0,1,0,2,1),\ \sqrt{\frac{70}{2431}}(0,0,2,0,2,1),$
	$\sqrt{\frac{84}{2431}}(0,0,1,0,3,1),\ \sqrt{\frac{84}{2431}}(1,0,0,0,3,1),\ \sqrt{\frac{7}{221}}(0,0,0,0,4,1)$
$1110_{[31]\rho}$	$\sqrt{\frac{21}{4199}}(0,1,0,0,5,0),\ \sqrt{\frac{315}{46189}}(0,1,1,0,4,0),\ \sqrt{\frac{350}{46189}}(0,1,2,0,3,0),$
	$\sqrt{\frac{350}{46189}}(0,1,3,0,2,0),\ \sqrt{\frac{315}{46189}}(0,1,4,0,1,0),\ \sqrt{\frac{21}{4199}}(0,1,5,0,0,0),$
	$\sqrt{\frac{525}{46189}}(1,1,0,0,4,0),\ \sqrt{\frac{700}{46189}}(1,1,1,0,3,0),\ \sqrt{\frac{750}{46189}}(1,1,2,0,2,0),$
	$\sqrt{\frac{700}{46189}}(1,1,3,0,1,0),\ \sqrt{\frac{525}{46189}}(1,1,4,0,0,0),\ \sqrt{\frac{2450}{138567}}(2,1,3,0,0,0),$
	$\sqrt{\frac{1050}{46189}}(2,1,1,0,2,0),\ \sqrt{\frac{1050}{46189}}(2,1,2,0,1,0),\ \sqrt{\frac{2450}{138567}}(2,1,0,0,3,0),$
	$\sqrt{\frac{1050}{46189}}(3,1,0,0,2,0),\ \sqrt{\frac{1260}{46189}}(3,1,1,0,1,0),\ \sqrt{\frac{1050}{46189}}(3,1,2,0,0,0),$
	$\sqrt{\frac{105}{4199}}(4,1,0,0,1,0),\ \sqrt{\frac{105}{4199}}(4,1,1,0,0,0),\ \sqrt{\frac{7}{323}}(5,1,0,0,0,0)$
$1110_{[31]\lambda}$	$\sqrt{\frac{21}{4199}}(0,0,0,1,5,0),\ \sqrt{\frac{315}{46189}}(1,0,0,1,4,0),\ \sqrt{\frac{350}{46189}}(2,0,0,1,3,0),$
	$\sqrt{\frac{350}{46189}}(3,0,0,1,2,0),\ \sqrt{\frac{315}{46189}}(4,0,0,1,1,0),\ \sqrt{\frac{21}{4199}}(5,0,0,1,0,0),$
	$\sqrt{\frac{525}{46189}}(0,0,1,1,4,0),\ \sqrt{\frac{700}{46189}}(1,0,1,1,3,0),\ \sqrt{\frac{750}{46189}}(2,0,1,1,2,0),$
	$\sqrt{\frac{700}{46189}}(3,0,1,1,1,0),\ \sqrt{\frac{525}{46189}}(4,0,1,1,0,0),\ \sqrt{\frac{2450}{138567}}(3,0,2,1,0,0),$
	$\sqrt{\frac{1050}{46189}}(1,0,2,1,2,0),\ \sqrt{\frac{1050}{46189}}(2,0,2,1,1,0),\ \sqrt{\frac{2450}{138567}}(0,0,2,1,3,0),$
	$\sqrt{\frac{1050}{46189}}(0,0,3,1,2,0),\ \sqrt{\frac{1260}{46189}}(1,0,3,1,1,0),\ \sqrt{\frac{1050}{46189}}(2,0,3,1,0,0),$
	$\sqrt{\frac{105}{4199}}(0,0,4,1,1,0),\ \sqrt{\frac{105}{4199}}(1,0,4,1,0,0),\ \sqrt{\frac{7}{323}}(0,0,5,1,0,0)$
$1110_{[31]\eta}$	$\sqrt{\frac{21}{4199}}(5,0,0,0,0,1),\ \sqrt{\frac{315}{46189}}(4,0,1,0,0,1),\ \sqrt{\frac{350}{46189}}(3,0,2,0,0,1),$
	$\sqrt{\frac{350}{46189}}(2,0,3,0,0,1),\ \sqrt{\frac{315}{46189}}(1,0,4,0,0,1),\ \sqrt{\frac{21}{4199}}(0,0,5,0,0,1),$
	$\sqrt{\frac{525}{46189}}(4,0,0,0,1,1),\ \sqrt{\frac{700}{46189}}(1,0,3,0,1,1),\ \sqrt{\frac{750}{46189}}(2,0,2,0,1,1),$
	$\sqrt{\frac{700}{46189}}(3,0,1,0,1,1),\ \sqrt{\frac{525}{46189}}(0,0,4,0,1,1),\ \sqrt{\frac{2450}{138567}}(0,0,3,0,2,1),$
	$\sqrt{\frac{1050}{46189}}(2,0,1,0,2,1),\ \sqrt{\frac{1050}{46189}}(1,0,2,0,2,1),\ \sqrt{\frac{2450}{138567}}(3,0,0,0,2,1),$

Table C.8 (Continued)

NLM	$C_{n_\rho,l_\rho,n_\lambda,l_\lambda,n_\eta,l_\eta}(n_\rho, l_\rho, n_\lambda, l_\lambda, n_\eta, l_\eta)$
	$\sqrt{\frac{1050}{46189}}(2,0,0,0,3,1),\ \sqrt{\frac{1260}{46189}}(1,0,1,0,3,1),\ \sqrt{\frac{1050}{46189}}(0,0,2,0,3,1),$
	$\sqrt{\frac{105}{4199}}(1,0,0,0,4,1),\ \sqrt{\frac{105}{4199}}(0,0,1,0,4,1),\ \sqrt{\frac{7}{323}}(0,0,0,0,5,1)$

Table C.9 Normalized pentaquark (q^4 symmetry) spatial wave functions with quantum number, $N' = 2n$ and $L' = M' = 1$

NLM	$C_{n_\rho,l_\rho,n_\lambda,l_\lambda,n_\eta,l_\eta}(n_\rho, l_\rho, n_\lambda, l_\lambda, n_\eta, l_\eta)$
$210_{[211]\rho}$	$(0,1,0,0,0,1)$
$210_{[211]\lambda}$	$(0,0,0,1,0,1)$
$210_{[211]\eta}$	$(0,1,0,1,0,0)$
$410_{[211]\rho}$	$\sqrt{\frac{5}{39}}(0,1,0,0,1,1),\ \frac{1}{\sqrt{13}}(0,1,1,0,0,1),\ \sqrt{\frac{5}{39}}(1,1,0,0,0,1)$
$410_{[211]\lambda}$	$\sqrt{\frac{5}{39}}(0,0,0,1,1,1),\ \frac{1}{\sqrt{13}}(1,0,0,1,0,1),\ \sqrt{\frac{5}{39}}(0,0,1,1,0,1)$
$410_{[211]\eta}$	$\sqrt{\frac{5}{39}}(0,1,1,1,0,0),\ \frac{1}{\sqrt{13}}(0,1,0,1,1,0),\ \sqrt{\frac{5}{39}}(1,1,0,1,0,0)$
$610_{[211]\rho}$	$\sqrt{\frac{7}{117}}(0,1,0,0,2,1),\ \sqrt{\frac{2}{39}}(0,1,1,0,1,1),\ \frac{1}{\sqrt{39}}(0,1,2,0,0,1),$
	$\sqrt{\frac{10}{117}}(1,1,0,0,1,1),\ \sqrt{\frac{2}{39}}(1,1,1,0,0,1),\ \sqrt{\frac{7}{117}}(2,1,0,0,0,1)$
$610_{[211]\lambda}$	$\sqrt{\frac{7}{117}}(0,0,0,1,2,1),\ \sqrt{\frac{2}{39}}(1,0,0,1,1,1),\ \frac{1}{\sqrt{39}}(2,0,0,1,0,1),$
	$\sqrt{\frac{10}{117}}(0,0,1,1,1,1),\ \sqrt{\frac{2}{39}}(1,0,1,1,0,1),\ \sqrt{\frac{7}{117}}(0,0,2,1,0,1)$
$610_{[211]\eta}$	$\sqrt{\frac{7}{117}}(0,1,2,1,0,0),\ \sqrt{\frac{2}{39}}(0,1,1,1,1,0),\ \frac{1}{\sqrt{39}}(0,1,0,1,2,0),$
	$\sqrt{\frac{10}{117}}(1,1,1,1,0,0),\ \sqrt{\frac{2}{39}}(1,1,0,1,1,0),\ \sqrt{\frac{7}{117}}(2,1,0,1,0,0)$
$810_{[211]\rho}$	$\sqrt{\frac{7}{221}}(0,1,0,0,3,1),\ \sqrt{\frac{7}{221}}(0,1,1,0,2,1),\ \sqrt{\frac{5}{221}}(0,1,2,0,1,1),$
	$\sqrt{\frac{7}{663}}(0,1,3,0,0,1),\ \sqrt{\frac{35}{663}}(1,1,0,0,2,1),\ \sqrt{\frac{10}{221}}(1,1,1,0,1,1),$
	$\sqrt{\frac{5}{221}}(1,1,2,0,0,1),\ \sqrt{\frac{35}{663}}(2,1,0,0,1,1),\ \sqrt{\frac{7}{221}}(2,1,1,0,0,1),$
	$\sqrt{\frac{7}{221}}(3,1,0,0,0,1)$
$810_{[211]\lambda}$	$\sqrt{\frac{7}{221}}(0,0,0,1,3,1),\ \sqrt{\frac{7}{221}}(1,0,0,1,2,1),\ \sqrt{\frac{5}{221}}(2,0,0,1,1,1),$
	$\sqrt{\frac{7}{663}}(3,0,0,1,0,1),\ \sqrt{\frac{35}{663}}(0,0,1,1,2,1),\ \sqrt{\frac{10}{221}}(1,0,1,1,1,1),$

Table C.9   (Continued)

NLM	$C_{n_\rho,l_\rho,n_\lambda,l_\lambda,n_\eta,l_\eta}(n_\rho, l_\rho, n_\lambda, l_\lambda, n_\eta, l_\eta)$
	$\sqrt{\frac{5}{221}}(2,0,1,1,0,1),\ \sqrt{\frac{35}{663}}(0,0,2,1,1,1),\ \sqrt{\frac{7}{221}}(1,0,2,1,0,1),$
	$\sqrt{\frac{7}{221}}(0,0,3,1,0,1)$
$810_{[211]\eta}$	$\sqrt{\frac{7}{221}}(3,1,0,1,0,0),\ \sqrt{\frac{7}{221}}(2,1,0,1,1,0),\ \sqrt{\frac{5}{221}}(1,1,0,1,2,0),$
	$\sqrt{\frac{7}{663}}(0,1,0,1,3,0),\ \sqrt{\frac{35}{663}}(2,1,1,1,0,0),\ \sqrt{\frac{10}{221}}(1,1,1,1,1,0),$
	$\sqrt{\frac{5}{221}}(0,1,1,1,2,0),\ \sqrt{\frac{35}{663}}(1,1,2,1,0,0),\ \sqrt{\frac{7}{221}}(0,1,2,1,1,0),$
	$\sqrt{\frac{7}{221}}(0,1,3,1,0,0)$
$1010_{[211]\rho}$	$\sqrt{\frac{77}{4199}}(0,1,0,0,4,1),\ \sqrt{\frac{84}{4199}}(0,1,1,0,3,1),\ \sqrt{\frac{70}{4199}}(0,1,2,0,2,1),$
	$\sqrt{\frac{140}{12597}}(0,1,3,0,1,1),\ \sqrt{\frac{21}{4199}}(0,1,4,0,0,1),\ \sqrt{\frac{140}{4199}}(1,1,0,0,3,1),$
	$\sqrt{\frac{140}{4199}}(1,1,1,0,2,1),\ \frac{10}{\sqrt{4199}}(1,1,2,0,1,1),\ \sqrt{\frac{140}{12597}}(1,1,3,0,0,1),$
	$\sqrt{\frac{700}{12597}}(2,1,0,0,2,1),\ \sqrt{\frac{140}{4199}}(2,1,1,0,1,1),\ \sqrt{\frac{70}{4199}}(2,1,2,0,0,1),$
	$\sqrt{\frac{140}{4199}}(3,1,0,0,1,1),\ \sqrt{\frac{84}{4199}}(3,1,1,0,0,1),\ \sqrt{\frac{77}{4199}}(4,1,0,0,0,1)$
$1010_{[211]\lambda}$	$\sqrt{\frac{77}{4199}}(0,0,0,1,4,1),\ \sqrt{\frac{84}{4199}}(1,0,0,1,3,1),\ \sqrt{\frac{70}{4199}}(2,0,0,1,2,1),$
	$\sqrt{\frac{140}{12597}}(3,0,0,1,1,1),\ \sqrt{\frac{21}{4199}}(4,0,0,1,0,1),\ \sqrt{\frac{140}{4199}}(0,0,1,1,3,1),$
	$\sqrt{\frac{140}{4199}}(1,0,1,1,2,1),\ \frac{10}{\sqrt{4199}}(2,0,1,1,1,1),\ \sqrt{\frac{140}{12597}}(3,0,1,1,0,1),$
	$\sqrt{\frac{700}{12597}}(0,0,2,1,2,1),\ \sqrt{\frac{140}{4199}}(1,0,2,1,1,1),\ \sqrt{\frac{70}{4199}}(2,0,2,1,0,1),$
	$\sqrt{\frac{140}{4199}}(0,0,3,1,1,1),\ \sqrt{\frac{84}{4199}}(1,0,3,1,0,1),\ \sqrt{\frac{77}{4199}}(0,0,4,1,0,1)$
$1010_{[211]\eta}$	$\sqrt{\frac{77}{4199}}(0,1,4,1,0,0),\ \sqrt{\frac{84}{4199}}(0,1,3,1,1,0),\ \sqrt{\frac{70}{4199}}(0,1,2,1,2,0),$
	$\sqrt{\frac{140}{12597}}(0,1,1,1,3,0),\ \sqrt{\frac{21}{4199}}(0,1,0,1,4,0),\ \sqrt{\frac{140}{4199}}(1,1,3,1,0,0),$
	$\sqrt{\frac{140}{4199}}(1,1,2,1,1,0),\ \frac{10}{\sqrt{4199}}(1,1,1,1,2,0),\ \sqrt{\frac{140}{12597}}(1,1,0,1,3,0),$
	$\sqrt{\frac{700}{12597}}(2,1,2,1,0,0),\ \sqrt{\frac{140}{4199}}(2,1,1,1,1,0),\ \sqrt{\frac{70}{4199}}(2,1,0,1,2,0),$
	$\sqrt{\frac{140}{4199}}(3,1,1,1,0,0),\ \sqrt{\frac{84}{4199}}(3,1,0,1,1,0),\ \sqrt{\frac{77}{4199}}(4,1,0,1,0,0)$

APPENDIX D

NUMERICAL CALCULATION IN HO BASIS

D.1 The Complete Basis Of Harmonic Oscillator Functions

The Schrödinger equation for the pentaquark systems described by the Hamiltonian is solved numerically by expanding the pentaquark wave functions in the completed bases ϕ_k and we can always expand our eigenfunction of the Hamiltonian in terms of HO basis which reads: $\Psi_m = a_{mk}\phi_k$.

In the coordinate state space,

$$
\begin{aligned}
\langle\psi_m|r|\psi_n\rangle &= \langle\psi_m|r'\rangle\langle r'|r|r''\rangle\langle r''|\psi_n\rangle \\
&= \langle\psi_m|r'\rangle\delta(r'-r'')\langle r''|\psi_n\rangle \\
&= \int dr\,\psi_m^*(r)r\psi_n(r)
\end{aligned}
\tag{D.1}
$$

The momentum described in the coordinate space as,

$$
\begin{aligned}
\langle\psi_m|p|\psi_n\rangle &= \langle\psi_m|r'\rangle\langle r'|p|r''\rangle\langle r''|\psi_n\rangle \\
&= \langle\psi_m|r'\rangle(-i\hbar)\frac{d}{dr'}\delta(r'-r'')\langle r''|\psi_n\rangle \\
&= \int dr\,\psi_m^*(r)(-i\hbar)\frac{d}{dr}\psi_n(r)
\end{aligned}
\tag{D.2}
$$

Following this, we can write our Hamiltonian in the coordinate space in the form below:

$$
\begin{aligned}
\langle\Psi_m|H|\Psi_n\rangle &= \langle a_{mk}\phi_k|H|\phi_k' a_{nk'}\rangle \\
&= \langle a_{mk}\phi_k|(\frac{-\hbar^2}{2m}\frac{d^2}{dr^2} - \frac{k}{r} + ar)|\phi_k' a_{nk'}\rangle
\end{aligned}
$$

$$= \langle a_{mk}|B_{kk}|a_{nk'}\rangle \tag{D.3}$$

B_{kk} is a $k \times k$ matrix, by solve the eigenvalue and eigenfunction of B_{kk}, we have the eigenvalues for the corresponding mass spectrum and eigenfunction for the expansion in the harmonic oscillator basis. Among them permutation symmetry of identical particles are applied to simplify the calculations shown as below:

For any operator O_i, i stands for i^{th} quark of the system. ϕ is the full wave function of hadron. (ij) is the any permutation of quark i and j then we have:

$$
\begin{aligned}
\langle\phi|O_i|\phi\rangle &= \langle\phi|(1i)^{-1}(1i)O_i(1i)(1i)^{-1}|\phi\rangle \\
&= \langle\phi|(1i)^{-1}O_1(1i)|\phi\rangle \\
&= \langle\phi(-1)|O_1|(-1)\phi\rangle \\
&= \langle\phi|O_1|\phi\rangle
\end{aligned}
\tag{D.4}
$$

So for any operator O_iO_j, we just repeat this process twice, we can always get:

$$
\begin{aligned}
\langle\phi|O_iO_j|\phi\rangle &= \langle\phi|O_1O_j|\phi\rangle \\
&= \langle\phi|O_1O_2|\phi\rangle
\end{aligned}
\tag{D.5}
$$

For q^3 baryon r_{ij} can be also treat as operator O_iO_j, so

$$\langle\phi|r_{ij}|\phi\rangle = \langle\phi|r_{12}|\phi\rangle \tag{D.6}$$

Same method for $q^4\bar{q}$ pentaquark, for $i < j$, $i, j < 5$

$$\langle\phi|r_{ij}|\phi\rangle = \langle\phi|r_{12}|\phi\rangle \tag{D.7}$$

for $i < 5$, $j = 5$

$$\langle\phi|r_{i5}|\phi\rangle = \langle\phi|r_{45}|\phi\rangle \tag{D.8}$$

CURRICULUM VITAE

NAME: Kai Xu   **GENDER**: Male

NATIONALITY: Chinese   **DATE OF BIRTH**: May 17, 1988

EDUCATIONS:

- B. Sc. Department of Physics, University of Science and Technology of China, China, 2011.

PUBLICATIONS

[1] K. Xu, N. Ritjoho, S. Srisuphaphon, Y. Yan, **"Estimation of ground state pentaquark masses "**, Int. J. Mod. Phys. Conf. Ser. 29 (2014) 1460251.

[2] W.Sreethawong, K. Xu, Y. Yan, **"Exclusion of $c\bar{c}$ interpretation for X(3940) "**, J. Phys. G: Nucl. Part. Phys. 42 (2015) no.2, 025001.

[3] T. Gutsche, M. A. Ivanov, J. G. Körner, V. E. Lyubovitskij and K. Xu, **"Test of the multiquark structure of $a_1(1420)$ in strong two-body decays "**, Phys. Rev. D96 (2017) no.11, 114004.

[4] K. Xu, A. Kaewsnod, X. Y. Liu, S. Srisuphaphon, A. Limphirat, and Y. Yan, **"Complete basis for pentaquark wave function in group theory approach "**, Phys. Rev. C100 (2019), 065207.

[5] K. Xu, A. Kaewsnod, Z. Zhao, X. Y. Liu, S. Srisuphaphon, A. Limphirat, and Y. Yan, **"Pentaquark components in low-lying baryon resonances "**, Phys. Rev. D101 (2020), 076025.